MODELING THE IMPACTS OF CHANGES IN SOIL MICROBES AND MOSSES ON ARCTIC TERRESTRIAL ECOSYSTEM CARBON DYNAMICS

by

Junrong Zha

A Dissertation

Submitted to the Faculty of Purdue University

In Partial Fulfillment of the Requirements for the degree of

Doctor of Philosophy

Department of Earth, Atmospheric, & Planetary Sciences

West Lafayette, Indiana

August 2019

THE PURDUE UNIVERSITY GRADUATE SCHOOL
STATEMENT OF COMMITTEE APPROVAL

Dr. Qianlai Zhuang, Chair

Department of Earth, Atmospheric, and Planetary Sciences, and Agronomy

Dr. Robert L. Nowack

Department of Earth, Atmospheric, and Planetary Sciences

Dr. Wen-Wen Tung

Department of Earth, Atmospheric, and Planetary Sciences

Dr. Harshvardhan Harshvardhan

Department of Earth, Atmospheric, and Planetary Sciences

Approved by:

Dr. Daniel J. Cziczo

Head of the Graduate Program

Dedicated to my parents and whom I love
for their unconditional support, help and selfless love.

ACKNOWLEDGMENTS

The PhD life in past four years is a precious and unforgettable journey, with harvest, happiness, as well as stress and bewilderment. There are so many people accompanied me through this journey. Without them, I won't be able to reach where I am now. In this section, I would like to express my deep gratitude to them for their support and help.

Above all, I would like to express my sincerest appreciation and gratitude to my advisor, Professor Qianlai Zhuang. He offered me the opportunity to pursue the PhD degree at Purdue University, supported my research with his stimulating instructions, and provided inspired advices when I was confused. It was his encouragement, patience and academic insight, which made me from an undergraduate with little experience in ecosystem modeling to a PhD with professional knowledge. This thesis would not have been possible without his solid support. I am proud to be a student of him and extremely grateful for all the nutrition he brought to my growth on both academic and personal levels.

I would also like to thank my advisory committee members: Drs. Robert L. Nowack, Wen-Wen Tung, and Harshvardhan. Thanks to Dr. Robert L. Nowack, his course of inverse theory helped me build a solid foundation of model parameterization. Besides, I also benefited a lot from the face-to-face meetings with him. His advices on both my PhD research and career choices could always inspired me. Thanks to Dr. Wen-Wen Tung, her openness to invite us attending the Geodata Science seminar, brought a big picture of intersections between data science and Earth Science, which broadens my scientific vision a lot. Thanks to Dr. Harshvardhan, his course of atmospheric physics served as theoretical fundamentals for my research in modeling. Their help and instructions played essential roles in the achievement of my PhD program.

I must also thank my lab-mates in the EBDL for their help and suggestions on my research and personal life. From thorough discussions with them, I learnt useful skills, inspiring suggestions on research and career, and invaluable experience. Thanks to the open-minded and stimulating academic environment built by them, and all the enjoyable moments we shared together in the past four years.

Last but not least, I want to convey special thanks to my parents and whom I love. Thanks to my parents, who raised me up, care for me and become my solid backing for the whole life. Thanks to my boyfriend, Hao Li, who has been supportive, tolerates my shortcomings and shares my ups and downs with his encouragements and trust.

Again, all your help, support and sacrifices made me who I am today, thank you!

TABLE OF CONTENTS

LIST OF TABLES

LIST OF FIGURES

ABSTRACT

Author: Zha, Junrong. PhD
Institution: Purdue University
Degree Received: August 2019
Title: Modeling the Impacts of Changes in Soil Microbes and Mosses on Arctic Terrestrial Ecosystem Carbon Dynamics
Committee Chair: Qianlai Zhuang

The land ecosystems in northern high latitudes (>45° N) occupy 22% of the global surface and store more than 1600 Pg soil organic carbon. Warming in this region has been documented during the past decades. Warming-induced changes in regional carbon dynamics are expected to loom large in the global carbon cycle and exert large feedbacks to the global climate system. Numerous Earth System Models have been widely used to quantify the response of terrestrial ecosystem carbon dynamics to climatic changes. However, predictions of terrestrial ecosystem carbon responses to increasing levels of atmospheric carbon dioxide (CO_2) and climate change is still uncertain due to model limitations. The limitations include relatively low levels of representation of ecosystem processes that determine the exchanges of water, energy, and carbon between land ecosystems and the atmosphere and omitting some key biogeochemical mechanisms. To improve model realism and provide a better projection of the Arctic carbon dynamics, this dissertation developed three new versions of a process-based biogeochemistry models that involve more fundamental processes of terrestrial ecosystems. First, microbial dynamics and enzyme kinetics that catalyze soil carbon decomposition have been incorporated into the extant terrestrial ecosystem model TEM to remedy the inadequate representation of soil decomposition process. Furthermore, a vital microbial life-history trait, microbial dormancy, has been implemented into previous microbial-based model to consider the impacts of microbial dormancy in modeling.

Additionally, the role of moss in the Arctic terrestrial ecosystem carbon quantification was also demonstrated by incorporating moss and higher plant interactions in modelling.

CHAPTER 1. INTRODUCTION

1.1 Research Background

Northern high-latitude ecosystems occupy a large proportion (22%) of the terrestrial surface and contain over 40% of the global soil organic carbon (SOC), which is more than 1600 Pg C (Allison et al., 2008; Jobbágy & Jackson, 2000; Kasischke, 2000; Tarnocai et al., 2009; McGuire & Hobbie, 1997). The total carbon in soils and plants in this region accounts for about 30% of global terrestrial carbon (Hugelius et al., 2014; Schuur et al., 2008). On the other hand, global warming has been pronounced since the middle of the 19th century (Jones and Mogberg 2003), especially at high latitudes (McGuire et al., 2009; Treseder et al., 2016). Previous studies showed that the increase of surface air temperature in this region is 1.5 to 4.5 times the global mean (Holland and Bitz, 2003; Serreze and Francis, 2006), and warming in this region is expected to continue through the 21st century (Serreze et al., 2000, Overland et al., 2004). This warming may induce environmental responses such as acceleration in soil carbon loss (Mack et al., 2004), a decrease in permafrost stability (Jorgenson et al., 2001) and snow cover duration (Stone et al., 2002, Euskirchen et al., 2009), which will further alter the carbon cycling in terrestrial arctic ecosystems (Chapin et al., 2005, Beringer et al., 2005). Given the large pool of carbon in northern high latitudes, warming-induced changes in carbon cycle of the Arctic are expected to exert large feedbacks on the global climate system (McGuire et al., 2009; Davidson and Janssens, 2006; Christensen and Christensen, 2007; Oechel et al., 2000; Bond-Lamberty & Thomson, 2010). Thus, explicit investigation of carbon-climate feedback in this region is essential (Wieder et al., 2013; Bond-Lamberty & Thomson, 2010). This dissertation therefore particularly focuses on exploring

regional carbon budgets in the Arctic terrestrial ecosystems in last and this century using a process-based biogeochemistry modeling approach.

Currently, numerous state-of-the-art process-based Earth System Models such as Terrestrial Ecosystem Model (TEM; Hayes et al., 2014; Raich and Schlesinger, 1992; McGuire et al., 1992; Zhuang et al., 2010, 2013), Biome-BGC (Running and Coughlan, 1988; Bond-Lamberty et al., 2005), CENTURY (Parton et al., 1994), and the Biosphere Energy Transfer Hydrology scheme (BETHY) (Knorr, 2000) have been employed to project future climate and carbon cycle feedbacks (Todd-Brown et al., 2011; Treseder et al., 2016). These models were built on consensus scientific representations of processes such as photosynthesis, respiration, nutrient and water cycling, and soil decomposition (Bond-Lamberty et al., 2005; Zhuang et al., 2003). Estimates from documented studies using those models indicate the region functioned as a sink of atmospheric CO_2 in recent decades (Schimel, 2013; McGuire et al., 2012). Globally, the terrestrial ecosystem was estimated as a carbon sink of 1.4 PgC yr^{-1} in the 1990s (Schimel et al., 2001), while the Arctic region was indicated on average of a CO_2 sink about 0.5 Pg C yr^{-1} in the same time period (McGuire et al., 2000), which accounts for roughly 36% of global carbon budget. In the late 20^{th} century, the net uptake of CO_2 by the Arctic terrestrial ecosystems was estimated in the range of 0.3 to 0.6 Pg C yr^{-1} (McGuire et al., 2000). However, the carbon dynamics response to climate change is still with a high uncertainty (Friedlingstein et al., 2006; Todd-Brown et al., 2013).

The uncertainty from process-based models depends in part on the components and processes that are built into the models (Zhuang et al. 2006; Turetsky et al., 2012; Oreskes et al., 1994). Low levels of representation of ecosystem processes that determine the exchanges of water, energy, and carbon between land ecosystems and the atmosphere (Wieder et al., 2013), and ignorance of some key biogeochemical mechanisms and ecological components (Schmidt et al.,

2011; Conant et al., 2011; Treseder et al., 2011) may induce biases in carbon budget quantification (Wieder et al., 2013; Todd-Brown et al., 2011, 2013). Firstly, in modeling soil decomposition, many contemporary models treated soil decomposition as a first-order Q_{10} relationship decay process, i.e., CO_2 respiration is directly proportional to soil organic carbon pool size (Todd-Brown et al., 2011; *van't Hoff*, 1898). However, recent empirical studies have shown that soil decomposition actually depends on the activity of biological communities dominated by microbes (Allison and Martiny, 2008; Schimel and Weintraub, 2003). Microbes control soil respiration by degrading complex organic matter and converting to CO_2 (Sinsabaugh, 1994; Todd-Brown et al., 2013). Thus, such first-order implementation of soil respiration is inconsistent with current understanding of decomposition mechanisms (Todd-Brown et al., 2013). The significant role of microbial community in soil carbon decomposition indicates the need for an explicit representation of microbial physiology and enzymatic activity on heterotrophic respiration (Schimel and Weintraub, 2003). Moreover, recent process-based models which explicitly incorporated the microbial dynamics and enzyme kinetics have produced notably different results and better reproduce field and satellite observations (Treseder et al., 2011; Wieder et al., 2013; Allison et al., 2010; Lawrence et al., 2009).

Although microbial ecology has been explicitly incorporated into some existing process-based models to remedy the inadequate representation of soil decomposition process (Zha & Zhuang, 2018; Allison et al., 2010; German et al., 2012), some vital common evolutionary traits such as microbial dormancy and community shifts are still rarely represented in these models (Graham et al., 2014, 2016; Wang et al., 2015; Kaiser et al., 2014). Dormancy is a prominent feature for microorganisms to cope with periodical environmental stresses in soil systems (Harder & Dijkhuizen, 1983; Wang et al., 2014), especially in arctic terrestrial ecosystems due to nitrogen-

limitation (Stolpovsky et al., 2011; Thullner et al., 2005). When environmental conditions limit growth and reproduction, microbes switch to the dormant state, which is a reversible state of low metabolic activity, until conditions improve to allow replication (Stolpovsky et al., 2011; Lennon & Jones, 2011; Wang et al., 2014). Previous studies have recognized that more than 50% of number of microbes are in dormant state at any given time in natural soils (Blagodatsky et al., 2011; Stolpovsky et al., 2011). Nevertheless, soil decomposition and nutrient cycling mainly depend on the active fraction of microbial communities, not the whole microbes (Blagodatskaya et al., 2013, 2014; Wang et al., 2014, 2015). Thus, neglecting microbial dormancy will lead to incorrect estimates of "active" microbial biomass and further bias the quantification of ecosystem carbon budget (Wang et al., 2015; Hagerty et al., 2014; He et al., 2015). It is important to represent microbial dormancy in Earth System Models to improve model realism and adequately quantify the carbon dynamics in northern high latitudes.

In addition, important components such as moss are also ignored in most existing models (Treseder et al., 2011; Bond-Lamberty et al., 2005). Mosses are ubiquitous in northern ecosystems, benefiting from their functional traits related to water, nutrient, and thermal tolerances through physiological responses (Turetsky et al., 2010, 2012; Oechel &Van Cleve, 1986; Jagerbrand et al., 2009). The activities of moss can influence several ecosystem processes such as soil decomposition, net primary productivity (NPP) and peat accumulation (Turetsky et al., 2012; Euskirchen et al., 2009; Nilsson & Wardle, 2005). First of all, unlike higher plants, mosses are productive with carbon assimilation even during low temperature, water content and irradiance (Kallio & Heinonen, 1975; Harley et al., 1989). It is gradually recognized that mosses can contribute comparable NPP to vascular plants as high as 350 g m^{-2} yr^{-1} in some arctic regions (Turetsky et al., 2010; Pakarinen & Vitt 1973). Besides, moss can compete with vascular plants for available nutrients because of

their rapid nutrient acquisition and slow nutrient loss, which can cause negative effects on vascular plant productivity (Oechel &Van Cleve, 1986; Gornall et al., 2007, 2011; Turetsky et al., 2010, 2012). Moreover, moss cover can prevent absorbed solar heat from being conducted down into the soil, and tends to decrease soil temperature in summer (Pedersen et al. 1999; Oechel &Van Cleve, 1986). It can also form an environment with water logging or low oxygen supply, which will exert effects on soil moisture (Skre & Oechel, 1979; Cornelissen et al., 2007). The effects of moss on soil thermal and hydrologic dynamics will further influence heterotrophic respiration (R_H) (Beringer et al. 2001, Zhuang et al. 2001). Including moss as a keystone plant functional type in ecosystem models is essential for improving model prediction of carbon dynamics (Zhuang et al., 2006; Bond-Lamberty et al., 2005, 2007; Frolking et al., 1996, 2010).

1.2 Research Questions

This dissertation addresses the following questions by developing and applying several new biogeochemistry models:

1) Can modification of the soil respiration process modeling schemes by considering more detailed microbial dynamics improve carbon budget quantification at both site-level and regional scales?

2) How do the long-term carbon dynamics in northern high latitudes estimated using microbial-based model differ from that estimated using a traditional model that is based on the first-order decay process?

3) What are differences in Arctic carbon budget during last and this century predicted by models with and without microbial dormancy?

4) What is the role of moss in the Arctic carbon quantification during last and this century?

The three new models that advance an extant process-based biogeochemistry model by modifying the soil respiration process and incorporating important microbial traits (microbial dormancy) and components (moss) were first developed. A series of model evaluation, model parameterization, and uncertainty analysis were conducted.

1.3 Outline of Dissertation

This dissertation consists of three main chapters and each corresponds to a study that addresses one or two of the research questions listed above. In Chapter 2, a second-order soil decomposition module that considers microbial dynamics and enzyme kinetics was explicitly incorporated into a highly aggregated, large-scale terrestrial ecosystem model (TEM) to improve projections of Arctic carbon dynamics. The new microbial-based model (MIC-TEM), as well as traditional Q_{10}-based model (TEM) were applied to the northern high-latitude region for the 20^{th} and 21^{st} centuries. In Chapter 3, an important microbial trait, microbial dormancy, was further implemented into previous microbial-based model to involve the dormant-active microbial physiology. Contrasting model performance with and without representation of microbial dormancy in Arctic region highlights the effects of microbial dormancy on Arctic carbon dynamics. In Chapter 4, moss, one ubiquitous community in northern ecosystems, was included in traditional terrestrial ecosystem model (TEM) to explore the role of moss in arctic carbon budget. The verified new model, which can support both activities of higher plants and mosses, was compared with TEM to examine the influence of moss on both historical and future Arctic carbon budget. Finally, Chapter 5 summarized the major findings from previous chapters and answered the five main questions raised in Section 1.2. A survey of a dozen recently published microbial models was conducted to examine the current state of microbial modeling and mechanisms that are commonly

under-represented in the majority of models. Future research directions for both modeling and experimental community were discussed.

CHAPTER 2. MICROBIAL DECOMPOSITION PROCESSES AND VULNERABLE ARCTIC SOIL ORGANIC CARBON IN THE 21ST CENTURY[1]

2.1 Abstract

Various levels of representations of biogeochemical processes in current biogeochemistry models contribute to a large uncertainty in carbon budget quantification. Here, we present an uncertainty analysis with a process-based biogeochemistry model, the Terrestrial Ecosystem Model (TEM) that was incorporated with detailed microbial mechanisms. Ensemble regional simulations with the new model (MIC-TEM) estimated the carbon budget of the Arctic ecosystems is 76.0±114.8 Pg C during the 20th century, -3.1±61.7 Pg C under the RCP 2.6 scenario and 94.7±46 Pg C under the RCP 8.5 scenario during the 21st century. Positive values indicate the regional carbon sink while negative values are source to the atmosphere. Compared to the estimates using a simpler soil decomposition algorithm in TEM, the new model estimated that the Arctic terrestrial ecosystems stored 12 Pg less carbon over the 20th century, 19 Pg C and 30 Pg C less under the RCP 8.5 and RCP 2.6 scenarios, respectively, during the 21st century. When soil carbon within depths 30 cm, 100 cm and 300 cm was considered as initial carbon in the 21st century simulations, the region was estimated to accumulate 65.4, 88.6, and 109.8 Pg C, respectively, under the RCP 8.5 scenario. In contrast, under the RCP 2.6 scenario, the region lost 0.7, 2.2, and 3 Pg C, respectively, to the atmosphere. We conclude that the future regional carbon budget evaluation largely depends on whether or not the adequate microbial activities are represented in earth system models and the sizes of soil carbon considered in model simulations.

[1]**Zha, J**. and Zhuang, Q.: Microbial decomposition processes and vulnerable arctic soil organic carbon in the 21st century, Biogeosciences, 15, 5621-5634, https://doi.org/10.5194/bg-15-5621-2018, 2018.

2.2 Introduction

Northern high-latitude soils and permafrost contain more than 1,600 Pg carbon (Tarnocai et al., 2009). Climate over this region has warmed in recent decades (Serreze and Francis, 2006) and the increase is 1.5 to 4.5 times the global mean (Holland and Bitz, 2003). Warming-induced changes in carbon cycling are expected to exert large feedbacks to the global climate system (Davidson and Janssens, 2006; Christensen and Christensen, 2007; Oechel et al., 2000).

Warming is expected to accelerate soil C loss by increasing soil respiration, but increasing nutrient mineralization, thereby stimulating plant net primary production (NPP) (Mack et al., 2004). Thus, the variation of climate may switch the role of the Arctic system between a C sink and a source if soil C loss overtakes NPP (Davidson et al., 2000; Jobbágy and Jackson, 2000). Process-based biogeochemical models such as TEM (Hayes et al., 2014; Raich and Schlesinger, 1992; McGuire et al., 1992; Zhuang et al., 2001, 2002, 2003, 2010, 2013), Biome-BGC (Running and Coughlan, 1988), CASA (Potter et al., 1993), CENTURY (Parton et al., 1994) and Biosphere Energy Transfer Hydrology scheme (BETHY) (Knorr, 2000) have been widely used to quantify the response of carbon dynamics to climatic changes (Todd-Brown et al., 2012). An ensemble of process-based model simulations suggests that arctic ecosystems acted as a sink of atmospheric CO_2 in recent decades (McGuire et al., 2012; Schimel et al., 2013). However, the response of this sink to increasing levels of atmospheric CO_2 and climate change is still uncertain (Todd-Brown et al., 2013). The IPCC 5th report also shows that land carbon storage is the largest source of uncertainty in the global carbon budget quantification (Ciais et al., 2013).

Much of the uncertainty is also due to the relatively lower levels of representation of ecosystem processes that determine the exchanges of water, energy and C between land ecosystems and the atmosphere (Wieder et al., 2013), and ignorance of some key biogeochemical

mechanisms (Schmidt et al., 2011). For example, heterotrophic respiration (R_H) is the primary loss pathway for soil organic carbon (Hanson et al., 2000; Bond-Lamberty and Thomson, 2010), and it generally increases with increasing temperature (Davidson and Janssens, 2006) and moisture levels in well-drained soils (Cook and Orchard, 2008). Moreover, this process is closely related to soil nitrogen mineralization that determines soil N availability and affects gross primary production (Hao et al., 2015). To date, most models treated soil decomposition as a first-order decay process, i.e., CO_2 respiration is directly proportional to soil organic carbon. However, it is not clear if these models are robust under changing environmental conditions (Lawrence et al., 2011; Schimel and Weintraub, 2003; Barichivich et al., 2013) since they often ignored the effects of changes in biomass and composition of decomposers, while recent empirical studies have shown that microbial abundance and community play a significant role in soil carbon decomposition (Allison and Martiny, 2008). The control that microbial activity and enzymatic kinetics imposed on soil respiration suggests the need for explicit representation of microbial physiology, enzymatic activity, in addition to the direct effects of soil temperature and soil moisture on heterotrophic respiration (Schimel and Weintraub, 2003). Recent mechanistically-based models explicitly incorporated with the microbial dynamics and enzyme kinetics that catalyze soil C decomposition have produced notably different results and a closer match to contemporary observations (Wieder et al., 2013; Allison et al., 2010) indicating the need for incorporating these microbial mechanisms into large-scale earth system models to quantify carbon dynamics under future climatic conditions ((Wieder et al., 2013; Allison et al., 2010).

This study advanced a microbe-based biogeochemistry model (MIC-TEM) based on an extant Terrestrial Ecosystem Model (TEM) (Raich and Schlesinger, 1992; McGuire et al., 1992; Zhuang et al., 2001, 2002, 2003, 2010, 2013; Hao et al., 2015). In MIC-TEM, the heterotrophic

respiration is not only a function of soil temperature, soil organic matter (SOM) and soil moisture, but also considers the effects of dynamics of microbial biomass and enzyme kinetics (Allison et al., 2010). The verified MIC-TEM was used to quantify the regional carbon dynamics in northern high latitudes (north 45 °N) during the 20th and 21st centuries.

2.3 Methods

2.3.1 Overview

Below we first briefly describe how we advanced the MIC-TEM by modifying the soil respiration process in TEM (Zhuang et al., 2003) to better represent carbon dynamics in terrestrial ecosystems. Second, we describe how we parameterized and verified the new model using observed net ecosystem exchange data at representative sites and how simulated net primary productivity (NPP) was evaluated with Moderate Resolution Imaging Spectroradiometer (MODIS) data to demonstrate the reliability of new model at regional scales. Third, we present how we applied the model to the northern high latitudes for the 20th and 21st centuries. Finally, we introduce how we conducted the sensitivity analysis on initial soil carbon input, using gridded observation-based soil carbon data of three soil depths during the 21st century.

2.3.2 Model description

TEM is a highly aggregated large-scale biogeochemical model that estimates the dynamics of carbon and nitrogen fluxes and pool sizes of plants and soils using spatially-explicit information on climate, elevation, soils and vegetation (McGuire et al., 1992; Zhuang et al., 2003, 2010; Melillo et al., 1993). To explicitly consider the effects of microbial dynamics and enzyme kinetics on large-scale carbon dynamics of northern terrestrial ecosystems, we developed MIC-TEM by

coupling version 5.0 of TEM (Zhuang et al., 2003, 2010) with a microbial-enzyme module (Hao et al., 2015; Allison et al., 2010). Our modification of the TEM improved the representation of the heterotrophic respiration (R_H) from a first-order structure to a more detailed structure (Figure 2.1).

In TEM, heterotrophic respiration R_H is calculated as a function of soil organic carbon (SOC), temperature sensitivity of heterotrophic soil respiration (Q_{10}), soil moisture (f (MOIST)), and the gram-specific decomposition constant K_d:

$$R_H = K_d * SOC * Q_{10}^{\frac{temp}{10}} * f(MOIST) \quad (1)$$

Where temp is soil temperature at top 20 cm (units: ℃). CO_2 production from SOC pool is directly proportional to the pool size, and the activity of decomposers only depends on the built-in relationships with soil temperature and moisture (Todd-Brown et al., 2012). Therefore, the changes in microbial community composition or adaption of microbial physiology to new conditions were not represented in TEM. However, current studies indicate that soil C decomposition depends on the activity of biological communities dominated by microbes (Schimel and Weintraub, 2003), implying that the biomass and composition of the decomposer community can't be ignored (Todd-Brown et al., 2012).

We thus revised the first-order soil C structure in TEM to a second-order structure considering microbial dynamics and enzyme kinetics according to Allison et al. (2010). In MIC-TEM, heterotrophic respiration (R_H) is calculated as:

$$R_H = ASSIM * (1 - CUE) \quad (2)$$

Where ASSIM and CUE represent microbial assimilation and carbon use efficiency, respectively. ASSIM is modeled with a Michaelis-Menten function:

$$ASSIM = Vmax_{uptake} * MIC * \frac{DOC}{Km_{uptake} + DOC} \quad (3)$$

Where DOC is dissolved organic carbon and $Vmax_{uptake}$ is the maximum velocity of the reaction and calculated using the Arrhenius equation:

$$Vmax_{uptake} = Vmax_{uptake_0} * e^{-\frac{Ea_{uptake}}{R*(temp+273)}} \quad (4)$$

Where $Vmax_{uptake_0}$ is the pre-exponential coefficient, Ea_{uptake} is the activation energy for the reaction ($Jmol^{-1}$), R is the gas constant (8.314 $Jmol^{-1}K^{-1}$), and temp is the temperature in Celsius under the reaction occurs. Here we used soil temperature at top 20 cm.

Besides, Km_{uptake} is calculated as a linear function of temperature:

$$Km_{uptake} = Km_{uptake_{slope}} * temp + Km_{uptake_0} \quad (5)$$

Microbial biomass MIC is modeled as:

$$\frac{dMIC}{dt} = ASSIM * CUE - DEATH - EPROD \quad (6)$$

Where microbial biomass death (DEATH) and enzyme production (EPROD) are modeled as proportional to microbial biomass with rate constants r_{death} and $r_{EnzProd}$:

$$DEATH = r_{death} * MIC \quad (7)$$

$$EPROD = r_{EnzProd} * MIC \quad (8)$$

Where r_{death} and $r_{EnzProd}$ are the rate constants of microbial death and enzyme production, respectively.

DOC is part of soil organic carbon:

$$\frac{dDOC}{dt} = DEATH * (1 - MICtoSOC) + DECAY + ELOSS - ASSIM \quad (9)$$

Where MICtoSOC is carbon input ratio as dead microbial biomass to SOC, representing the fraction of microbial death that flows into SOC, and is set as a constant value according to Allison et al. (2010). SOC dynamics are modeled:

$$\frac{dSOC}{dt} = Litterfall + DEATH * MICtoSOC - DECAY \quad (10)$$

Where Litterfall is estimated as a function of vegetation carbon (Zhuang et al., 2010). The enzymatic decay of SOC is calculated as:

$$\mathrm{DECAY} = \mathrm{V_{max}} * \mathrm{ENZ} * \frac{\mathrm{SOC}}{Km+\mathrm{SOC}} \quad (11)$$

Where V_{max} is the maximum velocity of the reaction and calculated using the Arrhenius equation:

$$V_{max} = \mathrm{Vmax_0} * \mathrm{e}^{-\frac{Ea}{\mathrm{R}*(\mathrm{temp}+273)}} \quad (12)$$

The parameters Km and carbon use efficiency (CUE) are temperature sensitive, and calculated as a linear function of temperature between 0 and 50°C:

$$Km = \mathrm{Km}_{slope} * \mathrm{temp} + \mathrm{Km_0} \quad (13)$$

$$\mathrm{CUE} = \mathrm{CUE_{slope}} * \mathrm{temp} + \mathrm{CUE_0} \quad (14)$$

Where CUEslope and CUE_0 are parameters for calculating CUE, and Km_{slope} and Km_0 are parameters for calculating Km. The values of $\mathrm{CUE_{slope}}$, $\mathrm{CUE_0}$, Km_{slope}, and Km_0 were derived from Allison et al. (2010).

ELOSS is also a first-order process, representing the loss of enzyme:

$$\mathrm{ELOSS} = \mathrm{r_{enzloss}} * \mathrm{ENZ} \quad (15)$$

Where $r_{enzloss}$ is the rate constant of enzyme loss. Enzyme pool (ENZ) is modeled:

$$\frac{\mathrm{dENZ}}{\mathrm{dt}} = \mathrm{EPROD} - \mathrm{ELOSS} \quad (16)$$

Heterotrophic respiration (R_H) is an indispensable component of soil respiration (Bond-Lamberty and Thomson, 2010), and closely coupled with soil nitrogen (N) mineralization that determines soil N availability, affecting gross primary production (GPP).

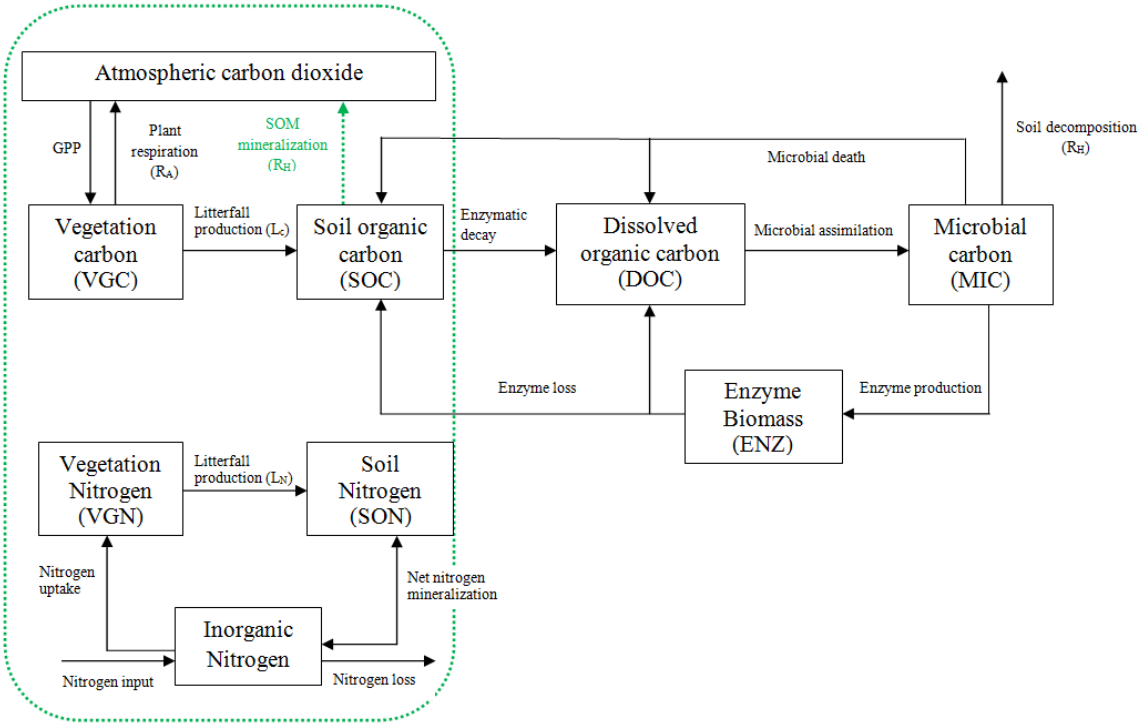

Figure 2.1. Schematic diagram of MIC-TEM. The green dashed circle is the previous structure used in TEM 5.0 (Zhuang et al., 2003), without considering the effects of detailed microbial dynamics. The previous heterotrophic respiration is proportional to SOC (green dashed arrow). In MIC-TEM, new heterotrophic respiration considers the effects of microbial dynamics and enzyme kinetics. In addition, three new carbon pools (DOC, MIC, and ENZ) and five carbon fluxes (decomposition of SOC, microbial assimilation and death, enzyme production and loss) are considered (Allison et al., 2010).

2.3.3 Model parameterization and validation

The variables and parameters of these microbial dynamics and their impacts on soil C decomposition were detailed in Allison et al. (2010) (Table 2.1). Here we parameterized MIC-TEM for representative ecosystem types in northern high latitudes based on monthly net ecosystem production (NEP, gCm^{-2} mon^{-1}) measurements from AmeriFlux network (Davidson et al., 2000) (Table 2.2). The results for model parameterization were presented in Figure 2.2. Another set of level 4 gap-filled NEP data was used for model validation at site level (Table 2.3). The site-level monthly climate data of air temperature (°C), precipitation (mm) and cloudiness (%) were used to drive the model. Gridded MODIS NPP data from 2001 to 2010 were used to evaluate regional NPP simulations. The MODIS NPP data was developed by the MOD17 MODIS project. The product name is Net Primary Production Yearly L4 Global 1 km. The critical parameter used in MOD17 algorithm is conversion efficiency parameter Ɛ. More information about the MODIS NPP product can be found at https://neo.sci.gsfc.nasa.gov/view.php?datasetId=MOD17A2_M_PSN.

In TEM, NPP is calculated as:

$$NPP = GPP - R_A \quad (17)$$

Where GPP is gross primary production, and R_A is autotrophic respiration. GPP is defined as:

$$GPP = C_{max} * f(PAR) * f(phenology) * f(foliage) * f(T) * f(CO_2) * f(NA) * f(FT) \quad (18)$$

Where C_{max} is the maximum rate of carbon assimilation, PAR is photosynthetically active radiation, and f(phenology) represents the effects of leaf area (Raich and Schlesinger, 1992). The function f(foliage) represents the ratio of canopy leaf biomass relative to maximum leaf biomass (Zhuang et al., 2002). T is monthly air temperature, and $f(CO_2)$ represents the effects of elevated atmospheric CO_2 (McGuire et al., 1997; Pan et al.,1998). The function f(NA) models the limiting effects of plant nitrogen status on GPP (McGuire et al., 1992; Pan et al., 1998). The function f (FT)

represents the effects of freeze-thaw (Zhuang et al., 2003). For detailed GPP and R_A calculations, see Zhuang et al. (2003).

The parameterization was conducted with a global optimization algorithm SCE-UA (Shuffled complex evolution) (Duan et al., 1994) to minimize the difference between the monthly simulated and measured NEE at these sites (Fig. S2). The cost function of the minimization is:

$$\mathrm{Obj} = \sum_{i=1}^{k}(\mathrm{NEP}_{obs,i} - \mathrm{NEP}_{sim,i})^2 \quad (19)$$

Where $\mathrm{NEP}_{obs,i}$ and $\mathrm{NEP}_{sim,i}$ are the observed and simulated NEP, respectively. k is the number of data pairs for comparison. Other parameters used in MIC-TEM were default values from TEM 5.0 (Zhuang et al., 2003, 2010). The optimized parameters were used for model validation and regional extrapolations.

Table 2.1. Parameters associated with more detailed microbial dynamics in MIC-TEM.

Process	Parameter	Units	Initial Value	Description	Parameter range	Reference
Assimilation	$Vmax_{uptake_0}$	mg DOC cm^{-3} (mg biomass cm^{-3})$^{-1}$ h^{-1}	9.97e6	Maximum microbial uptake rate	[1.0e4, 1.0e8]	Hao et al. (2015)
	Ea_{uptake}	kJ mol^{-1}	47	Activation energy	-	Allison et al. (2010)
	$Km_{uptake_{slope}}$	mg cm^{-3} degree^{-1}	0.01	Temperature regulator of MM for DOC uptake by microbes	-	Allison et al. (2010)
	Km_{uptake_0}	mg cm^{-3}	0.1	Temperature regulator of MM for DOC uptake by microbes	-	Allison et al. (2010)
CO_2 production	CUE_{slope}	degree^{-1}	-0.016	Temperature regulator of carbon use efficiency	-	Allison et al. (2010)
	CUE_0	-	0.63	Temperature regulator of carbon use efficiency	-	Allison et al. (2010)
Decay	$Vmax_0$	mg SOC cm^{-3} (mg Enz cm^{-3})$^{-1}$ h^{-1}	9.17e7	Maximum rate of converting SOC to soluble C	[1.0e5, 1.0e8]	Hao et al. (2015)
	Ea	kJ mol^{-1}	47	Activation energy	-	Allison et al. (2010)
	Km_{slope}	mg cm^{-3} degree^{-1}	5	Temperature regulator of MM for enzymatic decay	-	Allison et al. (2010)
	Km_0	mg cm^{-3}	500	Temperature regulator of MM for enzymatic decay	-	Allison et al. (2010)
MIC turnover	r_{death}	s^{-1}	0.02	Microbial death fraction	-	Allison et al. (2010)
	MICtoSOC		50	Partition coefficient for dead microbial biomass between the SOC and DOC pool	-	Allison et al. (2010)
ENZ turnover	$r_{EnzProd}$	s^{-1}	5.0e-4	Enzyme production fraction	-	Allison et al. (2010)
	$r_{EnzLoss}$	s^{-1}	0.1	Enzyme loss fraction	-	Allison et al. (2010)

Table 2.2. Site description and measured data used to calibrate MIC-TEM.

Site Name	Location (Longitude (degrees) /Latitude (degrees))	Elevation (m)	Vegetation type	Description	Data range	Citations
Univ. of Mich. Biological Station	84.71W 45.56 N	234	Temperate deciduous forest	Located within a protected forest owned by the University of Michigan. Mean annual temperature is 5.83˚C with mean annual precipitation of 803mm	01/2005-12/2006	Gough et al. (2013)
Howland Forest (main tower)	68.74W 45.20N	60	Temperate coniferous forest	Closed coniferous forest, minimal disturbance.	01/2004-12/2004	Davidson et al. (2006)
UCI-1964 burn site	98.38W 55.91N	260	Boreal forest	Located in a continental boreal forest, dominated by black spruce trees, within the BOREAS northern study area in central Manitoba, Canada.	01/2004-10/2005	Goulden et al. (2006)
KUOM Turfgrass Field	93.19W 45.0N	301	Grassland	A low-maintenance lawn consisting of cool-season turfgrasses.	01/2006-12/2008	Hiller et al. (2011)
Atqasuk	157.41W 70.47N	15	Wet tundra	100 km south of Barrow, Alaska. Variety of moist-wet coastal sedge tundra, and moist-tussock tundra surfaces in the more well-drained upland.	01/2005-12/2006	Oechel et al. (2014)
Ivotuk	155.75W 68.49N	568	Alpine tundra	300 km south of Barrow and is located at the foothill of the Brooks Range and is classified as tussock sedge, dwarf-shrub, moss tundra.	01/2004-12/2004	McEwing et al. (2015)

Table 2.3. Site description and measured data used to validate MIC-TEM

Site Name	Location (Longitude (degrees) /Latitude (degrees))	Elevation (m)	Vegetation type	Description	Data range	Citations
Bartlett Experimental Forest	71.29W/ 44.06N	272	Temperate deciduous forest	Located within the White Mountains National Forest in north-central New Hampshire, USA, with mean annual temperature of 5.61 °C and mean annual precipitation of 1246mm.	01/2005-12/2006	Jenkins et al. (2007); Richardson et al. (2007)
Howland Forest (main tower)	68.74W/ 45.20N	60	Temperate coniferous forest	Closed coniferous forest, minimal disturbance.	01/2003-12/2003	Davidson et al. (2006)
UCI-1964 burn site	98.38W/ 55.91N	260	Boreal forest	Located in a continental boreal forest, dominated by black spruce trees, within the BOREAS northern study area in central Manitoba, Canada.	01/2002-12/2003	Goulden et al. (2006)
Brookings	96.84W/ 44.35N	510	Grassland	Located in a private pasture, belonging to the Northern Great Plains Rangelands, the grassland is representative of many in the north central United States, with seasonal winter conditions and a wet growing season.	01/2005-12/2006	Gilmanov et al. (2005)
Atqasuk	157.41W/ 70.47N	15	Wet tundra	100 km south of Barrow, Alaska. Variety of moist-wet coastal sedge tundra, and moist-tussock tundra surfaces in the more well-drained upland.	01/2003-12/2004	Oechel et al. (2014)
Ivotuk	155.75W/ 68.49N	568	Alpine tundra	300 km south of Barrow and is located at the foothill of the Brooks Range and is classified as tussock sedge, dwarf-shrub, moss tundra.	01/2005-12/2005	McEwing et al. (2015)

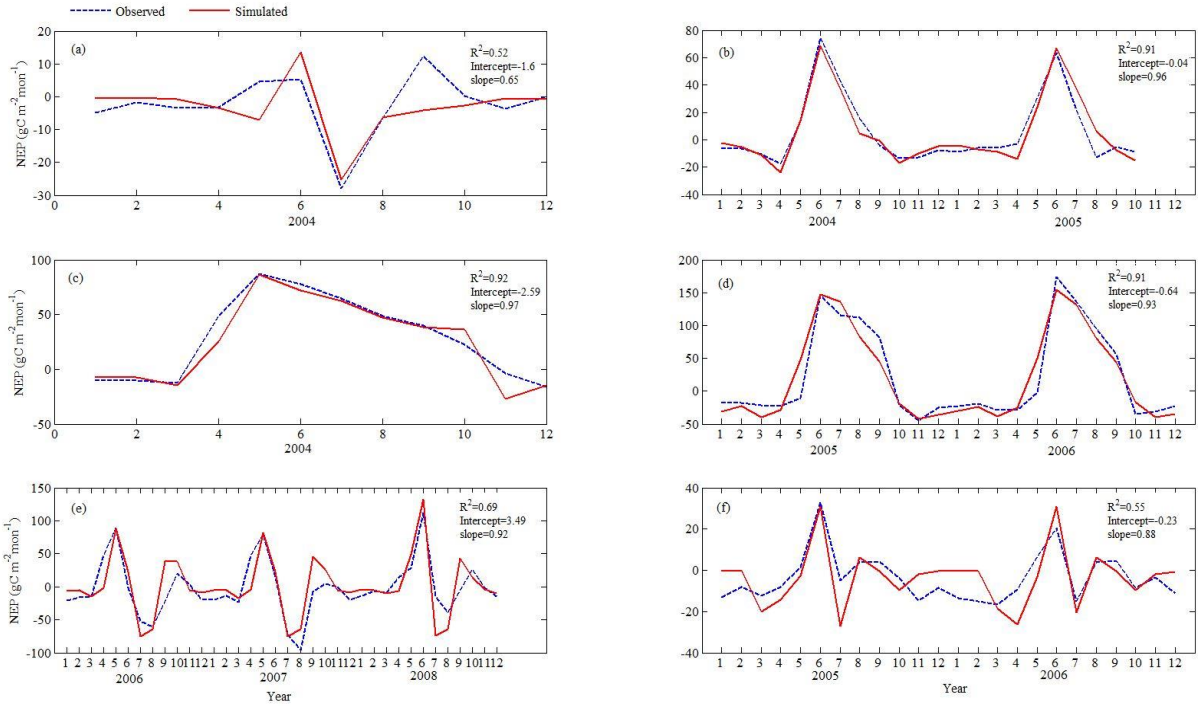

Figure 2.2. Comparison between observed and simulated NEP (gC $m^{-2}mon^{-1}$) at: (a) Ivotuk (alpine tundra), (b) UCI-1964 burn site (boreal forest), (c) Howland Forest (main tower) (temperate coniferous forest), (d) Univ. of Mich. Biological Station (Temperate deciduous forest), (e) KUOM Turfgrass Field (Grassland), and (f) Atqasuk (Wet tundra). Note: scales are different.

2.3.4 Regional simulations

Two sets of regional simulations for the 20th century using MIC-TEM and TEM at a spatial resolutions of 0.5° latitude × 0.5° longitude were conducted. Gridded forcing data of monthly air temperature, precipitation, and cloudiness were used, along with other ancillary inputs including historical atmospheric CO_2 concentrations, soil texture, elevation, and potential natural vegetation. Climatic inputs vary over time and space, whereas soil texture, elevation, and land cover data are assumed to remain unchanged throughout the 20th century, which only vary spatially. The transient climate data during the 20th century was organized from the Climatic Research Unit (CRU TS3.1) from the University of East Anglia (Harris et al., 2014). The spatially-explicit data include potential natural vegetation (Melillo et al., 1993), soil texture (Zhuang et al., 2003) and elevation (Zhuang et al., 2015).

Similarly, two sets of simulations were conducted driven with two contrasting climate change scenarios (RCP 2.6 and RCP 8.5) over the 21st century. The future climate change scenarios were derived from the HadGEM2-ES model, which is a member of CMIP5 project (https://esgf-node.llnl.gov/search/cmip5/). The future atmospheric CO_2 concentrations and climate forcing from each of the two climate change scenarios were used. The simulated NPP, R_H and NEP by both models (TEM 5.0 and MIC-TEM) were analyzed. The positive NEP represents a CO_2 sink from the atmosphere to terrestrial ecosystems, while a negative value represents a source of CO_2 from terrestrial ecosystems to the atmosphere.

Besides, in order to test the parameter uncertainty in our model, we conducted the regional simulations with 50 sets of parameters for both historical and future studies. The 50 sets of parameters were obtained according to the method in Tang and Zhuang (2008). The upper and lower bounds of the regional estimations were generated based on these simulations.

2.3.5 Sensitivity to initial soil carbon input

Future carbon dynamics can be affected by varying initial soil carbon amount. In the standard simulation of TEM, the initial soil carbon amount for transient simulations was obtained from equilibrium and spin-up periods directly for each grid cell in the region. To test the sensitivity to the initial soil carbon amount in transient simulations for the 21st century, we used empirical soil organic carbon data extracted from the Northern Circumpolar Soil Carbon Database (NCSCD) (Tarnocai et al., 2009), as the initial soil carbon amount. The 0.5° × 0.5° soil carbon data products for three different depths of 30cm, 100cm and 300cm were used. The sensitivity test was conducted for transient simulations under the RCP 2.6 and RCP 8.5 scenarios. To avoid the instability of C-N ratio caused by replacing the initial soil carbon pool with observed data at the beginning of transient period, initial soil nitrogen values were also generated based on the soil carbon data and corresponding C-N ratio map for transient simulations (Zhuang et al., 2003; Raich and Schlesinger, 1992).

2.4 Results

2.4.1 Model verification at site and regional levels

With the optimized parameters, MIC-TEM reproduces the carbon dynamics well for alpine tundra, boreal forest, temperate coniferous forest, temperate deciduous forest, grasslands and wet tundra with R^2 ranging from 0.70 for Ivotuk to 0.94 for Bartlett Experimental Forest (Figure 2.3, Table 2.4). In general, model performs better for forest ecosystems than for tundra ecosystems. The temporal NPP from 2001 to 2010 simulated by MIC-TEM and TEM were compared with MODIS NPP data (Figure 2.4). Pearson correlation coefficients are 0.84 (MIC-TEM and MODIS) and 0.66 (TEM and MODIS). NPP simulated by MIC-TEM showed higher spatial correlation

coefficients with MODIS data than TEM (Figure 2.5). By considering more detailed microbial activities, the heterotrophic respiration is more adequately simulated using the MIC-TEM. The simulated differences in soil decomposition result in different levels of soil available nitrogen, which influences the nitrogen uptake by plants, the rate of photosynthesis and NPP. The spatial correlation coefficient between NPP simulated by MIC-TEM and MODIS is close to 1 in most study areas, suggesting the reliability of MIC-TEM at the regional scale.

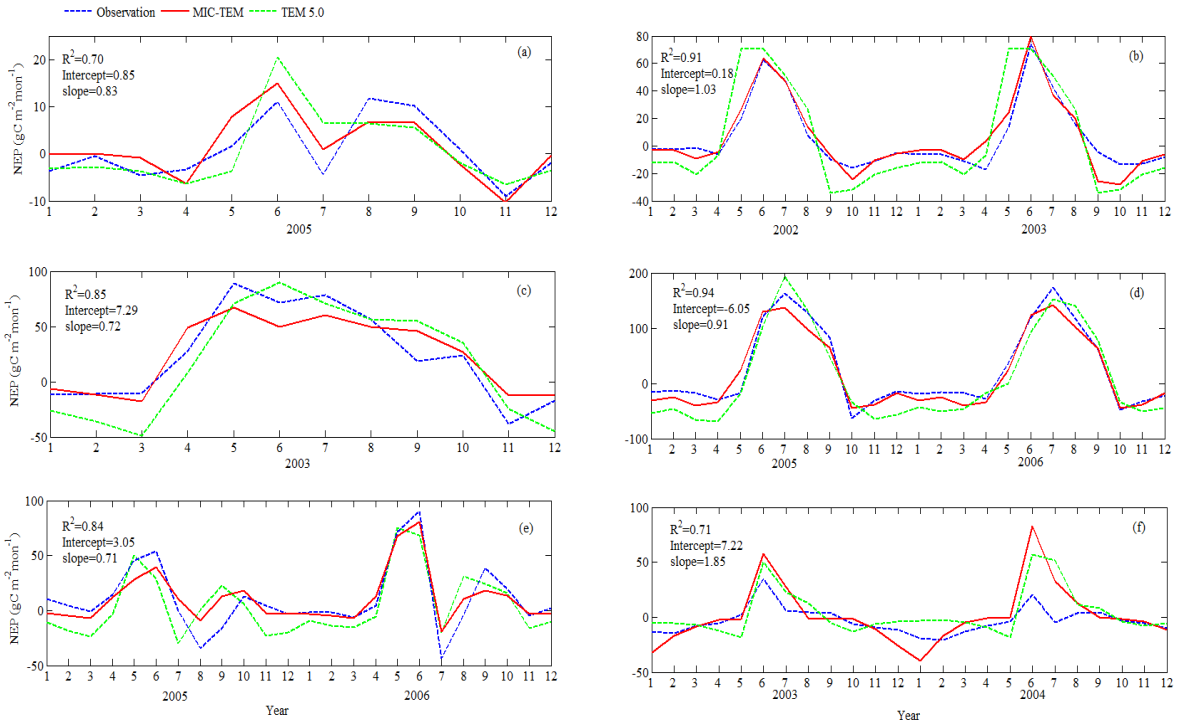

Figure 2.3. Comparison between observed and simulated NEP (gC m-2mon^{-1}) at: (a) Ivotuk (alpine tundra), (b) UCI-1964 burn site (boreal forest), (c) Howland Forest (main tower) (temperate coniferous forest), (d) Bartlett Experimental Forest (Temperate deciduous forest), (e) Brookings (Grassland), and (f) Atqasuk (Wet tundra). Note: scales are different.

Table 2.4. Comparison statistics between MIC-TEM and TEM in model validation

Site Name	Vegetation type	Model	Intercept (gC m^{-2} mon^{-1})	Slope	R-square	Adjusted R-square	p-value
Ivotuk	Alpine tundra	MIC-TEM	0.85	0.83	0.70	0.67	<0.001
		TEM 5.0	0.04	0.85	0.54	0.5	0.006
UCI-1964 burn site	Boreal forest	MIC-TEM	0.18	1.03	0.912	0.9080	<0.001
		TEM 5.0	-2.8	1.29	0.746	0.735	<0.001
Howland Forest (main tower)	Temperate coniferous forest	MIC-TEM	7.29	0.72	0.85	0.83	<0.001
		TEM 5.0	-8.18	1.1	0.82	0.804	<0.001
Bartlett Experimental Forest	Temperate deciduous forest	MIC-TEM	-6.05	0.91	0.944	0.941	<0.001
		TEM 5.0	-13.6	1.03	0.84	0.83	<0.001
Brookings	Grassland	MIC-TEM	3.05	0.71	0.84	0.83	<0.001
		TEM 5.0	-3.63	0.74	0.6	0.58	<0.001
Atqasuk	Wet tundra	MIC-TEM	7.22	1.85	0.71	0.70	<0.001
		TEM 5.0	6.64	1.15	0.42	0.39	<0.001

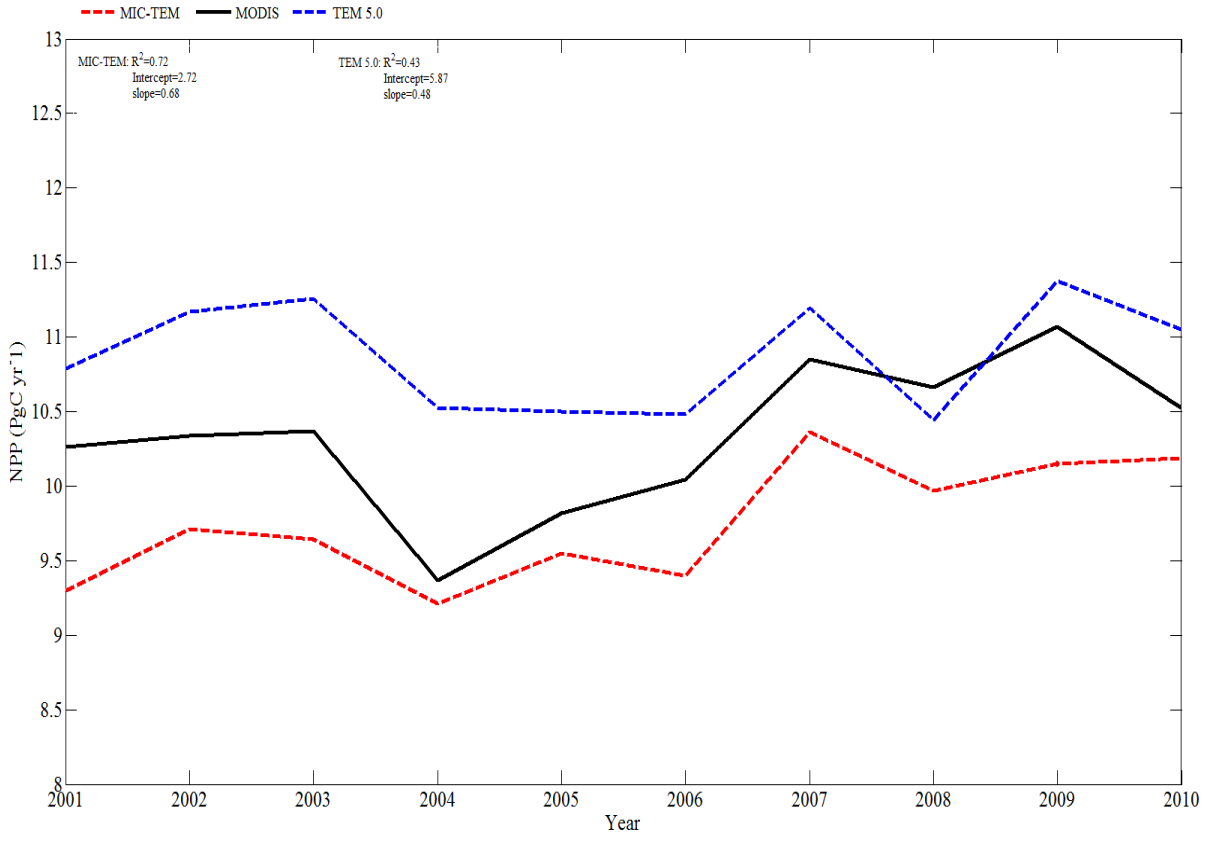

Figure 2.4. Comparison between regional NPP (PgC yr^{-1} simulated by MIC-TEM (red dashed line), TEM 5.0 (blue dashed line), and MODIS data (black solid line).

(a)

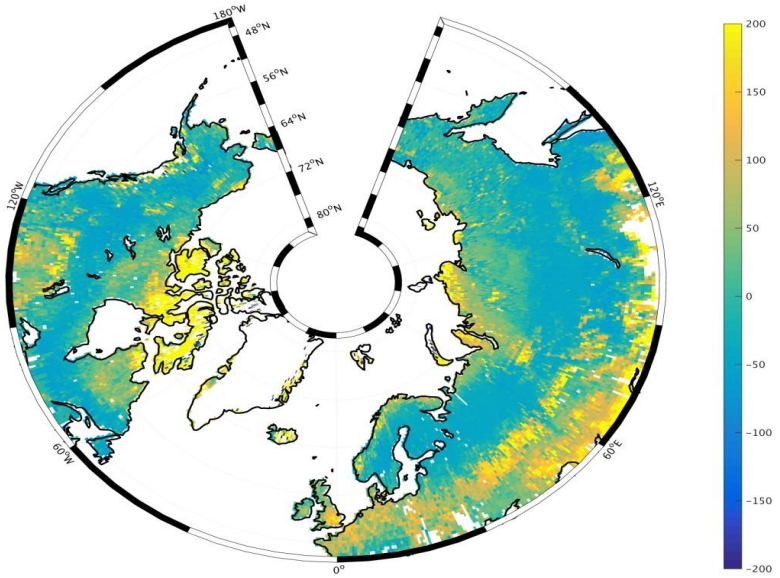

(b)

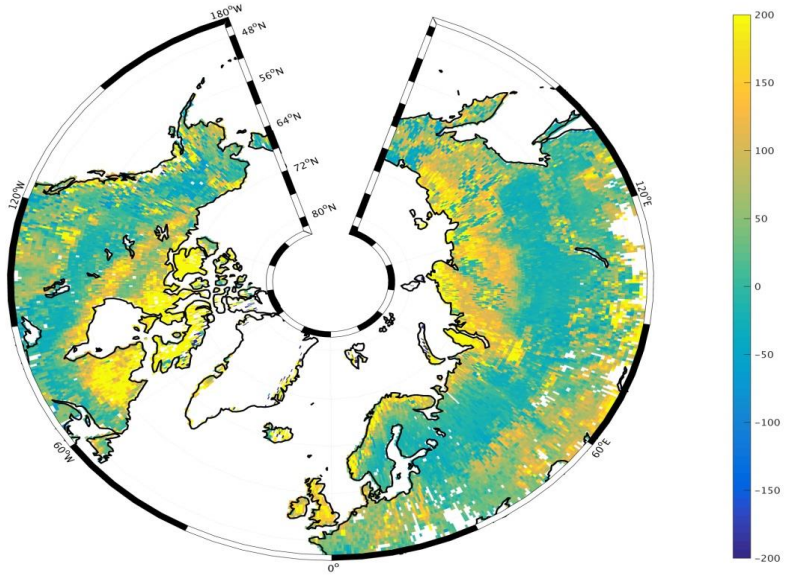

Figure 2.5. Comparisons between MODIS NPP as baseline and simulated NPP: (a) (MIC-TEM-MODIS)/ MODIS*100% (b) (TEM 5.0-MODIS)/ MODIS*100%. Positive values are overestimates and negative values are underestimates.

2.4.2 Regional carbon dynamics during the 20th century

The equifinality of the parameters in MIC-TEM was considered in our ensemble regional simulations to measure the parameter uncertainty (Tang and Zhuang, 2008). Here and below, the ensemble means and the inter-simulation standard deviations are shown for uncertainty measure, unless specified as others. These ensemble simulations indicated that the northern high latitudes act from a carbon source of 38.9 Pg C to a carbon sink of 190.8 Pg C by different ensemble members, with the mean of 64.2±21.4 Pg at the end of 20th century while the simulation with the optimized parameters estimates a regional carbon sink of 77.6 Pg with the interannual standard deviation of 0.21 Pg C yr^{-1} during the 20th century (Figure 2.6). Simulated regional NEP with optimized parameters using TEM and MIC-TEM showed an increasing trend throughout the 20th century except a slight decrease during the 1960s (Figure 2.7). The Spatial distributions of NEP simulated by MIC-TEM for different periods in the 20th century also show the increasing trend (Figure 2.8). Positive values of NEP represent sinks of CO_2 into terrestrial ecosystems, while negative values represent sources of CO_2 to the atmosphere. From 1900 onwards, both models estimated a regional carbon sink during the 20th century. With optimized parameters, TEM estimated higher NPP and R_H at 0.6 PgC yr^{-1} and 0.3 PgC yr^{-1} than MIC-TEM, respectively, at the end of the 20th century (Figure 2.7). The MIC-TEM estimated a carbon sink increase from 0.64 to 0.83 $PgCyr^{-1}$ during the century while the estimated increase by TEM was much higher (0.28 $PgCyr^{-1}$) (Figure 2.7). At the end of the century, MIC-TEM estimated NEP reached 1.0 $PgCyr^{-1}$ in comparison with TEM estimates of 0.3 $PgCyr^{-1}$. TEM estimated NPP and R_H are 0.5 Pg Cy r^{-1} and 0.3 Pg C yr^{-1} higher, respectively. As a result, TEM estimated that the region accumulated 11.4 Pg more carbon than MIC-TEM. Boreal forests are a major carbon sink at 0.55 and 0.63 Pg C yr^{-1} estimated by MIC-TEM and TEM, respectively. Alpine tundra contributes the least sink. Overall,

TEM overestimated the sink by 12.5% in comparison to MIC-TEM for forest ecosystems and 16.7% for grasslands. For wet tundra and alpine tundra, TEM overestimated about 20% and 33% in comparison with MIC-TEM, respectively (Table 2.5).

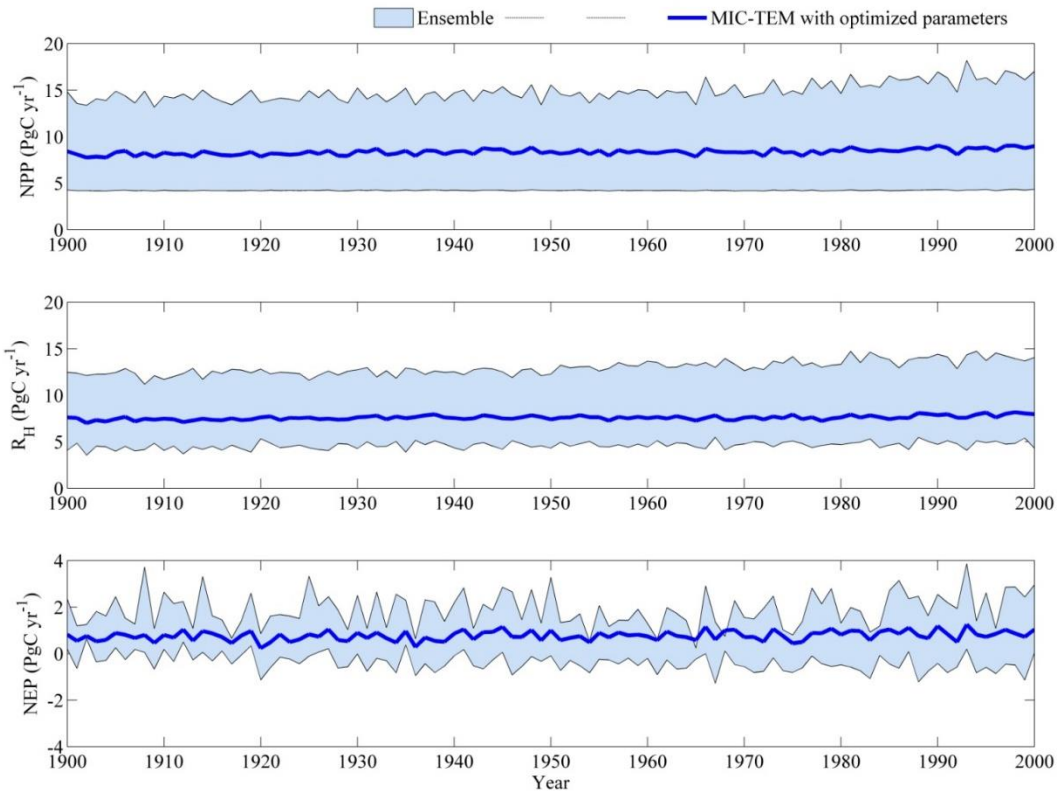

Figure 2.6. Simulated annual net primary production (NPP, top panel), heterotrophic respiration (R_H, center panel) and net ecosystem production (NEP, bottom panel) by MIC-TEM with ensemble of parameters.

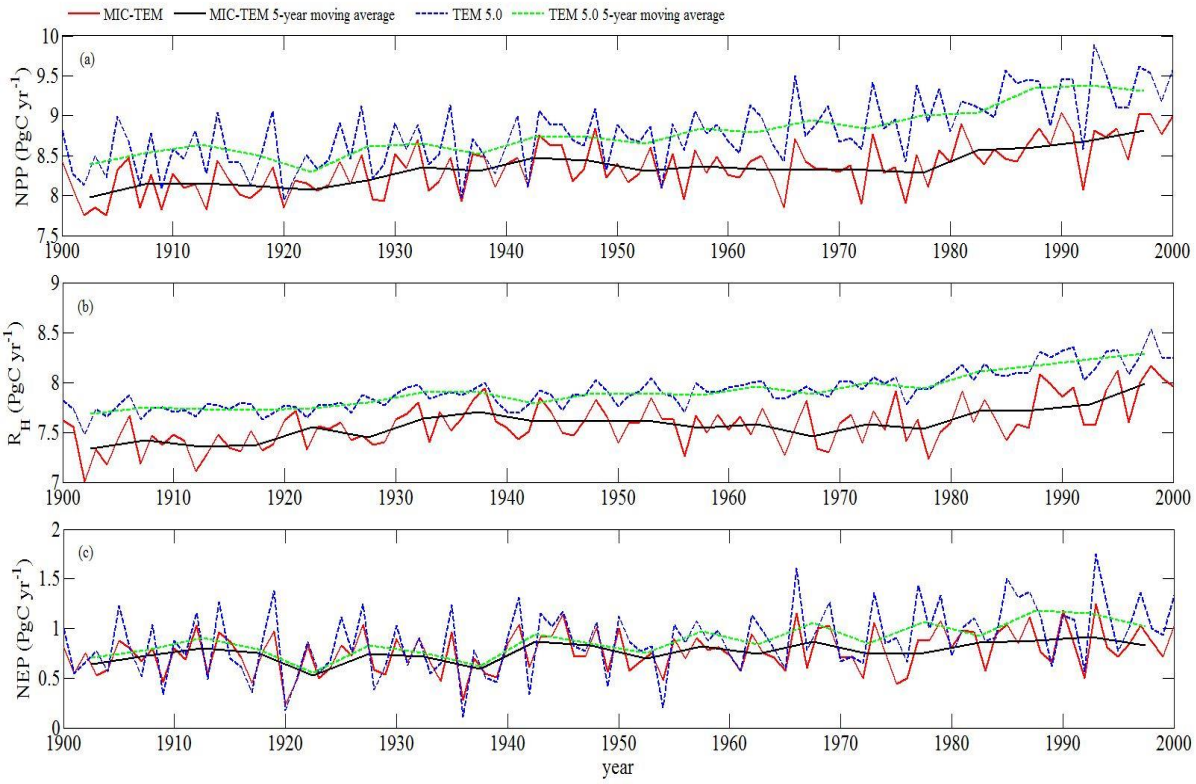

Figure 2.7. Simulated annual net primary production (NPP, top panel), heterotrophic respiration (R_H, center panel) and net ecosystem production (NEP, bottom panel) by MIC-TEM and TEM, respectively.

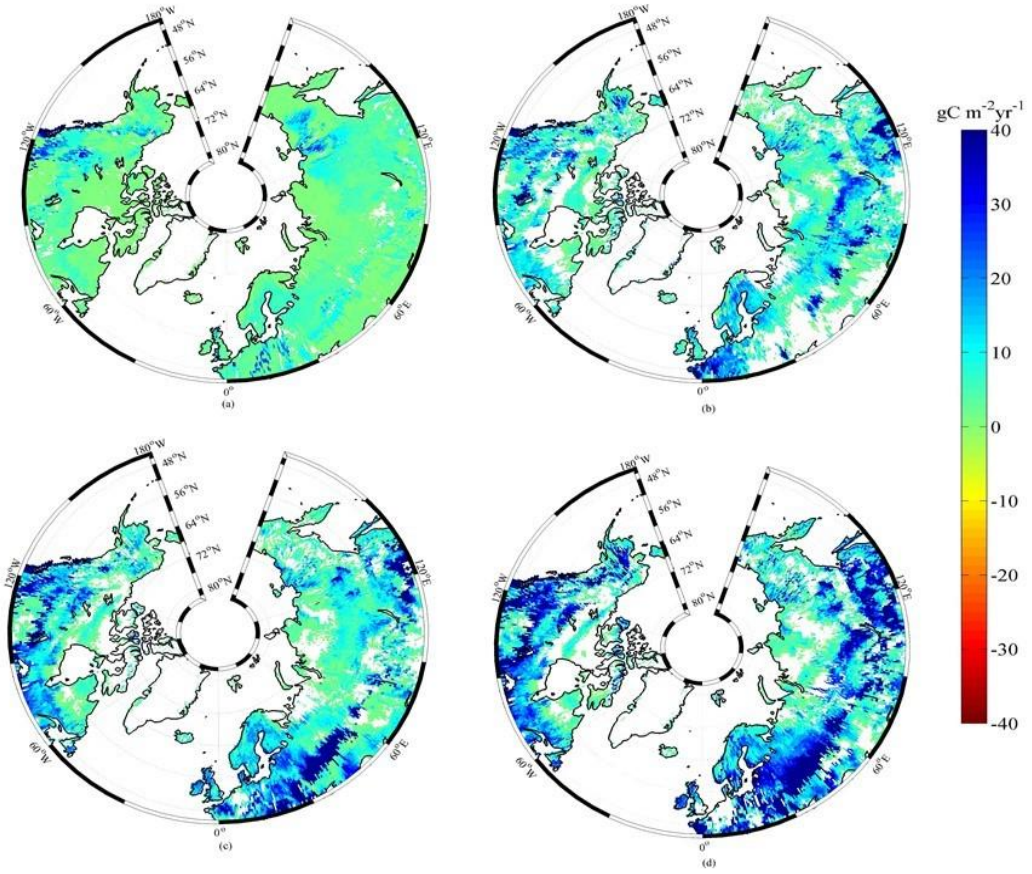

Figure 2.8. Spatial distribution of NEP simulated by MIC-TEM for the periods: (a) 1900-1930, (b) 1931-1960, (c) 1961-1990, and (d) 1991-2000. Positive values of NEP represent sinks of CO_2 into terrestrial ecosystems, while negative values represent sources of CO_2 to the atmosphere.

Table 2.5. Partitioning of average annual net ecosystem production (as Pg C per year) for six vegetation types during the 20th century

	MIC-TEM (PgC yr^{-1})	TEM 5.0 (PgC y^{-1})
Alpine tundra	0.03	0.04
Boreal forest	0.39	0.45
Conifer forest	0.09	0.09
Deciduous forest	0.16	0.18
Grassland	0.06	0.07
Wet tundra	0.05	0.06
Total	0.78	0.89

2.4.3 Regional carbon dynamics during the 21st century

Simulated regional annual NPP and R_H increases under the RCP 8.5 scenario with both models (Figure 2.9). With optimized parameters, MIC-TEM estimated NPP increases from 9.2 in the 2000s to 13.2 PgCyr^{-1} in the 2090s, while TEM-predicted NPP is 2.0 Pg C yr^{-1} higher in the 2000s and 0.3 Pg C yr^{-1} higher in the 2090s (Figure 2.9). Similarly, TEM also overestimated R_H by 1.7 Pg C yr^{-1} in the 2000s and 0.25 Pg C yr^{-1} higher in the 2090s, respectively (Figure 2.9). As a result, the regional sink increases from 0.53 Pg C yr^{-1} in the 2000s, 1.4 Pg C yr^{-1} in the 2070s, then decreases to 1.1 Pg C yr^{-1} in the 2090s estimated by MIC-TEM (Figure 2.9). Given the uncertainty in parameters, MIC-TEM predicted the region acts as a carbon sink ranging from 48.7 to 140.7 Pg, with the mean of 71.7±26.6 Pg at the end of 21st century, while the simulation with optimized parameters estimates a regional carbon source of 79.5 Pg with the interannual standard deviation of 0.37 Pg C yr^{-1} during the 21st century (Figure 2.9). TEM predicted a similar trend for NEP, which overestimated the carbon sink with magnitude of 19.2 Pg compared with the simulation by MIC-TEM with optimized parameters. Under the RCP 2.6 scenario (Figure 2.9), the increase of NPP and R_H is smaller from 2000 to 2100 compared to the simulation under the RCP 8.5. MIC-TEM predicted that NPP increases from 9.1 to 10.9 Pg C yr^{-1}, TEM estimated 1.6 Pg C yr^{-1} higher at the beginning and 0.9 Pg C yr^{-1} higher in the end of the 21st century (Figure 2.9). Consequently, MIC-TEM predicted NEP fluctuates between sinks and sources during the century, with a neutral before 2070, and a source between -0.2 - -0.3 Pg C yr^{-1} after the 2070s. As a result, the region acts as a carbon source of 1.6 Pg C with the interannual standard deviation of 0.24 Pg C yr^{-1} estimated with MIC-TEM and a sink of 27.6 Pg C with the interannual standard deviation of 0.2 Pg C yr^{-1} estimated with TEM during the century (Figure 2.9). When considering the uncertainty source of parameters, MIC-TEM predicted the region acts from a carbon source of

64.8 Pg C to a carbon sink of 58.6 Pg C during the century with the mean of -3.3±20.3 Pg at the end of 21st century (Figure 2.9).

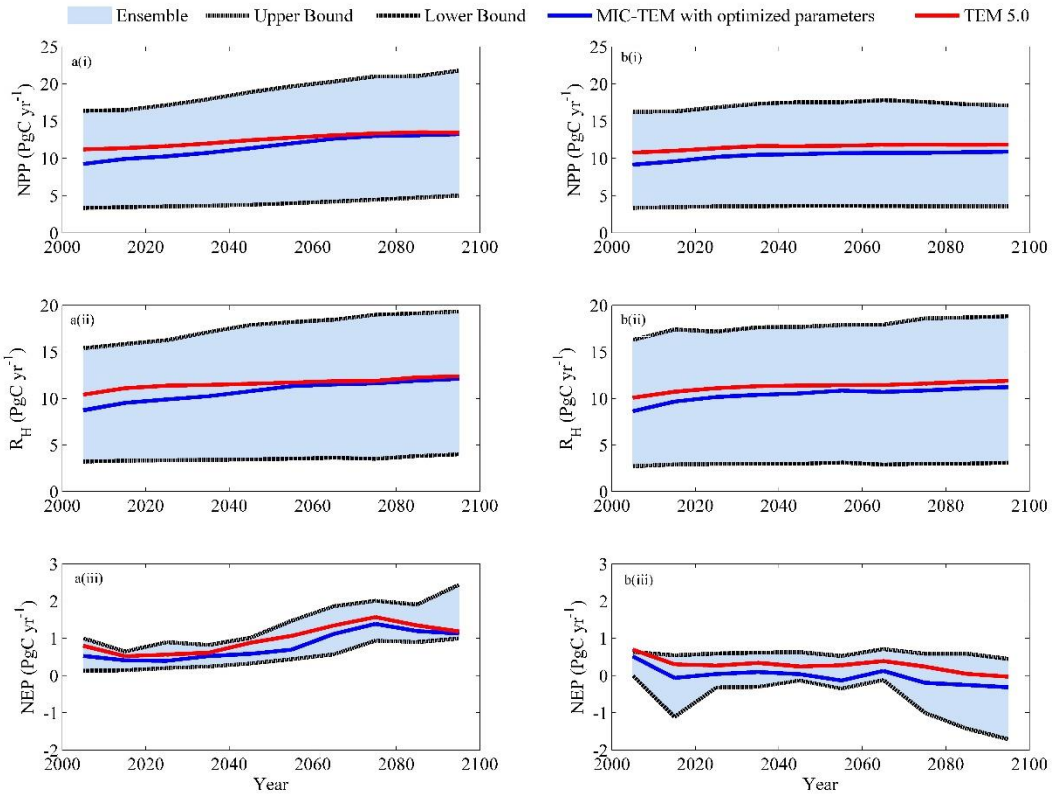

Figure 2.9. Predicted changes in carbon fluxes: (i) NPP, (ii) R_H, and (iii) NEP for all land areas north of 45 °N in response to transient climate change under (a) RCP 8.5 scenario and (b) RCP 2.6 scenario with MIC-TEM and TEM 5.0, respectively. The decadal running mean is applied. The grey area represents the upper and lower bounds of simulations.

2.4.4 Model sensitivity to initial soil carbon

Under the RCP 2.6, without replacing the initial soil carbon with inventory-based estimates (Tarnocai et al., 2009) in model simulations, TEM estimated that the regional soil organic carbon (SOC) is 604.2 Pg C and accumulates 12.1 Pg C during the 21st century. When using estimated soil carbon (Tarnocai et al., 2009), within depths of 30cm, 100cm and 300cm as initial pools in simulations, TEM predicted that regional SOC is 429.5, 689.3 and 1003.4 Pg C in 2000, and increases by 9.9, 16.0 and 22.8 Pg C at the end of the 21st century, and the regional cumulative carbon sink is 20.4, 34.0, and 48.1 Pg C, respectively during the century. In contrast, using the same inventory-based SOC estimates, MIC-TEM projected that the region acts from a cumulative carbon sink to a source at 0.7, 2.2, and 3.0 Pg C, respectively. Under the RCP 8.5, both models predicted that the region acts as a carbon sink, regardless of the magnitudes of initial soil carbon pools used, with TEM projected sink of 71.7, 120, and 155.6 Pg C and a much smaller cumulative sink of 65.4, 88.6, and 109.8 Pg C estimated with MIC-TEM, respectively (Table 2.6).

Table 2.6. Increasing of SOC, vegetation carbon (VGC), soil organic nitrogen (SON), vegetation nitrogen (VGN) from 1900 to 2000, and total carbon storage during the 21st century predicted by two models with observed soil carbon data of three different depths under (a) RCP 2.6 and (b) RCP 8.5.

(a)

Model	Units: Pg	Without (control)	30cm	100cm	300cm
TEM 5.0	SOC/SON in 2000	604.2/27.0	429.5/19.0	689.3/31.6	1003.4/46.2
	Increase of SOC during the 21st century	12.1	9.9	16.0	22.8
	VGC/VGN in 2000	318.3/1.48	238.4/1.05	394.2/1.80	556.7/2.53
	Increase of VGC during the 21st century	15.5	10.5	18.0	25.3
	Increase of total carbon storage during the 21st century	27.6	20.4	34.0	48.1
MIC-TEM	SOC/SON in 2000	591.5/26.8	420.3/18.6	686.0/31.2	990.7/45.3
	Increase of SOC during the 21st century	-2.0	-1.2	-2.4	-2.9
	VGC/VGN in 2000	309.7/1.42	230.1/1.02	374.4/1.71	548.6/2.45
	Increase of VGC during the 21st century	0.4	0.5	0.2	-0.1
	Increase of total carbon storage during the 21st century	-1.6	-0.7	-2.2	-3.0

(b)

Model	Units: Pg	Without (control)	30cm	100cm	300cm
TEM 5.0	SOC/SON in 2000	610.2 /27.9	431.9/19.1	693.8/31.8	1007.1/46.4
	Increase of SOC during the 21st century	44.2	33.0	56.5	74.6
	VGC/VGN in 2000	324.9/1.50	242.1/1.07	399.6/1.83	570.2/2.57
	Increase of VGC during the 21st century	54.5	38.7	63.5	81.0
	Increase of total carbon storage during the 21st century	98.7	71.7	120.0	155.6
MIC-TEM	SOC/SON in 2000	596.0/27.1	424.6/18.8	689.1/31.5	995.5/46.1
	Increase of SOC during the 21st century	33.3	27.4	36.9	42.9
	VGC/VGN in 2000	316.0/1.44	233.5/1.02	380.0/1.72	568.3/2.56
	Increase of VGC during the 21st century	46.2	37.0	51.7	56.9
	Increase of total carbon storage during the 21st century	79.5	65.4	88.6	109.8

2.5. Discussion

During the last few decades, a greening accompanying warming and rising atmospheric CO_2 in the northern high latitudes (>45° N) has been documented (McGuire et al., 1995; McGuire and Hobbie, 1997; Chapin and Starfield, 1997; Stow et al., 2004; Callaghan et al., 2005; Tape et al., 2006). The large stocks of carbon contained in the region (Tarnocai et al., 2009) are particularly vulnerable to climate change (Schuur et al., 2008; McGuire et al., 2009). To date, the degree to which the ecosystems may serve as a source or a sink of C in the future are still uncertain (McGuire et al., 2009; Wieder et al., 2013). Therefore, accurate models are essential for predicting carbon–climate feedbacks in the future (Todd-Brown et al., 2013). Our regional simulations indicate the region is currently a carbon sink, which is consistent with many previous studies (White et al., 2000; Houghton et al., 2007), and this sink will grow under the RCP 8.5 scenario, but shift to a carbon source under the RCP 2.6 scenario by 2100. MIC-TEM shows a higher correlation between NPP and soil temperature (R=0.91) than TEM (R=0.82), suggesting that MIC-TEM is more sensitive to environmental changes (Table S4).

Our regional estimates of carbon fluxes by MIC-TEM are within the uncertainty range from other existing studies. For instance, Zhuang et al. (2003) estimated the region as a sink of 0.9 Pg C yr^{-1} in extratropical ecosystems for the 1990s, which is similar to our estimation of 0.83 Pg C yr^{-1} by MIC-TEM. White et al. (2000) estimated that, during the 1990s, regional NEP above 50 °N region is 0.46 Pg C yr^{-1} while Qian et al. (2010) estimated that NEP increased from 0 to 0.3 Pg C yr^{-1} for the high-latitude region above 60 °N during last century, and reached 0.25 Pg C yr^{-1} during the 1990s. White et al. (2000) predicted that, from 1850 to 2100, the region accumulated 134 Pg C in terrestrial ecosystems, in comparison with our estimates of 77.6 Pg C with MIC-TEM and 89 Pg C with TEM. Our projection of a weakening sink during the second half of the 21st

century is consistent with previous model studies (Schaphoff et al., 2013). Our predicted trend of NEP is very similar to the finding of White et al. (2000), indicating that NEP increases from 0.46 Pg C yr^{-1} in the 2000s and reaches 1.5 Pg C yr^{-1} in the 2070s, then decreases to 0.6 Pg C yr^{-1} in the 2090s.

The MIC-TEM simulated NEP generally agrees with the observations. However, model simulations still deviate from the observed data, especially for tundra ecosystems. The deviation may be due to the uncertainty or errors in the observed data, which do not well constrain the model parameters. Uncertain driving data such as temperature and precipitation are also a source of uncertainty for transient simulations. In addition, we assumed that vegetation will not change during the transient simulation. However, over the past few decades in the northern high latitudes, temperature increases have led to vegetation changes (Hansen et al., 2006), including latitudinal treeline advance (Lloyd et al., 2005) and increasing shrub density (Sturm et al., 2001). Vegetation can shift from one type to another because of competition for light, N and water (White et al., 2000). For example, needleleaved trees tend to replace tundra gradually in response to warming. In some areas, forests even moved several hundreds of kilometers within 100 years (Gear and Huntley, 1991). The vegetation changes will affect carbon cycling in these ecosystems. In addition, we have not yet considered the effects of management of agriculture lands (Cole et al., 1997), but Zhuang et al. (2003) showed that the changes in agricultural land use in northern high latitudes have been small.

The largest limitation to this study is that we have not explicitly considered the fire effects. Warming in the northern high latitudes could favor fire in its frequency, intensity, seasonality and extent (Kasischke and Turetsky, 2006; Johnstone and Kasischke, 2005; Soja et al., 2007; Randerson et al., 2006; Bond-Lamberty et al., 2007). Fire has profound effects on northern forest

ecosystems, altering the N cycle and water and energy exchanges between the atmosphere and ecosystems. Increase in wildfires will destroy most of above-ground biomass and consume organic soils, resulting in less carbon uptake by vegetation (Harden et al., 2000), leading to a net release of carbon in a short term. However, a suite of biophysical mechanisms of ecosystems including post-fire increase in the surface albedo and rates of biomass accumulation may in turn, exert a negative feedback to climate warming (Amiro et al., 2006; Goetz et al., 2007), further influence the carbon exchanges between ecosystems and the atmosphere.

Moreover, carbon uptake in land ecosystems depends on new plant growth, which connects tightly with the availability of nutrients such as mineral nitrogen. Recent studies have shown that when soil nitrogen is in short supply, most terrestrial plants would form symbiosis relationships with fungi; hyphae provides nitrogen to plants, in return, plants provide sugar to fungi (Hobbie and Hobbie, 2008, 2006; Schimel and Hättenschwiler, 2007). This symbiosis relationship has not been considered in our current modeling, which may lead to a large uncertainty in our quantification of carbon and nitrogen dynamics.

Shift in microbial community structure was not considered in our model, which could affect the temperature sensitivity of heterotrophic respiration (Stone et al., 2012). Michaelis-Menten constant (K_m) could also adapt to climate warming, and it may increase more significantly with increasing temperature in cold-adapted enzymes than in warm-adapted enzymes (German et al., 2012; Somero et al., 2004; Dong and Somero, 2009). Carbon use efficiency (CUE) is also a controversial parameter in our model. Empirical studies in soils suggest that microbial CUE declines by at least 0.009 $^{o}C^{-1}$ (Steinweg et al., 2008), while other studies find that CUE is invariant with temperature (López-Urrutia and Morán, 2007). Another key microbial trait lacking in our modeling is microbial dormancy (He et al., 2015). Dormancy is a common, bet-hedging strategy

used by microorganisms when environmental conditions limit their growth and reproduction (Lennon and Jones, 2011). Microorganisms in dormancy are not able to drive biogeochemical processes such as soil CO_2 production, and therefore, only active microorganisms should be involved in utilizing substrates in soils (Blagodatskaya and Kuzyakov, 2013). Many studies have indicated that soil respiration responses to environmental conditions are more closely associated with the active portion of microbial biomass than total microbial biomass (Hagerty et al., 2014; Schimel and Schaeffer, 2012; Steinweg et al., 2013). Thus, the ignorance of microbial dormancy could fail to distinguish microbes with different physiological states, introducing uncertainties to our carbon estimation.

2.6. Conclusions

This study used a more detailed microbial biogeochemistry model to investigate the carbon dynamics in the region for the past and this century. Regional simulations using MIC-TEM indicated that, over the 20th century, the region is a sink of 77.6 Pg C. This sink could reach to 79.5 Pg C under the RCP 8.5 scenario or shift to a carbon source of 1.6 Pg under the RCP 2.6 scenario during the 21st century. On the other hand, traditional TEM overestimated the carbon sink under the RCP 8.5 scenario with magnitude of 19.2 Pg than MIC-TEM, and predicted this region acting as a carbon sink with magnitude of 27.6 Pg under the RCP 2.6 scenario during the 21st century. Using recent soil carbon stock data as initial soil carbon in model simulations, the region was estimated to shift from a carbon sink to a source, with total carbon release at 0.7- 3 Pg by 2100 depending on initial soil carbon pools at different soil depths under the RCP 2.6 scenario. In contrast, the region acts as a carbon sink at 55.4 - 99.8 Pg in the 21st century under the RCP 8.5 scenario. Without considering more detailed microbial processes, models estimated that the region

acts as a carbon sink under both scenarios. Under the RCP 2.6 scenario, the cumulative sink ranges from 9.9 to 22.8 Pg C. Under the RCP 8.5 scenario, the cumulative sink is even larger at 71.7 - 155.6 Pg C. This study indicated that more detailed microbial physiology-based biogeochemistry models estimate carbon dynamics very differently from using a relatively simple microbial decomposition-based model. The comparison with satellite products or other estimates for the 20th century suggests that the more detailed microbial decomposition shall be considered to adequately quantify C dynamics in northern high latitudes.

2.7. Acknowledgments

This research was supported by a NSF project (IIS-1027955), a DOE project (DE-SC0008092), and a NASA LCLUC project (NNX09AI26G) to Q. Z. We acknowledge the Rosen High Performance Computing Center at Purdue for computing support. We thank the National Snow and Ice Data center for providing Global Monthly EASE-Grid Snow Water Equivalent data, National Oceanic and Atmospheric Administration for North American Regional Reanalysis (NARR). We also acknowledge the World Climate Research Programme's Working Group on Coupled Modeling Intercomparison Project CMIP5, and we thank the climate modeling groups for producing and making available their model output. The data presented in this paper can be accessed through our research website (http://www.eaps.purdue.edu/ebdl/).

CHAPTER 3. MICROBIAL DORMANCY AND ITS IMPACTS ON ARCTIC TERRESTRIAL ECOSYSTEM CARBON BUDGET[2]

3.1. Abstract

A large amount of soil carbon in the Arctic terrestrial ecosystems could be emitted as greenhouse gases in a warming future. However, lacking detailed microbial processes such as microbial dormancy in current biogeochemistry models might have biased the quantification of the regional carbon dynamics. Here the effect of microbial dormancy was incorporated into a biogeochemistry model to improve the quantification for the last and this century. Compared with the previous model without considering the microbial dormancy, the new model estimated the regional soils stored 75.9 Pg more C in the terrestrial ecosystems during the last century, and will store 50.4 Pg and 125.2 Pg more C under the RCP 8.5 and RCP 2.6 scenarios, respectively, in this century. This study highlights the importance of the representation of microbial dormancy in earth system models to adequately quantify the carbon dynamics in the Arctic.

3.2. Introduction

The land ecosystems in northern high latitudes (>45° N) occupy 22% of the global surface and store over 40% of the global soil organic carbon (SOC) (McGuire & Hobbie, 1997; Melillo et al., 1993; Tarnocai et al., 2009; Hugelius et al., 2014). During the past decades, a greening accompanying a warming in the region has been documented (Zhou et al., 2001; Lloyd et al., 2002; Stow et al., 2004; Callaghan et al., 2005; Tape et al., 2006). The regional carbon dynamics are expected to loom large in the global carbon cycle and exert large feedbacks to the global climate system (McGuire et al., 2009; Davidson & Janssens, 2006; Bond-Lamberty & Thomson, 2010).

[2]**Zha, J.** and Zhuang, Q.: Microbial dormancy and its impacts on Arctic terrestrial ecosystem carbon budget, ***Biogeosciences Discuss.***, https://doi.org/10.5194/bg-2019-72, in review, 2019.

To date, numerous ecosystem models have been developed to project the feedbacks between terrestrial ecosystem carbon cycling and climate (Raich et al., 1991; Zhuang et al., 2001, 2002, 2015; Parton et al., 1993; Knorr et al., 2005; Running & Coughlan, 1988), but they can bias their quantifications due to missing detailed microbial mechanisms in these models (Schmidt et al., 2011; Todd-Brown et al., 2013; Conant et al., 2011; Treseder et al., 2011). Microorganisms play a central role in decomposition of litter and soil organic carbon, which further governs the global carbon cycling and climate change (Xu et al., 2014; Treseder et al., 2011; Wang et al., 2015). An emerging field of research has begun to incorporate microbial ecology into existing process-based models to remedy the inadequate representation of soil decomposition process (Zha & Zhuang, 2018; Schimel & Weintraub, 2003; Allison et al., 2010; German et al., 2012). These microbial-based models tend to better reproduce field and satellite observations than traditional ones that treat soil decomposition as a first-order decay process without considering microbial activities (Treseder et al., 2011; Wieder et al., 2013; Todd-Brown et al., 2011; Lawrence et al., 2009; Moorhead et al., 2006). However, some vital microbial traits such as microbial dormancy and community shifts are still rarely explicitly considered in large-scale ecosystem models, and this may introduce notable uncertainties (Graham et al., 2014, 2016; Wang et al., 2015; Bouskill et al., 2012; Kaiser et al., 2014).

Dormancy is broadly recognized as a strategy for microorganisms to cope with periodical environmental stresses (Harder & Dijkhuizen, 1983). When environmental conditions are unfavorable for growth, microbes switch to a dormant state, which is a reversible state of low to zero metabolic activity (Stolpovsky et al., 2011; Lennon & Jones, 2011). In this state, biogeochemical processes such as soil decomposition are slow (Blagodatskaya et al., 2013). At any given time, there is only a fraction of number of microbes, likely below 50% of live microbes,

in natural soils (Wang et al., 2015; Stolpovsky et al., 2011). Soil decomposition and nutrient cycling mainly depend on these active microbes because only active ones can consume organic matter and replicate themselves (Wang et al., 2015; Blagodatskaya et al., 2014). To date, most existing biogeochemistry models used total microbial biomass as indicator of microbial activities, rather than the active portion of microbial biomass, which could bias the estimates of soil decomposition and ecosystem carbon budget (Hagerty et al., 2014; He et al., 2015). Especially, the Arctic terrestrial ecosystems are nitrogen-limited, neglecting microbial dormancy will lead to incorrect estimates of nitrogen availability through soil decomposition, failing to capture nitrogen feedbacks to carbon dynamics (Wang et al., 2015; Stolpovsky et al., 2011; Thullner et al., 2005). Thus, incorporating dormancy effects will improve model realism and provide a better projection of the Arctic carbon dynamics.

This study incorporated the effects of microbial dormancy trait into an extant process-based biogeochemistry model (MIC-TEM) (Zha & Zhuang, 2018; He et al., 2015). The dormant and active microbial physiology has been considered explicitly in the new version of model (MIC-TEM-dormancy). The revised model was parameterized, validated, and then applied to evaluate the carbon dynamics during the last and this centuries in the Arctic terrestrial ecosystems (north 45 °N above).

3.3. Methods

3.3.1. Overview

First, we describe how we developed the new model (MIC-TEM-dormancy) by incorporating the microbial dormancy trait into an existing microbial-based biogeochemistry model (MIC-TEM)**.** Second, parameterization and validation of MIC-TEM-dormancy using

observed net ecosystem exchange data, and heterotrophic respiration data at representative sites have been shown. Third, we applied the model to northern high latitudes (above 45 °N) for the 20th and 21st centuries, to demonstrate the dormancy effects.

3.3.2 Model Description

A non-dormancy version of biogeochemistry model (MIC-TEM) has been developed by incorporating a microbial module (Allison et al., 2010) into an extant large-scale biogeochemical model (TEM) to explicitly (Zhuang et al., 2001, 2002, 2003) consider the effects of microbial dynamics and enzyme kinetics on carbon dynamics (Zha & Zhuang, 2018). Here we further advanced the MIC-TEM by incorporating algorithms that describe the effects of microbial dormancy dynamics based on He et al. (2015). Different from He et al. (2015), in which microbial module was driven with existing data of carbon stocks and fluxes, our study incorporated the microbial module into an extant MIC-TEM that simulates carbon data dynamically. This coupling enables us to extrapolate our model to whole northern high-latitudes region, rather than only for temperate forest region in He et al. (2015). In our new model (MIC-TEM-dormancy), microbial biomass pool was divided into two fractions, including the dormant and active microbial biomass pools. The two microbial biomass pools and the reversible transition between them have been considered explicitly in the new model, which was ignored in MIC-TEM (Figure 3.1).

In previous MIC-TEM, heterotrophic respiration (R_H) is calculated as:

$$R_H=ASSIM*(1-CUE) \quad (1)$$

Where ASSIM and CUE represent microbial assimilation and carbon use efficiency, respectively. For detailed carbon dynamics in MIC-TEM, see Zha & Zhuang (2018).

Here we revised MIC-TEM by incorporating microbial dormancy dynamics according to He et al. (2015). In the new model (MIC-TEM-dormancy), the soil heterotrophic respiration R_H is comprised of three parts: the maintenance respiration from the active and dormant microorganisms and the CO_2 production through the process of microbial assimilation (He et al., 2015):

$$R_H = m_R Q_{10mic}^{\frac{temp-15}{10}} B_a + \beta m_R Q_{10mic}^{\frac{temp-15}{10}} B_d + CO_2 \quad (2)$$

where the first two terms are maintenance respiration from the active and dormant microorganisms, respectively. The last term is the CO_2 produced during the process of microbial assimilation.

For first two terms, B_a and B_d represents the active and dormant microbial biomass pool, respectively. The parameter m_R denotes the specific maintenance rate at active state (h^{-1}), and β is the ratio of dormant maintenance rate to active maintenance rate. Thus, βm_R denotes the maximum specific maintenance rate at dormant state. Temperature sensitivity was expressed as the Q_{10} function ($Q_{10}^{\frac{temp-15}{10}}$), where temp is soil temperature at top 20 cm (units: ℃).

For the third term, the CO_2 produced through microbial assimilation is calculated as in He et al. (2015) and Allison et al. (2010):

$$CO_2 = ASSIM*(1-Y_g) \quad (3)$$

Where ASSIM represents the variable of microbial assimilation and the parameter Y_g represents carbon use efficiency. Microbial assimilation (ASSIM) is calculated as in He et al. (2015):

$$ASSIM = \frac{1}{Y_g} \frac{\Phi}{\alpha} m_R Q_{10enz}^{\frac{temp-15}{10}} Ba \left(\frac{CN_{soil}}{CN_{mic}}\right)^{0.6} \quad (4)$$

Here parameter α is called the maintenance weight (h^{-1}), CN_{soil} and CN_{mic} denotes the C:N ratio of soil and that of microbial biomass to consider substrate quality. Besides, Φ is called substrate saturation level and defined as in He et al. (2015) and Wang et al. (2014):

$$\Phi = \frac{S}{K_s + S} \quad (5)$$

Where K_s is the half saturation constant for substrate uptake as indicated by the Michaelis–Menten kinetic, and S is soluble C substrates that are directly accessible for microbial assimilation (Wang et al., 2014). Here we quantified concentration of soluble C substrates that are directly accessible for microbial assimilation by using conceptual framework from Davidson et al. (2012):

$$S = \text{Soluble C} * D_{liq} * \theta^3 \quad (6)$$

The term 'Soluble C' denotes the state variable of soluble carbon pool. D_{liq} is the diffusion coefficient of the substrate in the liquid phase, and is formulated as $D_{liq} = 1/(1-BD/PD)^3$. BD is the bulk density and PD is the soil particle density. θ is the volumetric soil moisture.

Different from MIC-TEM, the transitions between active and dormant microbial biomass are included in MIC-TEM-dormancy. We used $B_{a\rightarrow d}$ and $B_{d\rightarrow a}$ denotes the transition from the active to dormant microbe and from the dormant to active microbe, respectively (He et al., 2015; Wang et al., 2014):

$$B_{a\rightarrow d} = (1-\Phi) m_R Q_{10mic}^{\frac{temp-15}{10}} B_a \quad (7)$$

$$B_{d\rightarrow a} = \Phi m_R Q_{10mic}^{\frac{temp-15}{10}} B_d \quad (8)$$

Dormancy rate is affected by substrate availability (B_a, B_d), soil temperature (temp) and soil moisture (θ in Φ).

The active microbial biomass (B_a) is modeled as (He et al., 2015; Wang et al., 2014):

$$\frac{dBa}{dt} = ASSIM * Y_g - m_R Q_{10mic}^{\frac{temp-15}{10}} B_a - B_{a\to d} + B_{d\to a} - DEATH - EPROD \quad (9)$$

Where DEATH and EPROD denotes microbial biomass death and enzyme production, which are modeled as proportional to active microbial biomass with constant rates r_{death} and $r_{EnzProd}$ (Allison et al., 2010):

$$DEATH = r_{death} * Ba \quad (10)$$

$$EPROD = r_{EnzProd} * Ba \quad (11)$$

Where r_{death} and $r_{EnzProd}$ are the rate constants of microbial death and enzyme production, respectively.

The dormant microbial biomass (B_d) is modeled as (He et al., 2015; Wang et al., 2014):

$$\frac{dB_d}{dt} = -\beta m_R Q_{10mic}^{\frac{temp-15}{10}} B_d + B_{a\to d} - B_{d\to a} \quad (12)$$

The Soluble C pool is modeled as (He et al., 2015; Allison et al., 2010):

$$\frac{d\ Soluble\ C}{dt} = DECAY - ASSIM + ELOSS + DEATH \quad (13)$$

Where DECAY represents the enzymatic decay of soil organic carbon (SOC), and ELOSS represents the loss of enzyme.

DECAY is regulated by enzyme biomass (ENZ), soil organic carbon (SOC), soil temperature, and substrate quality (He et al., 2015):

$$DECAY = V_{max} * Q_{10enz}^{\frac{temp-15}{10}} * ENZ * \frac{SOC}{Km_{uptake}+SOC} * (120 - CN_{soil}) \quad (14)$$

Where V_{max} is the maximum SOC decay rate, Km_{uptake} is half saturation constant for enzymatic decay.

ELOSS is modeled as a first-order process (Allison et al., 2010) to represent enzyme turnover:

$$ELOSS = r_{enzloss} * ENZ \quad (15)$$

Where $r_{enzloss}$ is the rate constant of enzyme loss.

The soil organic carbon pool (SOC) is modeled as:

$$\frac{\mathrm{dSOC}}{\mathrm{dt}} = \mathrm{Litterfall} - \mathrm{DECAY} \qquad (16)$$

Where Litterfall is estimated as a function of vegetation carbon (Zhuang et al., 2010).

Last, enzyme pool (ENZ) is modeled as:

$$\frac{\mathrm{dENZ}}{\mathrm{dt}} = \mathrm{EPROD\text{-}ELOSS} \qquad (17)$$

With the modification of microbial carbon dynamics by considering microbial life-history trait, soil decomposition is changed since it is controlled by microbes. When microbial dormancy is considered, the number of active microbes that participate in soil decomposition is different. The changes in soil decomposition directly influence the amount of soil respiration, and further influence soil nitrogen (N) mineralization that determines soil N availability for plants, affecting gross primary production (GPP). Since both GPP and soil respiration (R_H) can be affected by microbial dormancy, net ecosystem production (NEP) will also be affected.

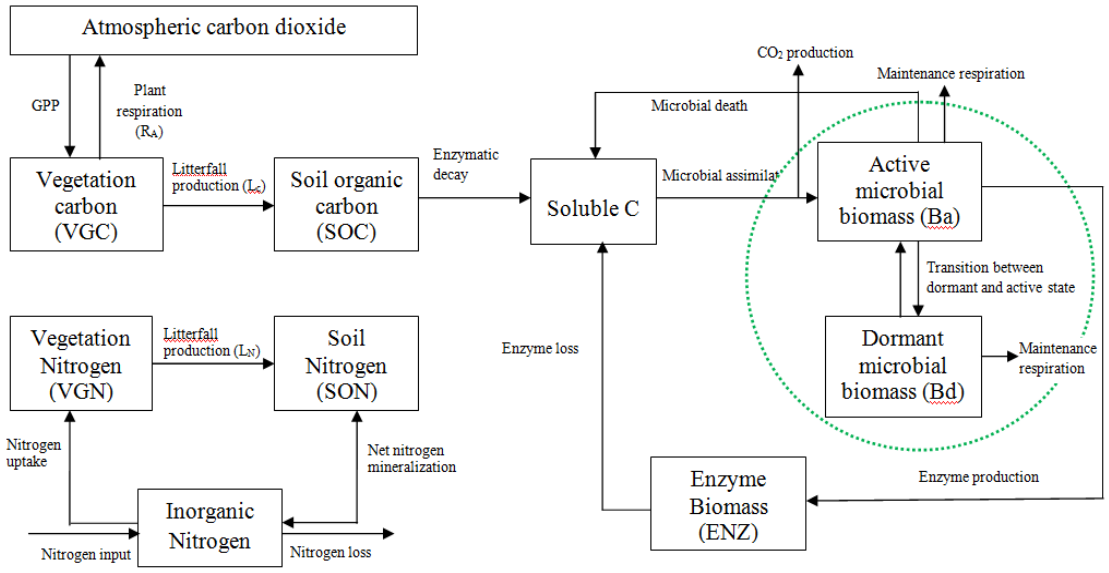

Figure 3.1. Framework of the dormancy model: microbial biomass is split into two parts, active microbial biomass and dormant microbial biomass (shown in the green dashed circle). Maintenance respiration from these two parts, and the CO2 production through microbial assimilation contributes to heterotrophic respiration. The model was revised based on Zha & Zhuang (2018).

3.3.3 Model parameterization and validation

The detailed description of parameters that are related to microbial dormancy can be found in He et al. (2015) (Table 3.1). Here we calibrated the MIC-TEM-dormancy at six representative sites with gap-filled monthly net ecosystem productivity (NEP, $gCm^{-2}mon^{-1}$) data in northern high latitudes (Table 3.2). Site-level climatic data and soil texture data were organized for driving model. All sites information can be found on AmeriFlux network (Davidson et al., 2000). The results for model parameterization were presented in Figure 3.2. We conducted the parameterization using a global optimization algorithm known as SCE-UA (Shuffled complex evolution) method (Duan et al., 1994). An ensemble of 50 independent sets of parameters were performed based on prior ranges from literature (Table 3.1) to minimize the difference between the monthly simulated and measured NEP at the chosen sites. The cost function of the minimization is:

$$\mathrm{Obj} = \sum_{i=1}^{k}(\mathrm{NEP}_{obs,i} - \mathrm{NEP}_{sim,i})^2 \qquad (17)$$

Where $\mathrm{NEP}_{obs,i}$ and $\mathrm{NEP}_{sim,i}$ are the observed and simulated NEP, respectively. k is the number of data pairs for comparison. Except for the parameters of microbial dormancy, other parameters are derived directly from MIC-TEM (Zha & Zhuang, 2018). The optimized parameters were used for model validation and regional simulations.

For model validation, we chose another six sites that containing monthly NEP data from AmeriFlux network (Table 3.3). Moreover, we also conducted site-level validations with monthly soil respiration data from AmeriFlux network and Fluxnet dataset. The site information was provided in Table 3.4. For these sites, we assumed 50% of soil respiration was heterotrophic respiration (R_H) for forest (Hanson et al., 2000), 60% and 70% of that was R_H for grassland (Wang et al., 2009) and tundra (Billings et al., 1977). Because there is a limited amount of measured data

of heterotrophic respiration, we could not conduct a regional validation for all pixels in northern high latitudes. Instead, we extracted 61 sites providing data of average annual heterotrophic respiration from ORNL global Soil Respiration Dataset (https://daac.ornl.gov/SOILS/guides/SRDB_V4.html, Bond-Lamberty et al., 2018) for model validation. The site-level observed average annual R_H was used to compare with simulated annual R_H by MIC-TEM-dormancy and MIC-TEM. The new model (MIC-TEM-dormancy) was run at monthly time step to keep consistent with the time step of MIC-TEM. Although microbial dynamics occur at fine temporal scales (Tang & Riley, 2014), we can still quantify the cumulative impacts of microbial dynamics on carbon and nitrogen cycling at monthly time by not changing the model structure.

Table 3.1. Parameters associated with detailed microbial dormancy in MIC-TEM-dormancy

parameter	unit	description	Parameter range	references
m_R	h^{-1}	Specific maintenance rate at active state	[0.001, 0.08]	Wang et al. (2014)
Q_{10mic}	-	Temperature effects on microbial metabolic activity (rate change per 10 °C increase in temperature). Based on 0.65 eV activation energy for soils	[1.5, 3.5]	He et al. (2015)
Q_{10enz}	-	Temperature effects on enzyme activity (rate change per 10 °C increase in temperature). Based on 6% rate increase per degree Celsius	1.79	He et al. (2015)
$\boldsymbol{\alpha}$	-	the ratio of m_R to the sum of maximum specific growth rate	[0.01, 0.5]	Wang et al. (2014)
β	-	Ratio of dormant microbial maintenance rate to m_R	[0.0005, 0.005]	Wang et al. (2014)
Y_g	-	carbon use efficiency	[0.3, 0.7]	He et al. (2015)
K_s	$mgC\ cm^{-2}$	Half-saturation constant for directly accessible substrate	[0.01, 10]	Wang et al. (2014)
Km_{uptake}	$mgC\ cm^{-2}$	Half-saturation constant for enzymatic decay of SOC	[200, 1000]	He et al. (2015)
r_{death}	h^{-1}	Potential rate of microbial death	[$2e^{-4}$, $2e^{-3}$]	Allison et al. (2010)
$r_{EnzProd}$	h^{-1}	Enzyme production rate of microbe	[$1e^{-4}$, $8e^{-4}$]	He et al. (2015)
$r_{enzloss}$	h^{-1}	Enzyme loss rate	[0.0005, 0.002]	Allison et al. (2010)
V_{max}	$mgC\ cm^{-2}\ h^{-1}$	Maximum SOC decay rate	[$1e^{-4}$, $5e^{-3}$]	He et al. (2015)

Table 3.2. Site description and measured NEP data used to calibrate MIC-TEM-dormancy

Site Name	Location (Longitude (degrees) /Latitude (degrees))	Elevation (m)	Vegetation type	Description	Data range	Citations
Univ. of Mich. Biological Station	84.71W 45.56 N	234	Temperate deciduous forest	Located within a protected forest owned by the University of Michigan. Mean annual temperature is 5.83˚C with mean annual precipitation of 803mm	01/2005-12/2006	Gough et al. (2013)
Howland Forest (main tower)	68.74W 45.20N	60	Temperate coniferous forest	Closed coniferous forest, minimal disturbance.	01/2004-12/2004	Davidson et al. (2006)
UCI-1964 burn site	98.38W 55.91N	260	Boreal forest	Located in a continental boreal forest, dominated by black spruce trees, within the BOREAS northern study area in central Manitoba, Canada.	01/2004-10/2005	Goulden et al. (2006)
KUOM Turfgrass Field	93.19W 45.0N	301	Grassland	A low-maintenance lawn consisting of cool-season turfgrasses.	01/2006-12/2008	Hiller et al. (2011)
Atqasuk	157.41W 70.47N	15	Wet tundra	100 km south of Barrow, Alaska. Variety of moist-wet coastal sedge tundra, and moist-tussock tundra surfaces in the more well-drained upland.	01/2005-12/2006	Oechel et al. (2014);
Ivotuk	155.75W 68.49N	568	Alpine tundra	300 km south of Barrow and is located at the foothill of the Brooks Range and is classified as tussock sedge, dwarf-shrub, moss tundra.	01/2004-12/2004	McEwing et al. (2015)

Table 3.3. Site description and measured NEP data used to validate MIC-TEM-dormancy

Site Name	Location (Longitude (degrees) /Latitude (degrees))	Elevation (m)	Vegetation type	Description	Data range	Citations
Bartlett Experimental Forest	71.29W/ 44.06N	272	Temperate deciduous forest	Located within the White Mountains National Forest in north-central New Hampshire, USA, with mean annual temperature of 5.61 °C and mean annual precipitation of 1246mm.	01/2005-12/2006	Jenkins et al. (2007); Richardson et al. (2007);
Howland Forest (main tower)	68.74W/ 45.20N	60	Temperate coniferous forest	Closed coniferous forest, minimal disturbance.	01/2003-12/2003	Davidson et al. (2006)
UCI-1964 burn site	98.38W/ 55.91N	260	Boreal forest	Located in a continental boreal forest, dominated by black spruce trees, within the BOREAS northern study area in central Manitoba, Canada.	01/2002-12/2003	Goulden et al. (2006)
Brookings	96.84W/ 44.35N	510	Grassland	Located in a private pasture, belonging to the Northern Great Plains Rangelands, the grassland is representative of many in the north central United States, with seasonal winter conditions and a wet growing season.	01/2005-12/2006	Gilmanov et al. (2005)
Atqasuk	157.41W/ 70.47N	15	Wet tundra	100 km south of Barrow, Alaska. Variety of moist-wet coastal sedge tundra, and moist-tussock tundra surfaces in the more well-drained upland.	01/2003-12/2004	Oechel et al. (2014);
Ivotuk	155.75W/ 68.49N	568	Alpine tundra	300 km south of Barrow and is located at the foothill of the Brooks Range and is classified as tussock sedge, dwarf-shrub, moss tundra.	01/2005-12/2005	McEwing et al. (2015)

Table 3.4. Site description and measured R_H data used to validate MIC-TEM-dormancy model

Site	Location (Longitude (degrees) /Latitude (degrees))	Elevation (m)	Vegetation type	Data range	Citations
US-EML	149.25W/ 63.88N	700	Alpine tundra	01/2009-12/2013	Belshe et al. (2012)
CA-SJ2	104.65W/ 53.95N	580	Boreal forest	01/2004-12/2008	Coursolle et al. (2006)
US-Ho2	68.75W/ 45.21N	91	Temperate coniferous forest	01/2000-12/2004	Davidson et al. (2006)
US-UMB	84.71W/ 45.56N	234	Temperate deciduous forest	01/2005-12/2006	Gough et al. (2013)
US-Ro4	93.07W/ 44.68N	274	Grasslands	01/2016-12/2017	Griffis et al. (2011)
RU-Che	161.34E/ 68.61N	6	Wet tundra	01/2002-12/2005	Merbold et al. (2009)

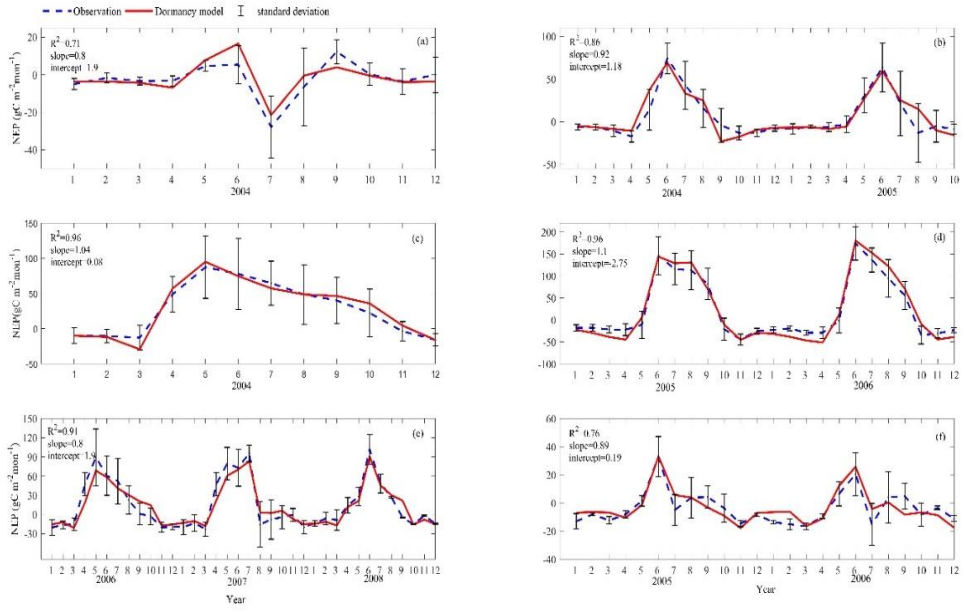

Figure 3.2. Comparison between observed and simulated NEP (gC $m^{-2}mon^{-1}$) at: (a) Ivotuk (alpine tundra), (b) UCI-1964 burn site (boreal forest), (c) Howland Forest (main tower) (temperate coniferous forest), (d) Univ. of Mich. Biological Station (Temperate deciduous forest), (e) KUOM Turfgrass Field (Grassland), and (f) Atqasuk (Wet tundra). Note: scales are different. Error bars represent standard errors among daily measure data in one month.

3.3.4 Spatial extrapolation

For historical simulations during the 20th century, two sets of regional simulations using MIC-TEM-dormancy and MIC-TEM at a spatial resolution of 0.5° latitude × 0.5° longitude were conducted. Our model simulation contains two parts: spin-up and transient simulation. A typical spin-up was conducted to get the model to a steady state for each spatial location, which will be used as initial conditions for transient simulations (McGuire et al., 1992). During spin-up procedure, cyclic forcing data was used to force the model run, and repeated continuously until dynamic equilibrium was achieved at which the modeled state variables show a cyclic pattern or become constant. Specifically, this study used the monthly historical climate data from 1900 to 1940 to repeatedly drive the model for the spin-up. Before spin-up procedure, the model was initialized with default built-in carbon stocks (Raich et al., 1991). During transient simulations, the calibrated ecosystem-specific parameters were used for regional simulations. The previous dynamic equilibrium was used as initial value for transient simulation. The historical climatic forcing data, including the monthly air temperature, precipitation, cloudiness, and atmospheric CO_2 concentrations, were organized from the Climatic Research Unit (CRU TS3.1) from the University of East Anglia (Harris et al., 2014). Gridded data of soil texture (Zhuang et al., 2003), elevation (Zhuang et al., 2015), and potential natural vegetation (Melillo et al., 1993) from literatures were also used. In our model, we assumed that soil texture, elevation, and potential natural vegetation data only vary spatially, not vary over time (Zhuang et al., 2015).

In addition, regional simulations over the 21st century were conducted under two Intergovernmental Panel on Climate Change (IPCC) climate scenarios (RCP 2.6 and RCP 8.5). The future climatic forcing data under these two climate change scenarios were derived from the HadGEM2-ESmodel, which is a member of CMIP5project213 (https://esgf-

node.llnl.gov/search/cmip5/). Then the regional estimations were obtained by summing up the gridded outputs for our study region. The positive simulated NEP represents a CO_2 sink from the atmosphere to terrestrial ecosystems, while a negative value represents a source of CO_2 from terrestrial ecosystems to the atmosphere.

3.4 Results

3.4.1 Inversed Model Parameters and model validation

Using SCE-UA ensemble method, 50 independent sets of parameters were converged to minimize the objective function. Then the optimized parameters are calculated as the mean of these 50 sets of inversed parameters. The boxplot of parameter posterior distributions reflects different ecosystem properties at these sites (Figure 3.3). For instance, carbon use efficiency (CUE) was much higher in tundra types than in forests, meaning microorganisms in environment with higher energy limitation tend to enhance the efficiency of energy transportation. Besides, alpha, the maintenance weight, was also much higher in tundra types than in forests. The opposite can be seen from parameter beta, the ratio of dormant maintenance rate to specific maintenance rate for active biomass. Other microbial related parameters did not differentiate much among different vegetation types.

After parameterization, the MIC-TEM-dormancy was validated with monthly NEP data for six representative ecosystems, and the comparisons between monthly observed NEP and simulated NEP were presented in Figure 3.4. With the optimized parameters, the dormancy-based model was used to reproduce NEP to compare with the measured NEP (Table 3.5). The statistical analysis shows that R^2 ranges from 0.67 for Atqasuk to 0.93 for Bartlett Experimental Forest (Table 3.5). Generally, our new model performs better for forest ecosystems than for

tundra ecosystems. Compared with MIC-TEM, which is no dormancy-based, dormancy model performs better for alpine tundra, temperate coniferous forest, and grassland. For other sites, two models show similar performance (Table 3.5). Another set of sites with monthly soil respiration data were selected to conduct model validation. The comparisons between monthly observed R_H and simulated R_H from two contrasting models were conducted (Figure 3.5). MIC-TEM-dormancy has higher R^2 and lower RMSE (Table 3.6). Sixty-one sites with average annual R_H in northern high-latitude region were used to further evaluate the new model performance. The dormancy model has lower intercept and slope with R^2 of 0.45, while R^2 of MIC-TEM is 0.3 (Figure 3.6). These analyses indicate that new model is more realistic in representing heterotrophic respiration (R_H) by considering microbial dormancy. This difference further affects soil available nitrogen dynamics, influencing nitrogen uptake by plants, the rate of photosynthesis and NPP.

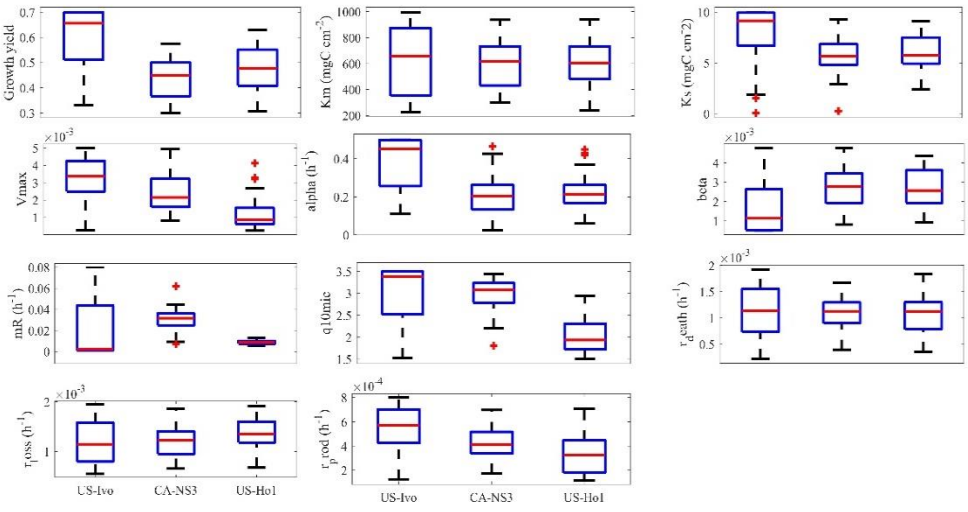

Figure 3.3. Boxplot of parameter posterior distribution that are obtained after ensemble inverse modeling for MIC-TEM-dormancy all six sites: US-Ivo: Ivotuk (alpine tundra), CA-NS3: UCI-1964 burn site (boreal forest), US-Ho1: Howland Forest (temperate coniferous forest), US-UMB: Univ. of Mich. Biological Station (temperate deciduous forest), US-KUT: KUOM Turfgrass Field (grassland), US-Atq: Atqasuk (wet tundra).

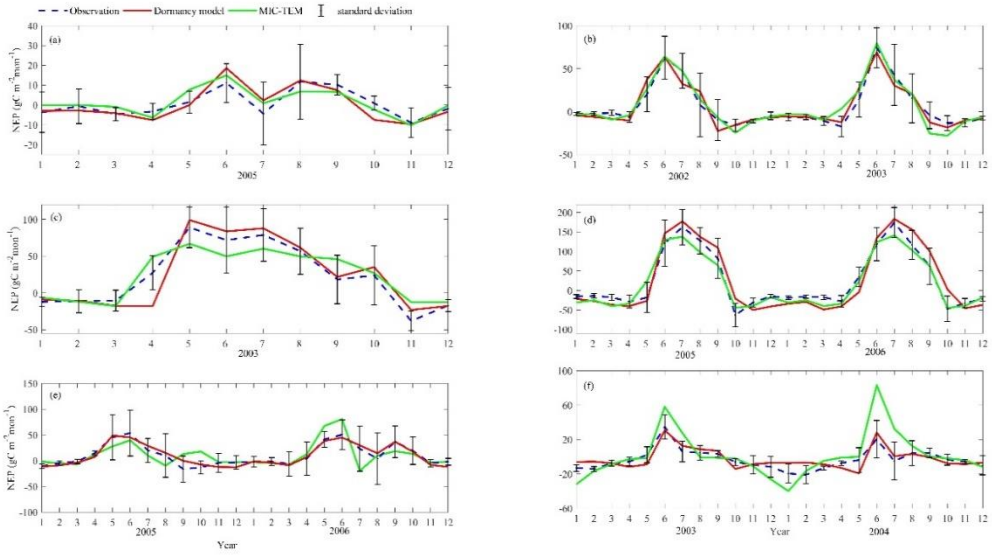

Figure 3.4. Comparison between observed and simulated NEP (gC $m^{-2}mon^{-1}$) at: (a) Ivotuk (alpine tundra), (b) UCI-1964 burn site (boreal forest), (c) Howland Forest (main tower) (temperate coniferous forest), (d) Bartlett Experimental Forest (Temperate deciduous forest), (e) Brookings (Grassland), and (f) Atqasuk (Wet tundra). Note: scales are different.

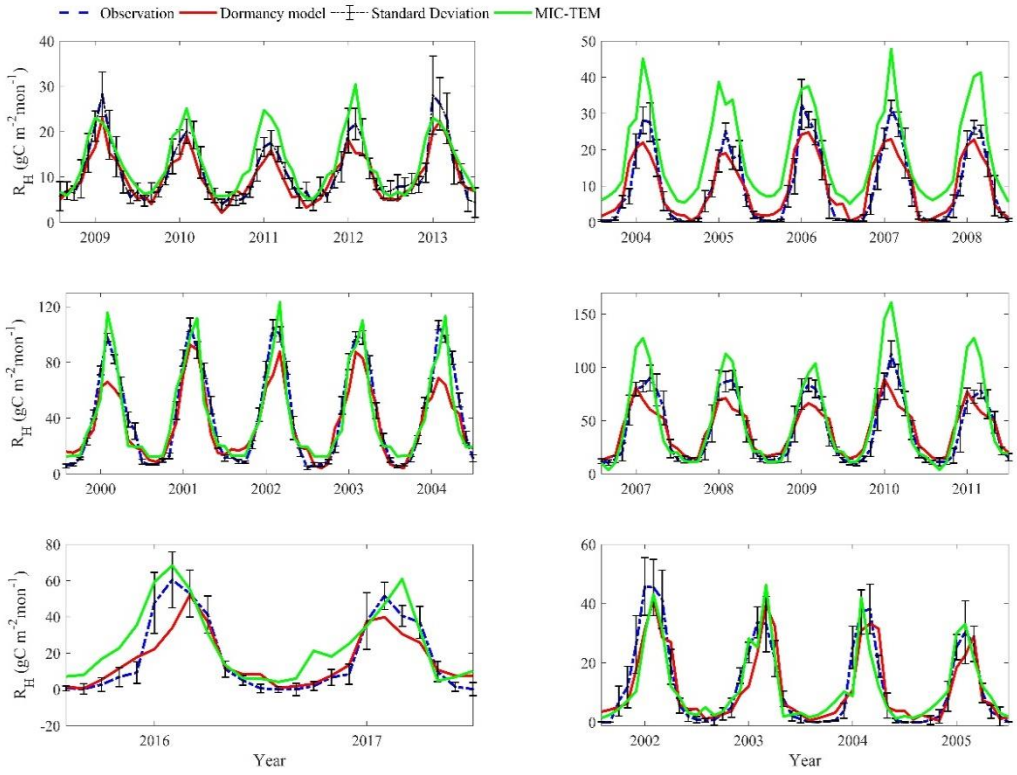

Figure 3.5. Comparison between observed and simulated R_H (gC $m^{-2}mon^{-1}$) at: (a) US-EML (alpine tundra), (b) CA-SJ2 (boreal forest), (c) US-Ho2 (temperate coniferous forest), (d) US-UMB (Temperate deciduous forest), (e) US-Ro4 (Grassland), and (f) RU-Che (Wet tundra). Note: scales are different.

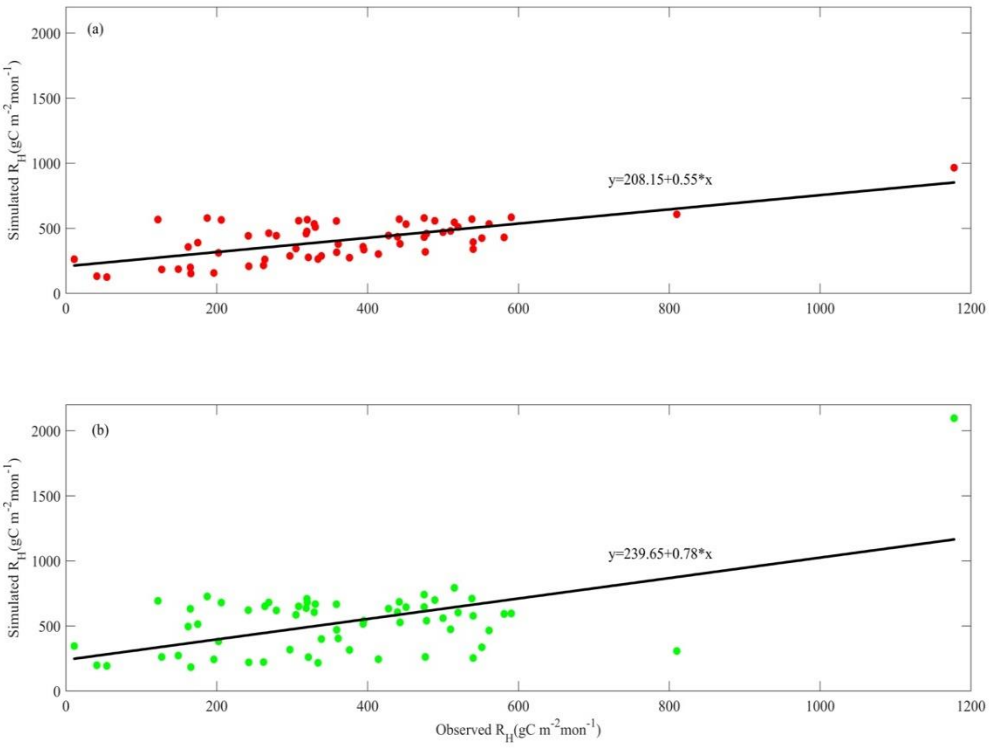

Figure 3.6. Linear regression between simulated and observed annual R_H (gC $m^{-2}yr^{-1}$) for: (a) MIC-TEM-dormancy, and (b) MIC-TEM.

Table 3.5. Model validation statistics for Dormancy model and MIC-TEM at six sites with NEP data

Site Name	Vegetation type	Models	Intercept	Slope	R-square	Adjusted R-square	p-value
Ivotuk	Alpine tundra	MIC-TEM	0.85	0.83	0.70	0.67	<0.001
		Dormancy	-0.51	1.09	0.75	0.73	<0.001
UCI-1964 burn site	Boreal forest	MIC-TEM	0.18	1.03	0.912	0.9080	<0.001
		Dormancy	-0.21	0.96	0.90	0.894	<0.001
Howland Forest (main tower)	Temperate coniferous forest	MIC-TEM	7.29	0.72	0.85	0.83	<0.001
		Dormancy	0.27	1.05	0.89	0.88	<0.001
Bartlett Experimental Forest	Temperate deciduous forest	MIC-TEM	-6.05	0.91	0.944	0.941	<0.001
		Dormancy	-2.34	1.13	0.93	0.924	<0.001
Brookings	Grassland	MIC-TEM	3.05	0.71	0.84	0.83	<0.001
		Dormancy	0.17	0.95	0.90	0.898	<0.001
Atqasuk	Wet tundra	MIC-TEM	7.22	1.85	0.71	0.70	<0.001
		Dormancy	0.19	0.82	0.67	0.66	<0.001

Table 3.6. Model validation statistics for Dormancy model and MIC-TEM at six sites with R_H data

Site ID	Vegetation type	Models	Intercept	Slope	R-square	Adjusted R-square	RMSE	p-value
US-EML	Alpine tundra	MIC-TEM	2.90	0.91	0.79	0.78	3.55	<0.001
		Dormancy	1.81	0.74	0.87	0.85	2.69	<0.001
CA-SJ2	Boreal forest	MIC-TEM	7.59	1.12	0.84	0.83	9.8	<0.001
		Dormancy	2.6	0.74	0.86	0.85	3.97	<0.001
US-Ho2	Temperate coniferous forest	MIC-TEM	4.07	0.89	0.86	0.84	12.39	<0.001
		Dormancy	6.59	0.71	0.91	0.89	11.83	<0.001
US-UMB	Temperate deciduous forest	MIC-TEM	-4.73	1.32	0.81	0.8	20.05	<0.001
		Dormancy	13.6	0.67	0.85	0.84	12.94	<0.001
US-Ro4	Grassland	MIC-TEM	9.34	0.87	0.81	0.79	11.25	<0.001
		Dormancy	4.81	0.65	0.86	0.84	9.21	<0.001
RU-Che	Wet tundra	MIC-TEM	2.5	0.67	0.72	0.71	6.24	<0.001
		Dormancy	1.96	0.77	0.81	0.79	5.95	<0.001

3.4.2 Regional carbon dynamics during the 20th century

Regional extrapolation with both models estimated a regional carbon sink but with different magnitudes (Figure 3.7c). Here positive values of NEP represent sinks of CO_2 into terrestrial ecosystems, while negative values represent sources of CO_2 to the atmosphere. With optimized parameters, MIC-TEM estimated a regional carbon sink of 77.6 Pg with the interannual standard deviation of 0.21 Pg C yr^{-1} during the 20th century. However, MIC-TEM-dormancy nearly doubles the sink at 153.5 Pg with the interannual standard deviation of 0.12 Pg C yr^{-1} during the last century, which estimates 75.9 Pg more carbon sink than MIC-TEM does but with less interannual variation (Figure 3.7c). At the end of the century, MIC-TEM estimated that NEP reaches 1.0 Pg C yr^{-1} in comparison with MIC-TEM-dormancy estimates of 1.5 Pg C yr^{-1} (Figure 3.7c). Both models simulated similar trends for regional NPP, R_H and NEP (Figure 3.7). Generally, they show an increasing trend in the 20th century except a slight decrease during the 1960s (Figure 3.7). Meanwhile, with optimized parameters, MIC-TEM-dormancy estimated NPP and R_H at 7.94 Pg C yr^{-1} and 6.4 Pg C yr^{-1}, which are 5.8% and 16.3% less than the estimations from MIC-TEM, respectively (Figures 3.7a and 3.7b). This pronounced difference of NEP between two models comes from the disparity between the simulated NPP and R_H with them. Without considering dormancy, MIC-TEM estimates more active microbial biomass since it assumes the whole microbial biomass pool will participate in soil decomposition. The fact is only active part of microbial biomass can work for soil decomposition, meaning MIC-TEM overestimates R_H. On the other hand, Overestimation of R_H can induce higher nitrogen uptake by plants, which will accelerate rate of photosynthesis and further enhance NPP projection. Although MIC-TEM estimates higher NPP and R_H than MIC-TEM-dormancy does, NEP estimated from MIC-TEM is actually lower.

The average annual seasonal patterns of NPP, R_H and NEP during the 1990s were also organized from regional simulations with two models (Figure 3.8). Temporally, both two models projected higher NPP and R_H in summer than in winter (Figures 3.8a and 3.8b) due to higher soil temperature and moisture (McGuire et al., 1992). MIC-TEM produced less R_H in winter but higher R_H in summer than MIC-TEM-dormancy (Figure 3.8b), which indicates that without dormancy, model tends to estimate lower soil respiration compared to dormancy model due to ignorance of dormant respiration in winter but estimate higher soil respiration due to higher estimation of active biomass in summer. In the meantime, seasonal cycle of NPP with MIC-TEM-dormancy shows a relative flattening pattern compared with MIC-TEM, which is similar to seasonal cycle of R_H (Figure 3.8a). This is because higher R_H can cause higher NPP due to the reasons we have mentioned above. Though R_H and NPP show the similar seasonal patterns, NEP can still show different pattern since it's the difference between NPP and R_H. Here seasonal cycles of NEP with models are close to each other (Figure 3.8c), but dormancy model projected slightly higher NEP in summer. Besides, setting the R_H projection from MIC-TEM as baseline, MIC-TEM-dormancy averagely projected 33% less R_H in summer (May to September), and 30% more in winter (other months). This suggested that relative difference of R_H between two models in summer was higher than in winter.

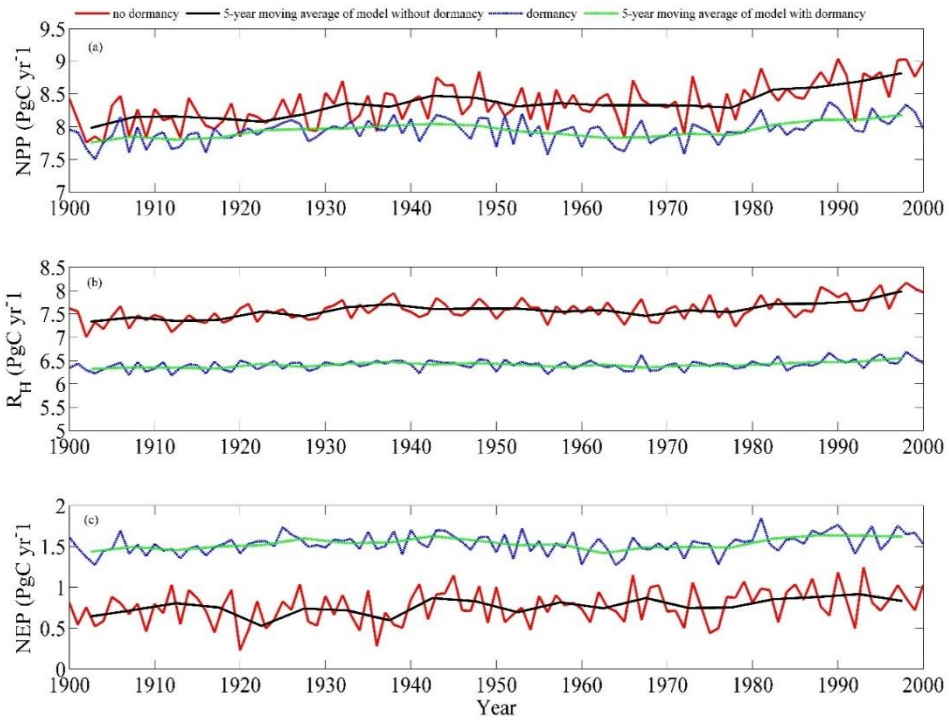

Figure 3.7. Simulated annual net primary production (NPP, top panel), heterotrophic respiration (R_H, center panel) and net ecosystem production (NEP, bottom panel) during the 20th century by dormancy model and MIC-TEM, respectively.

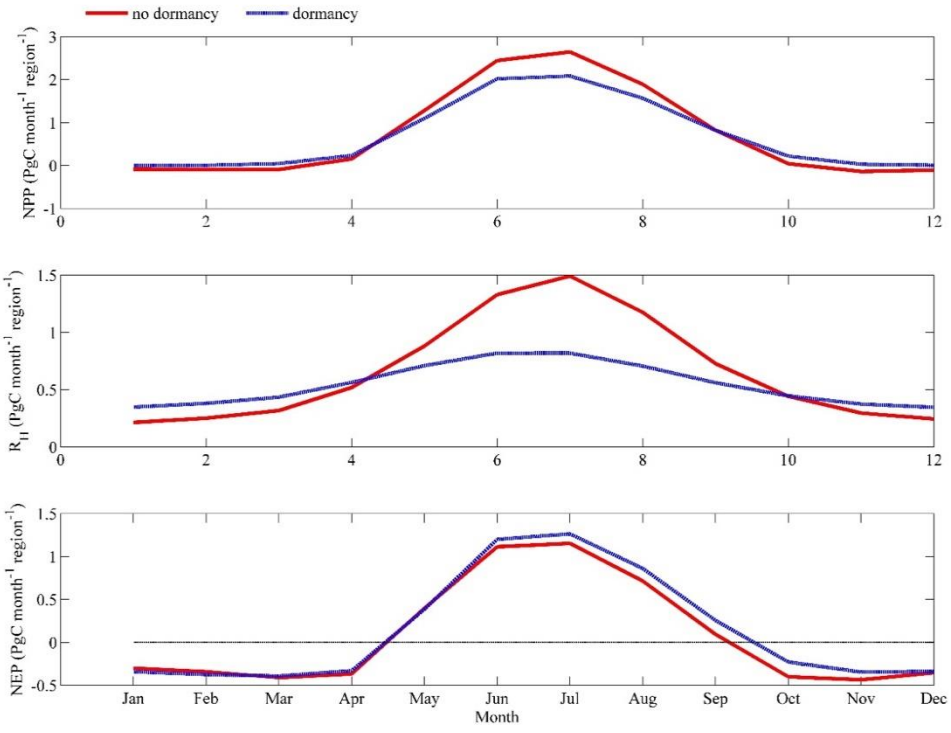

Figure 3.8. Annual seasonal pattern of simulated (a) net primary production (NPP, top panel), (b) heterotrophic respiration (R_H, center panel) and (c) net ecosystem production (NEP, bottom panel) during the 1990s from dormancy model and MIC-TEM.

3.4.3 Regional carbon dynamics during the 21st century

Under the RCP 8.5 scenario, both models estimated the region acts as a carbon sink (Figure 3.9). The MIC-TEM-dormancy predicted that the sink is 129.9 Pg with the interannual standard deviation of 0.13 Pg C yr^{-1}, whereas MIC-TEM estimates the sink is 79.5 Pg with the interannual standard deviation of 0.37 Pg C yr^{-1} during the 21st century (Figure 3.9). Thus, MIC-TEM-dormancy estimates an increase of 50.4 Pg regional carbon sequestration relative to MIC-TEM but with less interannual variation (Figure 3.9). Both models predict similar temporal trends for NEP, namely increasing from the 2000s and then decreasing from the 2070s onward (Figure 3.9). MIC-TEM-dormancy predicts that carbon sink reaches 1.36 Pg C yr^{-1} in the 2090s, which is 0.26 Pg C yr^{-1} more than projection of MIC-TEM. Moreover, MIC-TEM-dormancy estimated NPP and R_H at 10.2 Pg C yr^{-1} and 8.9 Pg C yr^{-1}, which are 1.3 Pg C yr^{-1} and 1.8 Pg C yr^{-1} less than the estimations from MIC-TEM, respectively (Figure 3.9). Under the RCP 2.6 scenario, the cumulative NEP from two models diverged by 125.2 Pg C by 2100. The trajectory of inter-annual NEP estimated with the two models also diverged. The MIC-TEM predicted the region fluctuates between carbon sinks and sources, and totally acts as a carbon source of 1.6 Pg C with the interannual standard deviation of 0.24 Pg C yr^{-1} during the 21st century. In contrast, MIC-TEM-dormancy projected the region acts as a carbon sink of 123.6 Pg C with the interannual standard deviation of 0.1 Pg C yr^{-1} (Figure 3.9). MIC-TEM-dormancy estimates NPP and R_H at 9.9 Pg C yr^{-1} and 8.7 Pg C yr^{-1}, which are 0.5 Pg C yr^{-1} and 1.7 Pg C yr^{-1} less than the estimations from MIC-TEM, respectively (Figure 3.9).

The average annual seasonal patterns of NPP, R_H and NEP during the 2990s by two models were also presented (Figure 3.10). MIC-TEM-dormancy estimated higher R_H in winter, but lower R_H in summer under both future scenarios (Figure 3.10). Similar seasonal cycle pattern

appears for NPP projection. The combined flattening patterns of NPP and R_H result in different patterns for NEP. Under the RCP 2.6 scenario, MIC-TEM-dormancy predicts higher NEP from June to October, but similar NEP in other months to MIC-TEM (Figure 3.10). Under the RCP 8.5 scenario, MIC-TEM-dormancy predicts higher NEP from June to September, but much lower NEP in other months than MIC-TEM (Figure 3.10).

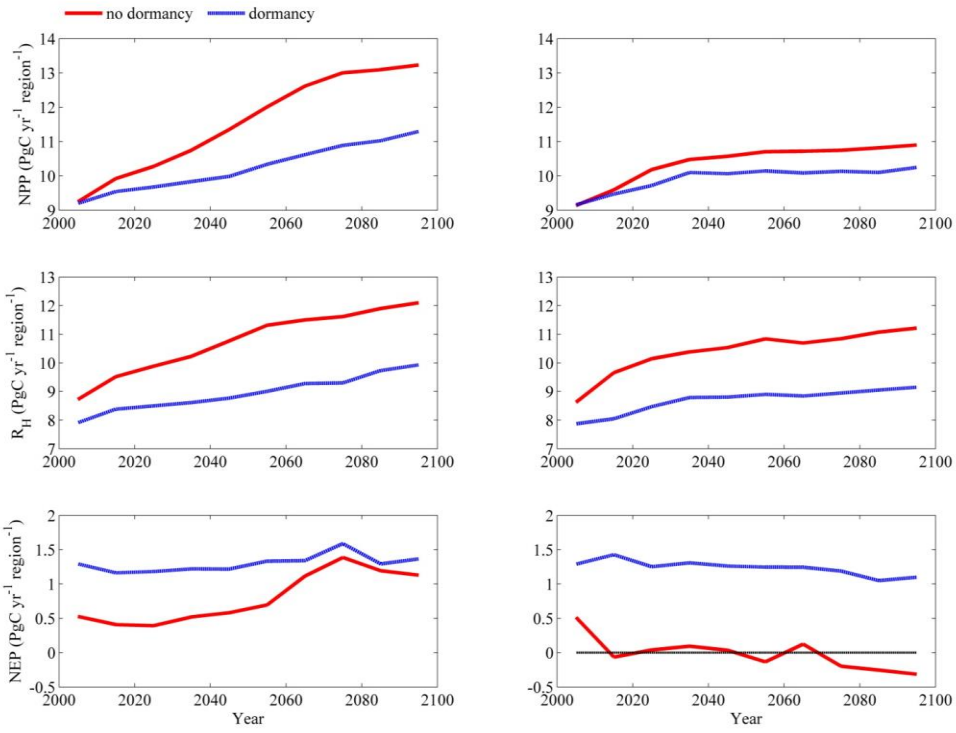

Figure 3.9. Predicted changes in carbon fluxes: (i) NPP, (ii) R_H, and (iii) NEP for all land areas north of 45 °N in response to transient climate change under the RCP 8.5 scenario (left panel) and RCP 2.6 scenario (right panel) with dormancy model and MIC-TEM, respectively. The decadal running mean is applied.

(a)

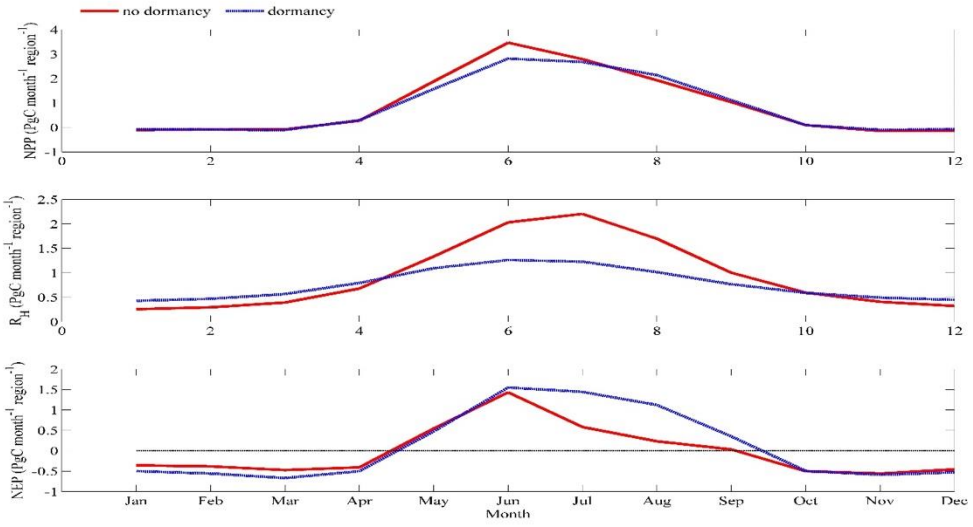

(b)

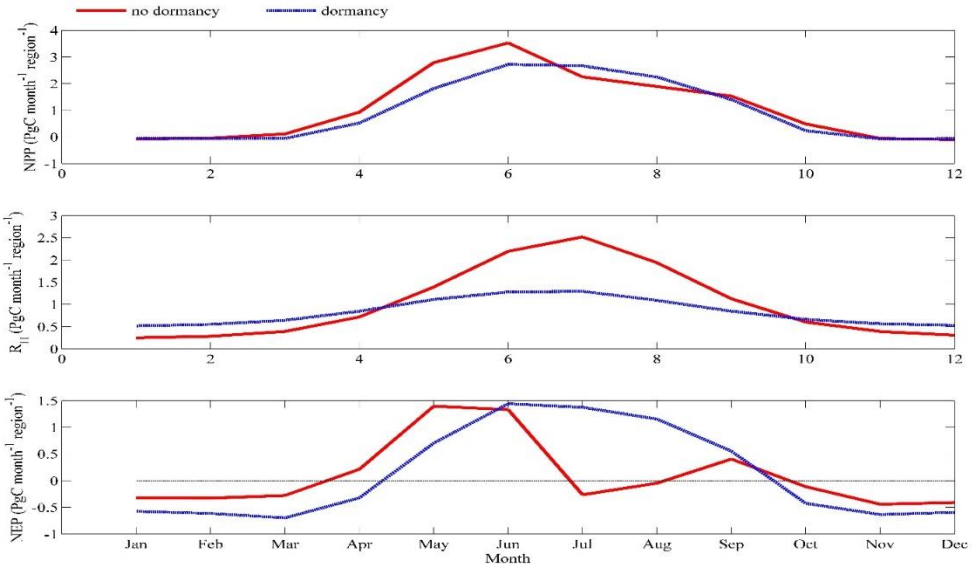

Figure 3.10. Annual seasonal pattern of simulated net primary production (NPP, top panel), heterotrophic respiration (R_H, center panel) and net ecosystem production (NEP, bottom panel) during the 2090s from dormancy model and MIC-TEM under: (a) RCP 2.6 scenario (top panel) and (b) RCP 8.5 scenario (bottom panel).

3.5. Discussion

Soils are the largest carbon repository in the terrestrial biosphere and hold 2.5 times more carbon than the atmosphere (Frey et al., 2013; Schlesinger & Andrews, 2000). Especially, a significant portion of soil organic carbon currently stored in northern high latitudes region (Tarnocai et al., 2009). Besides, climate over this region has warmed in recent decades (Serreze & Francis, 2006) and the changing climate is expected to alter the carbon cycle through influencing the activities of microorganisms in controlling soil decomposition (Manzoni et al., 2012; Melillo et al., 2011). Therefore, explicit consideration of microbial traits and functions in large-scale biogeochemistry models is necessary for better quantification of carbon-climate feedbacks (Thullner et al., 2005; Wang et al., 2015). Our regional simulations with two contrasting models (MIC-TEM, MIC-TEM-dormancy) indicate the region was a carbon sink in past decades, which is consistent with results from other process-based models (White et al., 2000; Houghton et al., 2007; McGuire et al., 2009; Schimel, 2013). However, the magnitudes of this sink are quite different in two models. Moreover, MIC-TEM-dormancy predicts the sink will decrease under both RCP 8.5 and RCP 2.6 scenarios during the 21st century, while MIC-TEM projects that the sink will increase under the RCP 8.5 but change to carbon source under the RCP 2.6 scenario. The large difference in two models suggests the importance of incorporating microbial dormancy effects.

The large bias between dormancy and non-dormancy models mainly comes from two parts. First, most important microbial activities such as soil organic carbon decomposition and nutrient cycling largely depend on the active fraction of microbial communities, not total microbial biomass (Wang et al., 2014; Blagodatsky et al., 2000). However, only a small part (about 0.1-2%, seldom exceed 5%) of the total soil microbial biomass is recognized to be active under natural conditions (Blagodatsky et al., 2011; Werf & Verstraete, 1987). Thus, dormancy

could be a prominent feature in soil systems (Wang et al., 2014). Without considering dormancy, the "effective" microbial biomass for soil decomposition could be overestimated, resulting in overestimation of heterotrophic respiration (He et al., 2015). Our regional estimate of R_H is 6.4 Pg C yr^{-1} during the 20th century by MIC-TEM-dormancy, while 7.7 Pg C yr^{-1} by MIC-TEM. No dormancy model simulated 20.3% higher respiration than dormancy model. For future simulations, MIC-TEM-dormancy predicted 8.7 Pg C yr^{-1} and 9.0 Pg C yr^{-1} of R_H under RCP 2.6 and RCP 8.5 scenarios during the 21st century, respectively. Nevertheless, no dormancy model simulated 19.5% and 21.2% higher respiration than dormancy model under RCP 2.6 and RCP 8.5 scenarios, respectively. He et al. (2015) predicted total soil R_H of all temperate forests (25°N-50°N) from the dormancy model amounted to 7.28 Pg C yr^{-1} and 8.83 Pg C yr^{-1} from a no-dormancy model, which is 21.3% higher than the dormancy model. Although their study region and simulation period are different from our study, the results can still be comparable. Both studies indicated that the magnitude of R_H and proportion from no-dormancy model are higher than dormancy models. Second, high soil respiration stimulates N mineralization in soils (Zhuang et al., 2001, 2002), making more nutrients for photosynthesis of plants (Raich et al., 1991; McGuire et al., 1995). Therefore, NPP will be higher due to the N enrichment from higher R_H. However, how NEP will change is still unclear. Our regional estimate of NEP during the 20th century by MIC-TEM-dormancy is 1.54 Pg C yr^{-1}, and is 0.78 Pg C yr^{-1} by MIC-TEM. Schimel et al. (2001) reported that a range of estimates of the northern extratropical NEP is from 0.6 to 2.3 PgC yr^{-1} in the 1980s. In comparison with our estimates of 1.61 Pg C yr^{-1} with MIC-TEM-dormancy and 0.84 Pg C yr^{-1} with MIC-TEM, our regional estimates of NEP are in reasonable range. Moreover, our predicted trend of NEP is very similar to the finding of White et al. (2000), indicating that NEP increases from the 2000s to the 2070s, and then decreases in the 2090s.

Moreover, future simulations under two contrasting climate scenarios (RCP 2.6 and RCP 8.5) exhibit a large difference of 81.1 Pg C of cumulative NEP during the 21st century by MIC-TEM, but only 6.3 Pg C of that by MIC-TEM-dormancy. This difference indicates microbes provide a resistant response to climate change due to dormancy to some extent (Treseder et al., 2011).

Although our dormancy model can project reasonable carbon fluxes and indicate the importance of incorporating microbial dormancy when compared with no dormancy model (MIC-TEM; Zha & Zhuang et al., 2018), there are some other microbial traits have not yet been considered in our model. For instance, one vital common evolutionary trait of microbe is the community shift (Wang et al., 2015) with changing environment, including warming, N fertilization and precipitation (Treseder et al., 2011; Frey et al., 2013; Allison et al., 2009; Evans & Wallenstein, 2011). Community shift will influence microbial physiology, temperature sensitivity and growth rates (Classen et al., 2015), which will further affect the rate of soil decomposition and other carbon dynamics (Treseder et al., 2011; Schimel & Schaeffer, 2012; Todd-Brown et al., 2011). Moreover, microbial acclimation is another important trait to affect soil decomposition. Recent studies have found the capacity of the microbial community to maintain the warming-induced elevated respiration could decrease over time because of acclimation (Melillo et al. 1993; Todd-Brown et al., 2011). This mechanism of adaption to a new temperature regime shall be factored into future soil decomposition analysis. Besides, microbial community composition was ignored in our model. We didn't separate among functional microbial groups, but gather microbes into one "box". However, microbial community composition could influence ecosystem functioning, and their variance in responses to environmental conditions could alter the prediction of the rates of decomposition of organic material (Balser et al. 2002; Fierer et al. 2007). Especially, some narrowly-distributed functions

can be more sensitive to microbial community composition, and these might benefit most from explicit consideration of distinguishing functional groups in ecosystem models (McGuire & Treseder, 2010; Schimel 1995). Thus, functional dissimilarity in microbial communities can be considered in next step for model development (Strickland et al., 2009; Moorhead et al., 2006).

Except for above model limitations, additional uncertainties may come from inadequate model parameterization and model assumptions. For example, a critical microbial parameter, carbon use efficiency (CUE), is a primary control to soil CO_2 efflux. Higher CUE indicates more microbial growth and more carbon uptake by plants, while lower CUE indicates higher soil decomposition (Manzoni et al., 2012). Theoretical and empirical studies have suggested that CUE depends on both temperature and substrate quality (Frey et al., 2013) and decreases as temperature increases and nutrient availability decreases (Manzoni et al., 2012). Our study considered the CUE sensitivity to temperature, but not nutrient availability. On the other hand, some model assumptions can also cause uncertainties. For example, we assumed that vegetation will not change during the transient simulation. However, over the past few decades in northern high latitudes, temperature increases have led to vegetation shift from one type to another (Hansen et al., 2006; White et al., 2000). The vegetation changes will affect carbon cycling in these ecosystems.

3.6. Conclusions

This study incorporated microbial dormancy into a detailed microbial-based soil decomposition biogeochemistry model to examine the fate of large Arctic soil carbon under changing climate conditions. Regional simulations using MIC-TEM-dormancy indicated that, over the 20th century, the region is a carbon sink of 153.5 Pg. This sink could decrease to 129.9 Pg under the RCP 8.5 scenario or 123.6 Pg under the RCP 2.6 scenario during the 21st century.

Whether considering microbial dormancy or not can cause large differences in soil decomposition estimation between two models. Meanwhile, due to available nitrogen affected by soil decomposition, net primary production is consequently influenced in these two centuries. The combined changes in soil decomposition and net primary production led to large differences in carbon budget estimation between two models. Compared with MIC-TEM, MIC-TEM-dormancy projected 75.9 Pg more C stored in the terrestrial ecosystems over the last century, 50.4 Pg and 125.2 Pg more C under the RCP 8.5 and RCP 2.6 scenarios, respectively. This study highlights the importance of the representation of microbial dormancy in earth system models in order to adequately quantify the carbon dynamics in northern high latitudes.

3.7. Acknowledgments

This research was supported by a NSF project (IIS-1027955), a DOE project (DE-SC0008092), and a NASA LCLUC project (NNX09AI26G) to Q. Z. We acknowledge the Rosen High Performance Computing Center at Purdue for computing support. We thank the National Snow and Ice Data center for providing Global Monthly EASE-Grid Snow Water Equivalent data, National Oceanic and Atmospheric Administration for North American Regional Reanalysis (NARR). We also acknowledge the World Climate Research Programme's Working Group on Coupled Modeling Intercomparison Project CMIP5, and we thank the climate modeling groups for producing and making available their model output. The data presented in this paper can be accessed through our research website (http://www.eaps.purdue.edu/ebdl/).

CHAPTER 4. MODELING THE ROLE OF MOSS IN TERRESTRIAL ECOSYSTEM CARBON DYNAMICS IN NORTHERN HIGH-LATITUDES[3]

4.1 Abstract

In addition to higher plants, mosses are ubiquitous in northern terrestrial ecosystems, which play an important role in regional carbon, water and energy cycling. Traditional models without considering moss may bias the quantification of the regional carbon dynamics. Here we incorporated moss into a process-based biogeochemistry model, the Terrestrial Ecosystem Model (TEM 5.0), as a plant functional type to develop a new model (TEM_Moss). The new TEM explicitly modeled the interactions between higher plants and mosses and their competition for energy, water, and nutrient. Compared to the estimates using TEM 5.0, the new model estimated that the regional terrestrial soils stored 132.7 Pg more C during the last century, and will store 157.5 Pg and 179.1 Pg more C under the RCP 8.5 and RCP 2.6 scenarios, respectively, in this century. Ensemble regional simulations for the 21st century with TEM_Moss predicted that the region will accumulate 161.1±142.1 Pg C under the RCP 2.6 scenario, and 186.7±166.1 Pg C under the RCP 8.5 scenario over the century. Our study highlights the necessity of coupling moss into Earth System Models to adequately quantify terrestrial carbon-climate feedbacks in the Arctic.

4.2 Introduction

Northern High latitude ecosystems occupy up to 30% of global terrestrial carbon (C) in soils and plants (Allison and Treseder, 2008; Jobbágy and Jackson, 2000; Kasischke, 2000; Tarnocai et al., 2009; Hugelius et al., 2014), and contain about 1024 Pg soil organic carbon (Treseder et al., 2016; Schuur et al., 2008). This large amount of carbon is potentially responsive

[3]**Zha, J.** and Zhuang, Q (2019), Modeling the role of moss in terrestrial ecosystem carbon dynamics in northern high-latitudes (Submitted to Journal of Advances in Modeling Earth Systems).

to ongoing global warming (McGuire et al., 1995; Melillo et al., 1993; McGuire and Hobbie, 1997), which is especially pronounced at high latitudes (Treseder et al., 2016; IPCC, 2014). Thus, explicit investigation of carbon-climate feedback is important (Wieder et al., 2013; Bond-Lamberty and Thomson, 2010).

Ecosystem models are important tools for understanding the role of boreal ecosystems in climate warming (Bond-Lamberty et al., 2005; Chadburn et al., 2017; Zhuang et al., 2002; Treseder et al., 2016). Process-based biogeochemical models such as TEM (Hayes et al., 2014; Raich et al., 1991; Melillo et al., 1993; McGuire et al., 1992; Zhuang et al., 2001, 2002, 2010, 2013), Biome-BGC (Running and Coughlan, 1988; Bond-Lamberty et al., 2007), and Biosphere Energy Transfer Hydrology scheme (BETHY) (Knorr, 2000) are increasingly employed to simulate current and future carbon dynamics. Those models estimate carbon dynamics by simulating processes such as photosynthesis, respiration, nutrient and water cycling, and soil decomposition (Bond-Lamberty et al., 2005; Zhuang et al., 2015). The results from these models are influenced by components and processes that are built into the model (Turetsky et al., 2012; Oreskes et al., 1994). However, whether boreal forests act as a carbon sink or source haven't reached consensus yet due to model uncertainties and limitations (Cahoon et al., 2012; Hayes et al., 2011; Todd-Brown et al., 2013).

One limitation in many models is that they only concern higher plants for simplification, but ignore some important components such as understory processes, although they play crucial roles in biogeochemical cycles (Zhuang et al., 2002; Treseder et al., 2012; Bond-Lamberty et al., 2005). For instance, mosses are ubiquitous in northern ecosystems, and show a pattern of increasing abundance with increasing latitude (Turetsky et al., 2012; Jägerbrand et al., 2006). Their functional traits, including tolerance to drought and a broad response of net assimilation

rates to temperature, allow them to persist in high-latitude regions (Kallio and Heinonen, 1975; Harley et al., 1989). The activities of moss that related to water, nutrient, and energy may influence several ecosystem processes such as permafrost formation and thaw, peat accumulation, soil decomposition and net primary productivity (NPP) (Turetsky et al., 2012; Nilsson and Wardle, 2005). Mosses can have positive or negative interactions with vascular plants (Skre and Oechel, 1979; Turetsky et al., 2010). On the one hand, mosses compete with vascular plants for available nutrients, which can cause negative effects on vascular plant productivity (Skre and Oechel, 1979; Gornall et al., 2011; Turetsky et al., 2012). Besides, a thick moss cover can form an environment with water logging or low oxygen supply, which is common in high-latitude regions (Skre and Oechel, 1979; Cornelissen et al., 2007). The moss cover prevents absorbed solar heat from being conducted down into the soil, and tends to decrease soil temperature in summer. Therefore, soil decomposition rates can be affected since it is mediated by soil temperature, which will further influence growth of vascular plants (Gornall et al., 2007). On the other hand, some species of mosses can serve as an important source of nitrogen because of their ability of facilitating biological nitrogen fixation and low nitrogen-use efficiency (Basilier, 1979; DeLuca et al., 2007; Markham, 2009; Kip et al., 2011). Thus, mosses can also exert positive effects on plant growth due to their regulation on nitrogen availability for vascular plants (Hobbie et al., 2000; Gornall et al., 2007). It is gradually recognized that mosses can have comparable influences on high-latitude ecosystems to vascular plants, due to their large density and essential function in plant competition, soil climate, and carbon and nutrient cycling (Longton, 1988; Lindo and Gonzalez, 2010; Okland, 1995; Pharo and Zartman, 2007). They can on average contribute 20% of aboveground NPP in boreal forests (Turetsky et al., 2010), and their annual NPP may reach as high as 350 g m^{-2} in some regions in the Arctic (Pakarinen and

Vitt 1973), even exceed that of vascular plants (Oechel and Collins, 1976; Clarke et al., 1971). Thus, ignorance of mosses, the keystone species of boreal ecosystems, can pose large biases in model predictions and limit the utility of models. To date, a number of ecosystem models have included moss activities to explore the response of moss to disturbance (Bond-Lamberty et al., 2007; Euskirchen et al., 2009; Frolking et al., 2010), or improve model prediction of carbon dynamics (Bond-Lamberty et al., 2005).

This study developed a new version of Terrestrial Ecosystem Model (Raich et al., 1991; McGuire et al., 1992; Zhuang et al., 2001, 2002, 2010, 2013, 2015), hereafter referred to as TEM-Moss, by explicitly considering moss impacts on terrestrial ecosystem carbon dynamics. The interactions and competition of water, energy and nutrient between higher plants and mosses are explicitly modeled. The verified TEM-Moss and previous TEM were compared against the observed data of ecosystem carbon, soil temperature and moisture dynamics. Both models were then used to analyze the regional carbon dynamics in northern high latitudes (north of 45 °N) during the 20th and 21st centuries.

4.3 Methods

4.3.1 Overview

First, we briefly describe how we developed the TEM_Moss by modifying the previous TEM 5.0 to consider their interactions between higher plants and mosses. Second, parameterization and validation of TEM_Moss using measured gap-filled carbon flux data and meteorological data at representative sites is presented. Third, we present how we have applied both models (TEM_Moss and TEM 5.0) to the northern high latitudes (above 45 °N) to quantify regional carbon dynamics for the 20th and 21st centuries.

4.3.2 Model description

TEM is a process-based, large-scale biogeochemical model that uses monthly climatic data and spatially explicit vegetation and soil information to simulate the dynamics of carbon and nitrogen fluxes and pool sizes of plants and soils (Raich et al., 1991; McGuire et al., 1992; Zhuang et al., 2010, 2015). However, in previous versions of TEM, only processes of higher plants have been included. Here we developed a TEM_Moss model by modifying model structure and incorporating activities of moss into extant TEM 5.0 (Zhuang et al., 2003). Based on the structure of TEM 5.0, we added carbon and nitrogen pools and fluxes to simulate activities of moss including photosynthesis, respiration, litterfall and nutrient and water cycling (Figure 4.1). Thus, internal data structure of TEM_Moss include processes of both higher plants and mosses (Figure 4.1).

In TEM_Moss, moss photosynthesis (GPP_m) is described as a maximum rate, reduced by influence of photosynthetically active radiation, mean air temperature, mean atmospheric carbon dioxide concentrations, moss moisture, and indirectly, nitrogen availability (Frolking et al., 1996; Launiainen et al., 2015; Zhuang et al., 2002). For each time step, GPP_m is calculated as:

$$GPP_m = C_{max} * f(PAR) * f(T) * f(w_m) * f([CO_2]) * f(NA) \quad (1)$$

Where C_{max} denotes the maximum rate of carbon assimilation by moss (units: gC $m^{-2}mon^{-1}$), $f(PAR)$ is a scalar function that depends on monthly photosynthetically active radiation (PAR), which is calculated as (Frolking et al., 1996; Launiainen et al., 2015; Kulmala et al., 2011):

$$f(PAR) = \frac{PAR}{b+PAR} \quad (2)$$

And b (units: μmol m^{-2} s^{-1}) is the half saturation constant for PAR use by moss as indicated by the Michaelis–Menten kinetic.

The temperature effect on moss photosynthesis is modeled as a multiplier (Frolking et al., 1996; Raich et al., 1991):

$$f(\mathrm{T}) = \frac{(\mathrm{T}-\mathrm{T_{min}})*(\mathrm{T}-\mathrm{T_{max}})}{(\mathrm{T}-\mathrm{T_{min}})*(\mathrm{T}-\mathrm{T_{max}})-(\mathrm{T}-\mathrm{T_{opt}})^2} \qquad (3)$$

Where T is the monthly mean air temperature (units: ℃), and T_{min}, T_{max}, and T_{opt} are parameters (units: ℃) that limit f (T) to a range of zero to one.

The moisture effect is also modeled as a multiplier (Frolking et al., 1996; Raich et al., 1991):

$$f(\mathrm{w_m}) = \frac{(\mathrm{w_m}-\mathrm{w_{min}})*(\mathrm{w_m}-\mathrm{w_{max}})}{(\mathrm{w_m}-\mathrm{w_{min}})*(\mathrm{w_m}-\mathrm{w_{max}})-(\mathrm{w_m}-\mathrm{w_{opt}})^2} \qquad (4)$$

Where w_m is moss moisture (units: mm), and w_{min}, w_{max}, and w_{opt} are related parameters (units: mm) that limit f (w_m) to a range of zero to one.

f ([CO_2]) is also a scalar function that depends on monthly mean atmospheric carbon dioxide concentration (Zhuang et al., 2002; Raich et al., 1991):

$$f([\mathrm{CO_2}]) = \frac{[\mathrm{CO_2}]}{\mathrm{k_m}+[\mathrm{CO_2}]} \qquad (5)$$

Where [CO_2] (units: μL/L) represents monthly mean atmospheric carbon dioxide concentration, the k_m (units: μL/L) is the internal CO_2 concentration at which moss C assimilation proceeds at one-half its maximum rate.

The function f (NA) models the limiting effects of plant nitrogen status on GPP (McGuire et al., 1992; Zhuang et al., 2002), which is a unitless multiplier.

Meanwhile, in TEM_Moss, we defined the moss respiration rate (R_m) as a function of moss respiration rate at 10 ℃, moss respiration temperature sensitivity which was expressed as a Q_{10} function, and moss moisture (Launiainen et al., 2015; Frolking et al., 1996):

$$\mathrm{R_m} = \mathrm{R_{10,m}} * \mathrm{Q_{10,m}}^{\frac{\mathrm{T_m}-10}{10}} * f^*(\mathrm{w_m}) \qquad (6)$$

Where $R_{10,m}$ (units: gC $m^{-2}mon^{-1}$) represents the moss respiration rate at 10 ℃, the parameter $Q_{10,m}$ is moss respiration temperature sensitivity, T_m is moss temperature (℃) and w_m is moss moisture (mm).

The function $f^*(w_m)$ denotes the moisture effect on moss respiration. Here we used $f^*(w_m)$ to distinguish with the function $f(w_m)$, which is moisture effect on moss photosynthesis as mentioned earlier. $f^*(w_m)$ is defined as (Frolking et al., 1996; Zhuang et al, 2002):

$$f^*(w_m) = 1 - \frac{(w_m - w_{min} - w_{opt,r})^2}{(w_m - w_{min}) * w_{opt,r} + {w_{opt,r}}^2} \qquad (7)$$

Where $w_{opt,r}$ (units: mm) denotes the optimal water content for moss respiration.

Besides, the carbon in litter production from mosses to soil ($L_{C,m}$) is modeled as proportional to moss carbon biomass with a constant ratio (Zhuang et al., 2002):

$$L_{C,m} = cfall_m * MOSSC \qquad (8)$$

Where MOSSC denotes the moss carbon biomass, and $cfall_m$ is the corresponding constant proportion.

Thus, moss carbon pool (MOSSC) can be modeled as:

$$\frac{dMOSSC}{dt} = GPP_m - R_m - L_{C,m} \qquad (9)$$

On the other hand, nitrogen uptake by moss ($Nuptake_m$) is modelled as a function of available soil nitrogen, moss moisture, and mean air temperature, and the relative amount of energy allocated to N versus C uptake (Zhuang et al., 2002; Raich et al., 1991):

$$Nuptake_m = N_{max} * \frac{K_s * N_{av}}{k_n + K_s * N_{av}} * e^{0.0693T} * (1 - A_m) \qquad (10)$$

Where N_{max} is the maximum rate of nitrogen uptake by mosses (units: gC $m^{-2}mon^{-1}$), and N_{av} (units: g m^{-2}) represents available soil nitrogen, which is treated as a state variable in our model.

k_n(units: g m^{-2}) is the concentration of available soil nitrogen at which nitrogen uptake proceeds at one-half its maximum rate. T is the monthly mean air temperature (°C), and A_m is a unitless parameter ranging from 0 to 1, which represents relative allocation of effort to carbon vs. nitrogen uptake. K_s is a parameter accounting for relative differences in the conductance of the soil to N diffusion, which can be calculated through moss moisture (Zhuang et al., 2002; Raich et al., 1991):

$$K_s = 0.9 * \left(\frac{w_m}{w_f}\right)^3 + 0.1 \qquad (11)$$

Where w_f (units: mm) denotes the moss field capacity.

The nitrogen in litter production from mosses to soil ($L_{N,m}$) is modeled as proportional to moss nitrogen biomass with a constant ratio (Zhuang et al., 2002):

$$L_{N,m} = nfall_m * MOSSN \qquad (12)$$

Where $nfall_m$ is the constant proportion to moss nitrogen biomass (MOSSN).

Thus, moss nitrogen pool (MOSSN) can be modeled as:

$$\frac{dMOSSN}{dt} = Nuptake_m - L_{N,m} \qquad (13)$$

At the same time, total carbon and nitrogen in litterfall, and total nitrogen uptake from soil available nitrogen are changed due to incorporation of mosses:

$$Litterfall_C = L_{C,v} + L_{C,m} \qquad (14)$$

$$Litterfall_N = L_{N,v} + L_{N,m} \qquad (15)$$

$$Nuptake = Nuptake_v + Nuptake_m \qquad (16)$$

Where $L_{C,v}$ and $L_{N,v}$ are carbon and nitrogen in litter production from higher plants to soil, and $Nuptake_v$ is nitrogen uptake by higher plants (Raich et al., 1991; Melillo et al., 1993; Zhuang et al., 2003).

Except for above equations, other governing equations in TEM 5.0 have not been changed. More equations of TEM 5.0 have been documented in previous studies (Raich et al., 1991; McGuire et al., 1992; Zhuang et al., 2003; Zha & Zhuang, 2018).

In TEM 5.0, a soil thermal module (STM) simulates soil thermal dynamics considering the effects of moss thickness, soil moisture, and snowpack (Zhuang et al., 2001, 2002). In STM, soil profile was treated as a three soil-layer system: (1) a moss plus fibric soil organic layer, (2) a humic organic soil layer, and (3) a mineral soil layer, and temperature for each layer can be output from STM (Zhuang et al., 2001, 2002, 2003). Temperature in moss layer is estimated with STM.

A water balance module (WBM) was also incorporated into TEM 5.0 to simulate soil hydrologic dynamics (Vörösmarty et al., 1989; Zhuang et al., 2001). The WBM receives information on precipitation, air temperature, potential evapotranspiration, vegetation, soils and elevation to predict soil moisture evapotranspiration and runoff (Vörösmarty et al., 1989). The whole soil was treated as a single profile in WBM (Vörösmarty et al., 1989; Zhuang et al., 2001). To simulate moss moisture, we added a moss layer on the soil profile by modifying the WBM (Figure 4.2). Similar to soil moisture, moss moisture is also treated as a state variable in the revised WBM, which is modeled as:

$$\frac{dw_m}{dt} = \text{snowfall} + \text{rainfall} - \text{percolation} - \text{moss evapotranspiration} \qquad (17)$$

Where the term "percolation" denotes the percolation from moss, which is the sum of rainfall percolation and snowmelt percolation from moss. We assume that there is no runoff from moss layer.

Accompanied by the above equation, changes in soil water (SM) is modified as:

$$\frac{dSM}{dt} = \text{percolation} - \text{rain excess} - \text{snow excess} - \text{plant evapotranspiration} \qquad (18)$$

Calculations for these water fluxes regarding higher plants were not changed. More details about an earlier version of WBM were described in Vörösmarty et al. (1989) and Zhuang et al. (2001).

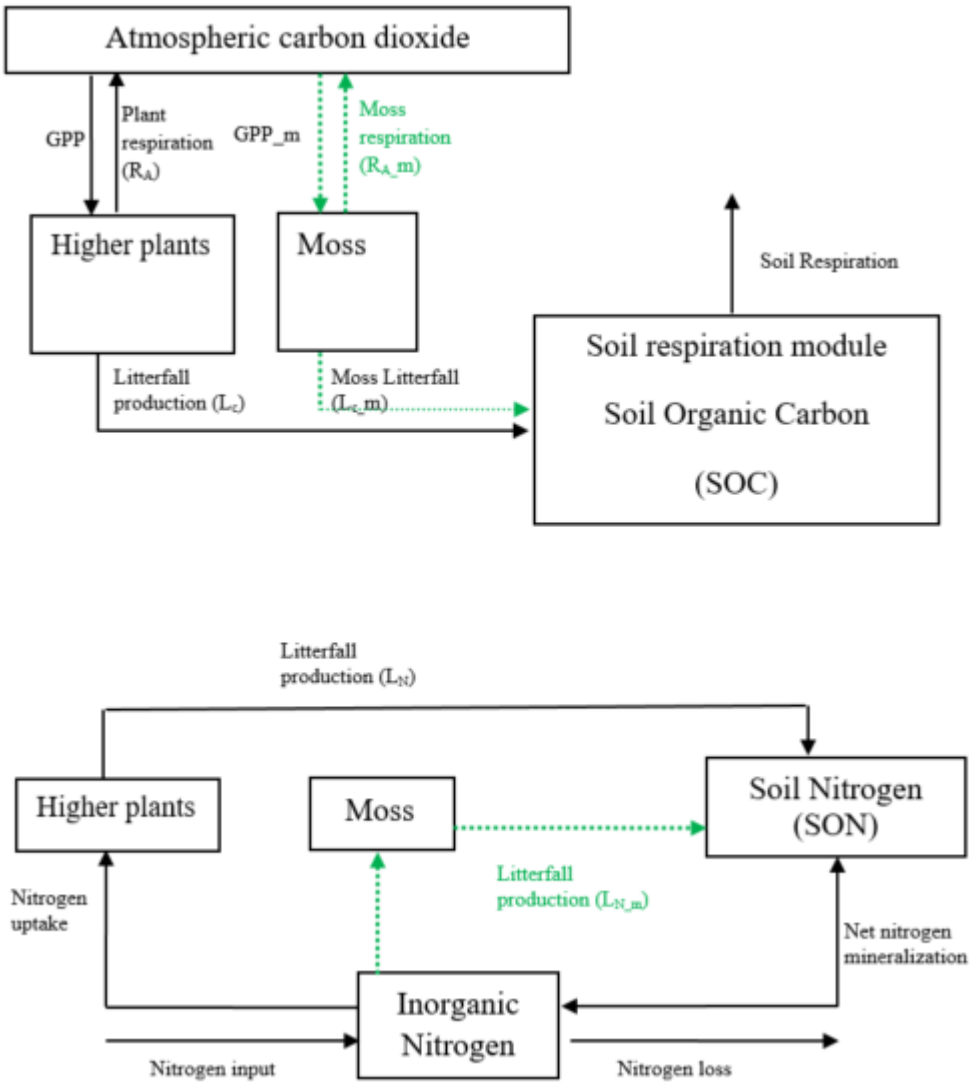

Figure 4.1. Schematic diagram of TEM_Moss: Green dashed arrows are new carbon and nitrogen fluxes, representing moss production, moss respiration and litterfall of moss. Black arrows were in TEM 5.0 (Zhuang et al., 2013).

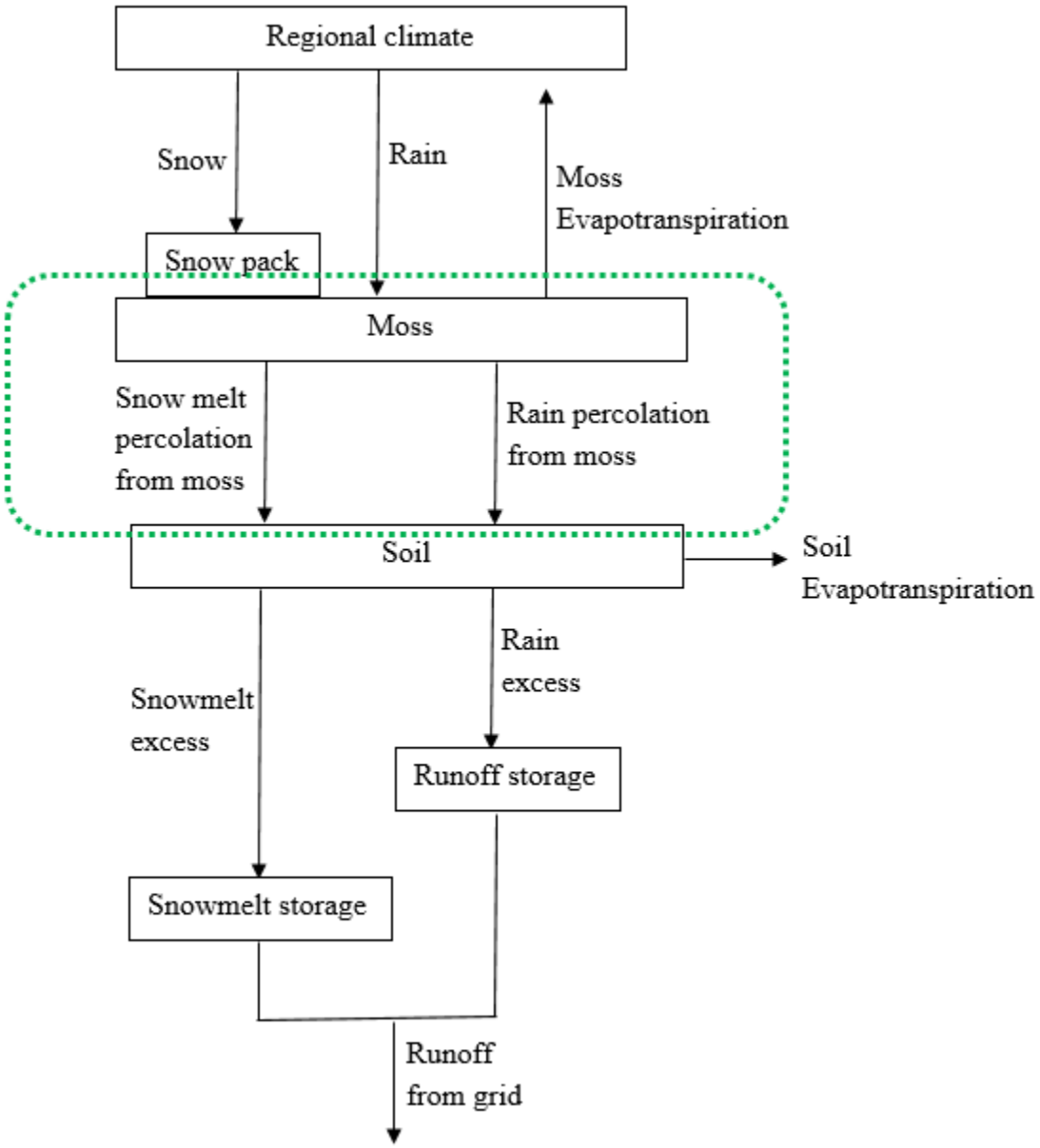

Figure 4.2. The revised Water Balance Model: Green dashed circle represents the hydrology dynamics for moss (Vorosmarty et al., 1989).

4.3.3 Model parameterization and validation

The newly introduced parameters that are associated with moss activities were documented in Table 4.1. We parameterized the TEM_Moss for six representative ecosystem types in northern high latitudes with gap-filled monthly net ecosystem productivity (NEP, $gCm^{-2}mon^{-1}$) data from the AmeriFlux network (Davidson et al., 2000). The information of six sites that we chose to calibrate the TEM_Moss was compiled in Table 4.2. The parameterization was conducted using a global optimization algorithm known as SCE-UA (Shuffled complex evolution) method, which aims to minimize the difference between model simulations and measurements (Duan et al., 1994). In our calibration, the cost function of the minimization is:

$$\mathrm{Obj} = \sum_{i=1}^{k}(\mathrm{NEP}_{obs,i} - \mathrm{NEP}_{sim,i})^2 \qquad (19)$$

Where $\mathrm{NEP}_{obs,i}$ and $\mathrm{NEP}_{sim,i}$ are the measured and simulated NEP, respectively. k is the number of data pairs for comparison. Fifty independent sets of parameters were converged to minimize the objective function, and finally the optimized parameters were derived as the mean of these 50 sets of inversed parameters. We presented the boxplot of parameter posterior distributions at sites chosen for calibration (Figure 4.4). At the same time, the results of model parameterization were shown in Figure 4.3. Besides these parameters related to moss, all other parameters use their default values in TEM 5.0 (Zhuang et al., 2010, 2015). These optimized parameters were used for model validation and extrapolation.

We verified the TEM_Moss simulated NEP, soil moisture and soil temperature. First, we conducted site-level simulations at six sites that contain level-4 gap-filled monthly NEP data from the AmeriFlux network (Table 4.3). Site-level monthly gap-filled soil moisture and soil temperature data were organized from the ORNL DAAC Dataset (https://daac.ornl.gov/) to make comparison with model simulations (Table 4.4 and Table 4.5). Local climate data including

monthly air temperature (°C), precipitation (mm), and cloudiness (%) were obtained to drive these model simulations.

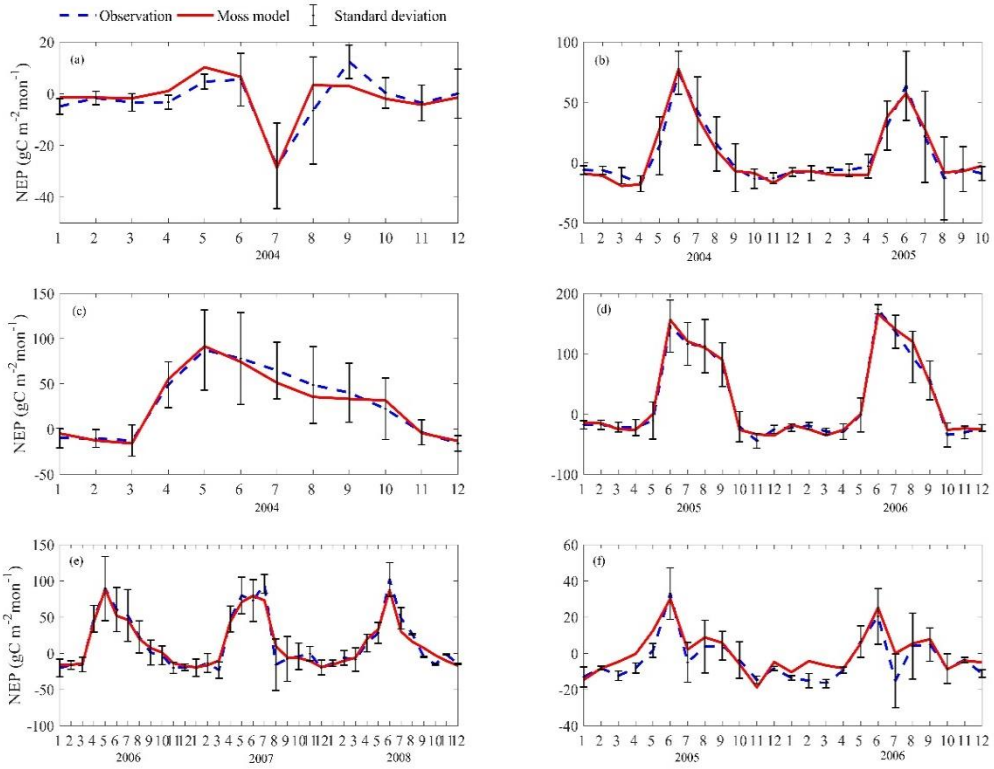

Figure 4.3. Comparison between observed and simulated NEP (gC $m^{-2}mon^{-1}$) at: (a) Ivotuk (alpine tundra), (b) UCI-1964 burn site (boreal forest), (c) Howland Forest (main tower) (temperate coniferous forest), (d) Univ. of Mich. Biological Station (Temperate deciduous forest), (e) KUOM Turfgrass Field (Grassland), and (f) Atqasuk (Wet tundra). Note: scales are different. Error bars represent standard errors among daily measure data in one month.

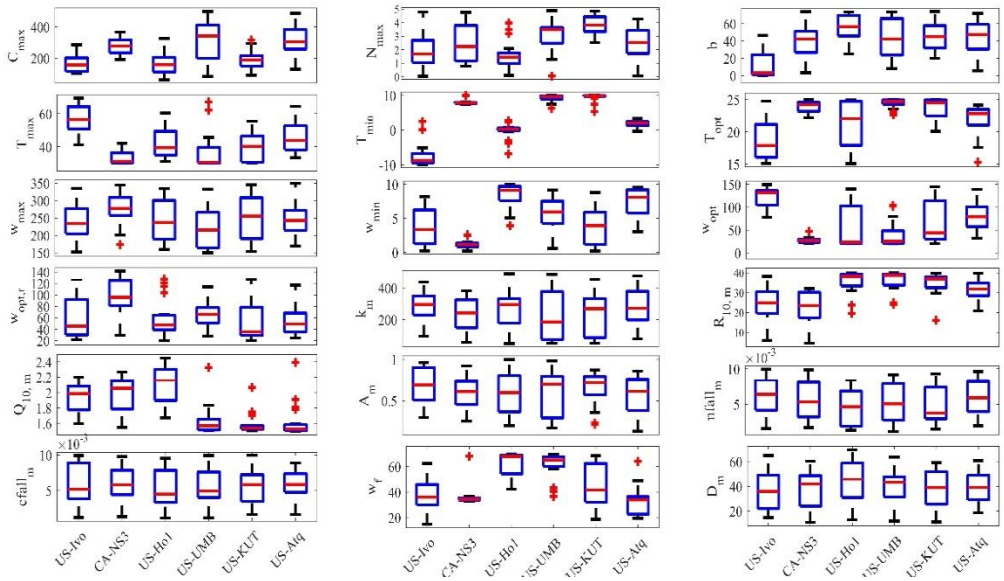

Figure 4.4. Boxplot of parameter posterior distribution that are obtained after ensemble inverse modeling for TEM_Moss all six sites: US-Ivo: Ivotuk (alpine tundra), CA-NS3: UCI-1964 burn site (boreal forest), US-Ho1: Howland Forest (temperate coniferous forest), US-UMB: Univ. of Mich. Biological Station (temperate deciduous forest), US-KUT: KUOM Turfgrass Field (grassland), US-Atq: Atqasuk (wet tundra).

Table 4.1. Parameters associated with moss activities in TEM_Moss

Parameters	Units	descriptions	Parameter range	references
C_{max}	gC m^{-2}	maximum rate of C assimilation	[50,500]	Launiainen et al. (2015); Williams
b	µmol	Light half-saturation level	[5, 150]	Launiainen et al. (2015); Raich et
T_{min}	℃	minimum temperature	[-10, 10]	Frolking et al. (1996); Raich et al.
T_{max}	℃	maximum temperature	[30, 80]	Frolking et al. (1996); Raich et al.
T_{opt}	℃	optimal temperature	[15, 30]	Frolking et al. (1996); Raich et al.
w_{min}	mm	minimum water content for moss	[0.5, 15]	Frolking et al. (1996); Launiainen et
w_{max}	mm	maximum water content for moss	[150, 380]	Frolking et al. (1996); Launiainen et
w_{opt}	mm	optimal water content for moss	[10, 150]	Frolking et al. (1996); Zhuang et al.
k_m	µL/L	CO_2 concentration half-saturation	[50, 500]	Zhuang et al. (2002); Raich et al.
$R_{10, m}$	gC m^{-2}	moss respiration rate at 10 ℃	[0,40]	Frolking et al. (1996); Launiainen et
$Q_{10, m}$	-	moss respiration temperature	[1.5, 2.5]	Frolking et al. (1996); Launiainen et
$w_{opt, r}$	mm	optimal water content for moss	[10, 150]	Frolking et al., 1996; Zhuang et al.
$cfall_m$	$g^{-1}g^{-1}$	constant proportion for carbon	[0.001,	Zhuang et al. (2002); Raich et al.
N_{max}	gN m^{-2}	maximum rate of N uptake by	[0.1,5]	Zhuang et al. (2002); Raich et al.
k_n	g m^{-2}	Half-saturation constant for N	1.0	Zhuang et al. (2002); Raich et al.
A_m	-	relative allocation of effort to C vs.	[0,1]	Raich et al. (1991)
w_f	mm	moss field capacity	[10, 80]	Frolking et al. (1996); Raich et al.
$nfall_m$	$g^{-1}g^{-1}$	constant proportion for nitrogen	[0.001,	Zhuang et al. (2002); Raich et al.
D_m	mm	Moss thickness	[0, 100]	Zhuang et al. (2002)

Table 4.2. Site description and measured NEP data used to calibrate TEM_Moss

Site Name	Location (Longitude (degrees) /Latitude (degrees))	Elevation (m)	Vegetation type	Description	Data range	Citations
Univ. of Mich. Biological Station	84.71W 45.56 N	234	Temperate deciduous forest	Located within a protected forest owned by the University of Michigan. Mean annual temperature is 5.83°C with mean annual precipitation of 803mm	01/2005-12/2006	Gough et al. (2013)
Howland Forest (main tower)	68.74W 45.20N	60	Temperate coniferous forest	Closed coniferous forest, minimal disturbance.	01/2004-12/2004	Davidson et al. (2006)
UCI-1964 burn site	98.38W 55.91N	260	Boreal forest	Located in a continental boreal forest, dominated by black spruce trees, within the BOREAS northern study area in central Manitoba, Canada.	01/2004-10/2005	Goulden et al. (2006)
KUOM Turfgrass Field	93.19W 45.0N	301	Grassland	A low-maintenance lawn consisting of cool-season turfgrasses.	01/2006-12/2008	Hiller et al. (2011)
Atqasuk	157.41W 70.47N	15	Wet tundra	100 km south of Barrow, Alaska. Variety of moist-wet coastal sedge tundra, and moist-tussock tundra surfaces in the more well-drained upland.	01/2005-12/2006	Oechel et al. (2014);
Ivotuk	155.75W 68.49N	568	Alpine tundra	300 km south of Barrow and is located at the foothill of the Brooks Range and is classified as tussock sedge, dwarf-shrub, moss tundra.	01/2004-12/2004	McEwing et al. (2015)

Table 4.3. Site description and measured NEP data used to validate TEM_Moss

Site Name	Location (Longitude (degrees) /Latitude (degrees))	Elevation (m)	Vegetation type	Description	Data range	Citations
Bartlett Experimental Forest	71.29W/ 44.06N	272	Temperate deciduous forest	Located within the White Mountains National Forest in north-central New Hampshire, USA, with mean annual temperature of 5.61 °C and mean annual precipitation of 1246mm.	01/2005-12/2006	Jenkins et al. (2007); Richardson et al. (2007);
Howland Forest (main tower)	68.74W/ 45.20N	60	Temperate coniferous forest	Closed coniferous forest, minimal disturbance.	01/2003-12/2003	Davidson et al. (2006)
UCI-1964 burn site	98.38W/ 55.91N	260	Boreal forest	Located in a continental boreal forest, dominated by black spruce trees, within the BOREAS northern study area in central Manitoba, Canada.	01/2002-12/2003	Goulden et al. (2006)
Brookings	96.84W/ 44.35N	510	Grassland	Located in a private pasture, belonging to the Northern Great Plains Rangelands, the grassland is representative of many in the north central United States, with seasonal winter conditions and a wet growing season.	01/2005-12/2006	Gilmanov et al. (2005)
Atqasuk	157.41W/ 70.47N	15	Wet tundra	100 km south of Barrow, Alaska. Variety of moist-wet coastal sedge tundra, and moist-tussock tundra surfaces in the more well-drained upland.	01/2003-12/2004	Oechel et al. (2014);
Ivotuk	155.75W/ 68.49N	568	Alpine tundra	300 km south of Barrow and is located at the foothill of the Brooks Range and is classified as tussock sedge, dwarf-shrub, moss tundra.	01/2005-12/2005	McEwing et al. (2015)

Table 4.4. Site descriptions and measured volumetric soil moisture data used to validate TEM_Moss

Site	Location (Longitude (degrees) /Latitude (degrees))	Elevation (m)	Vegetation type	Data range	Citations
US-Ivo	155.75W/ 68.49N	579	Alpine tundra	01/2015-12/2016	Oechel & Kalhori (2018)
BOREAS NSA-OBS	98.48W/ 55.88N	259	Boreal forest	07/1995-06/1997	Stangel & Kelly (1999)
NL-Loo	5.74E/ 52.17N	25	Temperate coniferous forest	05/1997-12/1998	Falge et al. (2005)
DK-Sor	11.64E/ 55.49N	40	Temperate deciduous forest	01/1997-12/1999	Falge et al. (2005)
US-Bkg	96.84W/ 44.35N	510	Grasslands	01/2005-12/2006	Gilmanov et al. (2005)
US-Atq	157.41W/ 70.47N	25	Wet tundra	01/2015-12/2016	Oechel & Kalhori (2018)

Table 4.5. Site description and measured soil temperature at 5cm depth data used to validate TEM_Moss

Site	Location (Longitude (degrees) /Latitude (degrees))	Elevation (m)	Vegetation type	Data range	Citations
US-Ivo	155.75W/ 68.49N	579	Alpine tundra	01/2015-12/2016	Oechel & Kalhori (2018)
BOREAS NSA-OBS	98.48W/ 55.88N	259	Boreal forest	01/1995-12/1998	Stangel & Kelly (1999)
US-Ho1	68.74W/ 45.2N	60	Temperate coniferous forest	01/1996-12/1997	Falge et al. (2005)
BE-Vie	6.0E/ 50.3N	493	Temperate deciduous forest	01/1997-12/1998	Falge et al. (2005)
US-Bkg	96.84W/ 44.35N	510	Grasslands	01/2005-12/2006	Gilmanov et al. (2005)
US-Atq	157.41W/ 70.47N	25	Wet tundra	01/2015-12/2016	Oechel & Kalhori (2018)

4.3.4 Regional Extrapolation

Both TEM_Moss and TEM 5.0 were applied to northern high latitudes (above 45 °N) for historical (20th century) and future (21st century) quantifications on carbon dynamics. The difference of carbon dynamics simulated by these two models mostly comes from the effects of moss. For historical simulations, climatic forcing data (monthly air temperature, precipitation, and cloudiness) and atmospheric CO_2 concentrations during the 20th century, were collected from the Climatic Research Unit (CRU TS3.1) from the University of East Anglia (Harris et al., 2014). Other ancillary inputs including gridded soil texture (Zhuang et al., 2003), elevation (Zhuang et al., 2015), and potential natural vegetation (Melillo et al., 1993) were also organized. For future simulations, two contrasting Intergovernmental Panel on Climate Change (IPCC) climate scenarios (RCP 2.6 and RCP 8.5) were used to drive our simulations. The future climate forcing data and atmospheric CO_2 concentrations during the 21st century under these two climate change scenarios were derived from the HadGEM2-ESmodel, which is a member of CMIP5project213 (https://esgf-node.llnl.gov/search/cmip5/, January 2017).

Simulations were conducted at a spatial resolution of 0.5° latitude × 0.5° longitude (Zhuang et al., 2001, 2002). A typical spin-up was run to reach an equilibrium for each pixel, and the values of state variables at equilibrium were treated as initial values for transient simulations (McGuire et al., 1992). We chose the first 30 years in the whole 100-year climatic forcing data to spin-up the models when conducting historical and future simulations. For each of the simulations, net primary production (NPP), heterotrophic respiration (R_H), and net ecosystem production (NEP) were analyzed. We denoted that a positive NEP represents a CO_2 sink from the atmosphere to terrestrial ecosystems, while a negative value represents a source of CO_2 from terrestrial ecosystems to the atmosphere.

4.4 Results

4.4.1 Model Validation

TEM_moss was able to reproduce the monthly NEP and performed better than TEM 5.0 at chosen sites, with larger R-square values and smaller RMSE (Figure 4.5, Table 4.6). R-square for TEM_Moss reached 0.94 at Bartlett Experimental Forest site and 0.72 at Ivotuk site (Table 4.6). R-square values for TEM 5.0 showed a similar pattern, reaching 0.91 and with minimum value of 0.43 at Bartlett Experimental Forest and Ivotuk sites, respectively (Table 4.6). Except for Ivotuk site, R-squares for TEM_Moss are all higher than 0.8 at the chosen sites, while most R-squares for TEM 5.0 are from 0.62 to 0.75 (Table 4.6). On the other hand, RMSE for TEM_Moss is lower than that for TEM 5.0 at each site (Table 4.6).

We presented the comparisons between measured and simulated volumetric soil moisture (VSM) from TEM_Moss and TEM 5.0 (Figure 4.6). Statistical analysis shows that TEM_Moss reproduces the soil moisture well with R-squares ranging from 0.51 at US-Bkg to 0.87 at US-Atq (Table 4.7). R-squares for TEM_Moss are substantially higher than that for TEM 5.0 at most chosen sites, except for US-Atq (Table 4.7). RMSE for TEM_Moss is lower than that for TEM 5.0 at each site (Table 4.7). Similarly, comparisons between measured and simulated soil temperature at 5 cm depth (ST_5) from TEM_Moss and TEM 5.0 indicated that TEM_Moss can reproduce the soil temperature with R-squares ranging from 0.81 at US-Ho1 to 0.91 at US-Bkg, while TEM 5.0 reproduces the soil temperature with R-squares ranging from 0.69 at BE-Vie to 0.89 at US-Bkg (Figure 4.7; Table 4.8). Although R-squares for both models are relatively high and RMSE for them are relatively low, TEM_Moss still shows higher R-squares and lower RMSE than TEM 5.0 (Table 4.8).

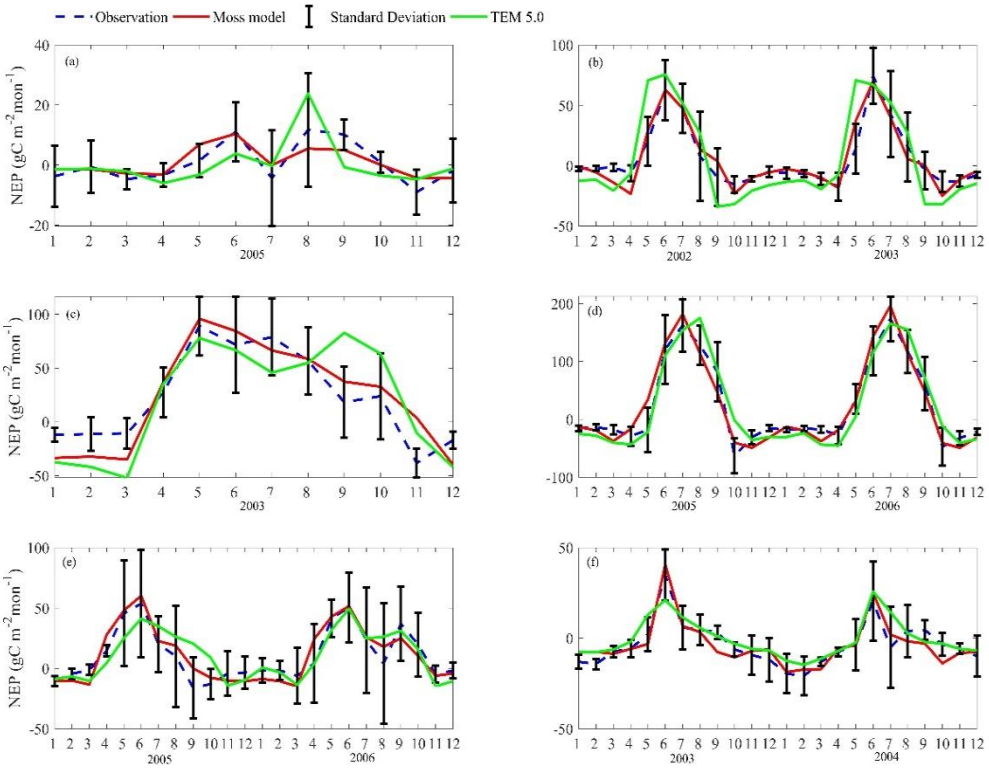

Figure 4.5. Comparison between observed and simulated NEP (gC $m^{-2}mon^{-1}$) at: (a) Ivotuk (alpine tundra), (b) UCI-1964 burn site (boreal forest), (c) Howland Forest (main tower) (temperate coniferous forest), (d) Bartlett Experimental Forest (Temperate deciduous forest), (e) Brookings (Grassland), and (f) Atqasuk (Wet tundra). Note: scales are different.

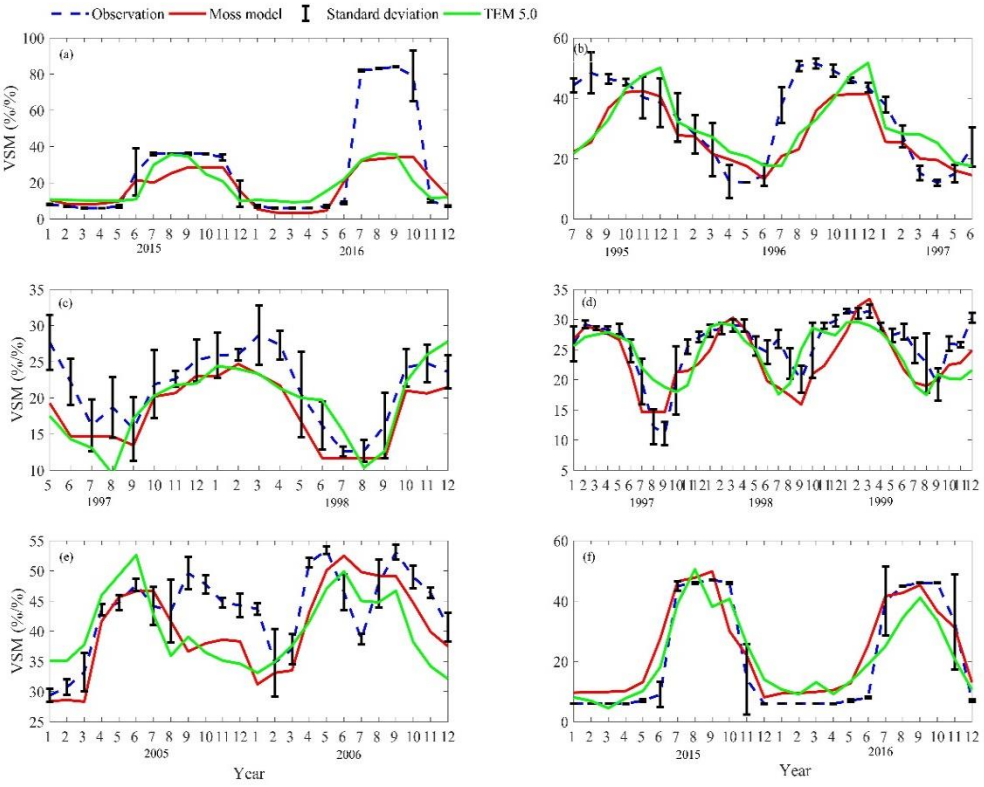

Figure 4.6. Comparison between observed and simulated volumetric soil moisture (VSM, %/%) at: (a) US-Ivo (alpine tundra), (b) BOREAS NSA-OBS (boreal forest), (c) NL-Loo (temperate coniferous forest), (d) DK-Sor (Temperate deciduous forest), (e) US-Bkg (Grassland), and (f) US-Atq (Wet tundra). Note: scales are different.

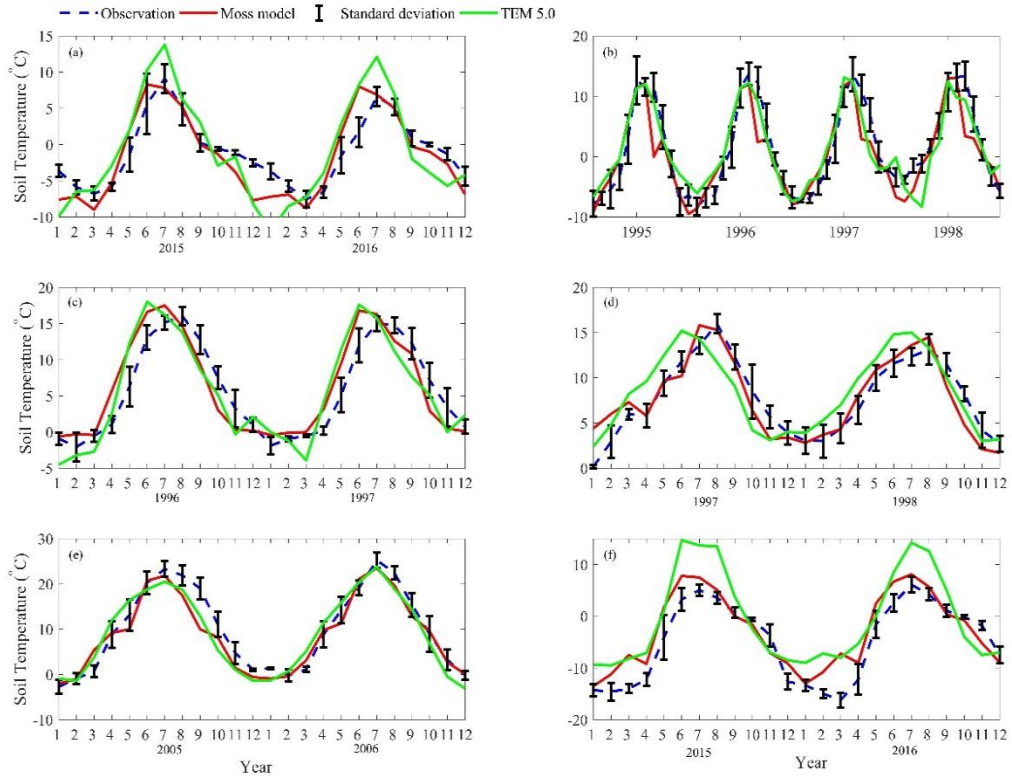

Figure 4.7. Comparison between observed and simulated soil temperature at 5cm depth (°C) at: (a) US-Ivo (alpine tundra), (b) BOREAS NSA-OBS (boreal forest), (c) US-Ho1 (temperate coniferous forest), (d) BE-Vie (Temperate deciduous forest), (e) US-Bkg (Grassland), and (f) US-Atq (Wet tundra). Note: scales are different.

Table 4.6. Model validation statistics for TEM_Moss and TEM 5.0 at six sites with NEP data

Site Name	Vegetation type	Models	Intercept	Slope	R-square	Adjusted R-square	RMSE	p-value
Ivotuk	Alpine tundra	TEM_Moss	0.46	0.61	0.72	0.70	3.57	<0.001
		TEM 5.0	-0.22	0.75	0.43	0.41	5.88	0.02
UCI-1964 burn site	Boreal forest	TEM_Moss	-0.13	1.01	0.91	0.90	8.33	<0.001
		TEM 5.0	-2.45	1.29	0.75	0.74	20.1	<0.001
Howland Forest (main tower)	Temperate coniferous forest	TEM_Moss	-1.28	1.05	0.83	0.81	19.69	<0.001
		TEM 5.0	-2.22	0.97	0.62	0.61	31.23	0.002
Bartlett Experimental Forest	Temperate deciduous forest	TEM_Moss	-0.49	1.03	0.94	0.94	19.06	<0.001
		TEM 5.0	-2.49	1.04	0.91	0.89	23	<0.001
Brookings	Grassland	TEM_Moss	0.36	1.02	0.85	0.84	8.95	<0.001
		TEM 5.0	2.58	0.75	0.62	0.6	13.07	<0.001
Atqasuk	Wet tundra	TEM_Moss	-0.36	0.97	0.84	0.83	5.13	<0.001
		TEM 5.0	1.99	0.75	0.75	0.74	6.56	<0.001

Table 4.7. Model validation statistics for TEM_Moss and TEM 5.0 at six sites with volumetric soil moisture data

Site ID	Vegetation type	Models	Intercept	Slope	R-square	Adjusted R-square	RMSE	p-value
US-Ivo	Alpine tundra	TEM_Moss	8.56	0.34	0.74	0.72	20.8	<0.001
		TEM 5.0	10.67	0.29	0.64	0.62	21.76	<0.001
BOREAS NSA-OBS	Boreal forest	TEM_Moss	10.71	0.51	0.52	0.51	11.1	<0.001
		TEM 5.0	16.47	0.43	0.32	0.31	11.96	<0.001
NL-Loo	Temperate coniferous forest	TEM_Moss	0.47	0.82	0.83	0.81	4.0	<0.001
		TEM 5.0	3.75	0.72	0.49	0.48	4.5	<0.001
DK-Sor	Temperate deciduous forest	TEM_Moss	1.39	0.86	0.67	0.65	3.65	<0.001
		TEM 5.0	10.41	0.54	0.4	0.39	4.06	<0.001
US-Bkg	Grassland	TEM_Moss	5.64	0.8	0.51	0.49	6.05	<0.001
		TEM 5.0	22.24	0.41	0.21	0.2	7.34	0.027
US-Atq	Wet tundra	TEM_Moss	7.76	0.77	0.87	0.85	7.38	<0.001
		TEM 5.0	6.74	0.68	0.85	0.84	7.63	<0.001

Table 4.8. Model validation statistics for TEM_Moss and TEM 5.0 at six sites with soil temperature at 5cm depth data

Site ID	Vegetation type	Models	Intercept	Slope	R-square	Adjusted R-square	RMSE	p-value
US-Ivo	Alpine tundra	TEM_Moss	-0.34	1.16	0.83	0.82	2.54	<0.001
		TEM 5.0	0.54	1.36	0.75	0.73	3.94	<0.001
BOREAS NSA-OBS	Boreal forest	TEM_Moss	-0.05	0.91	0.9	0.88	2.24	<0.001
		TEM 5.0	0.27	0.81	0.84	0.82	2.9	<0.001
US-Ho1	Temperate coniferous forest	TEM_Moss	0.7	0.95	0.81	0.79	2.93	<0.001
		TEM 5.0	-0.06	0.99	0.77	0.76	3.41	<0.001
BE-Vie	Temperate deciduous forest	TEM_Moss	0.57	0.92	0.83	0.81	1.82	<0.001
		TEM 5.0	1.88	0.85	0.69	0.68	2.56	<0.001
US-Bkg	Grassland	TEM_Moss	0.17	0.87	0.91	0.89	2.87	<0.001
		TEM 5.0	-0.01	0.91	0.89	0.87	3.04	<0.001
US-Atq	Wet tundra	TEM_Moss	1.36	0.86	0.84	0.82	3.63	<0.001
		TEM 5.0	4.33	0.99	0.75	0.74	6.17	<0.001

4.4.2 Regional carbon dynamics during the 20th century

Both TEM-Moss and TEM 5.0 were used to simulate northern high-latitude regional carbon balance during the 20th century (Figure 4.8). Higher NEP was correlated with the combination of relatively higher NPP and lower heterotrophic respiration (R_H). TEM-Moss indicated that the northern high latitudes acted as a carbon sink of 221.9 Pg with an inter-annual standard deviation of 0.31 PgC yr^{-1} during the 20th century, which is 132.7 Pg larger than 89.2 Pg simulated by TEM 5.0 (Figure 4.8). The simulated NEP by TEM-Moss ranges from 1.38 PgC yr^{-1} to 3.05 PgC yr^{-1}, while the range by TEM 5.0 was from 0.11 PgC yr^{-1} to 1.75 PgC yr^{-1} (Figure 4.8). The patterns of the simulated NEP from two models were similar, both showing a general increasing trend throughout the 20th century (Figure 4.8). By 2000, the TEM-Moss simulation indicated that the northern high-latitude region stored 3.05 PgC yr^{-1}, which is more than twice as the storage estimated by TEM 5.0 (1.33 PgC yr^{-1}, Figure 4.8). Both models indicated that carbon uptake by the northern ecosystems during the second half of the 20th century was higher than the first half for most part of the region, and only a small portion of the region lost carbon in last century (Figure 4.9).

Simulated total NPP by TEM-Moss was 9.6 PgC yr^{-1}, ranging from 8.52 PgC yr^{-1} to 10.65 PgC yr^{-1} in the 20th century, with 1.69 PgC yr^{-1} of moss NPP and 7.93 PgC yr^{-1} of higher plant NPP (Figure 4.8, Table 4.9). Moss NPP ranges from 1.23 PgC yr^{-1} to 2.14 PgC yr^{-1} and the ratio of moss NPP to higher plant NPP is 0.21 (Figure 4.8). TEM 5.0 estimated 0.8 PgC yr^{-1} lower total NPP than TEM-Moss, but 0.87 PgC yr^{-1} higher NPP for higher plants (Figure 4.8, Table 4.9). On the other hand, average heterotrophic respiration in the 20th century was 7.38 PgC yr^{-1} and all years were within about 5% of this value (Figure 4.8, Table 4.9). TEM 5.0 projected 0.53 PgC yr^{-1} higher

R_H than TEM-Moss (7.91 PgC yr^{-1}, Figure 4.8). Overall, TEM-Moss predicted higher total NPP but lower R_H, which jointly caused a pronounced difference in NEP between two models.

Both models estimated that soil organic carbon and vegetation carbon were accumulating continuously in the 20th century (Figure 4.10). TEM-Moss indicated that regional SOC and VEGC accumulated 96.3 PgC and 115.2 PgC, respectively, and the carbon uptake by moss was 10.4 Pg in the period (Figure 4.10, Table 4.10). As simulated by TEM-Moss, 43.4%, 51.9% and 4.7% of total carbon uptake in the region was assimilated to soils, higher plants and mosses, respectively (Table 4.10). TEM 5.0 simulated that SOC increased by 31.7 Pg at the end of the 20th century, which is 64.6 PgC less than the value estimated by TEM-Moss (Table 4.10). TEM 5.0 estimated 57.7 PgC in plants less than the value estimated by TEM-Moss (57.5 PgC, Table 4.10). 35.5% and 64.5% of total carbon was as SOC and VEGC, respectively.

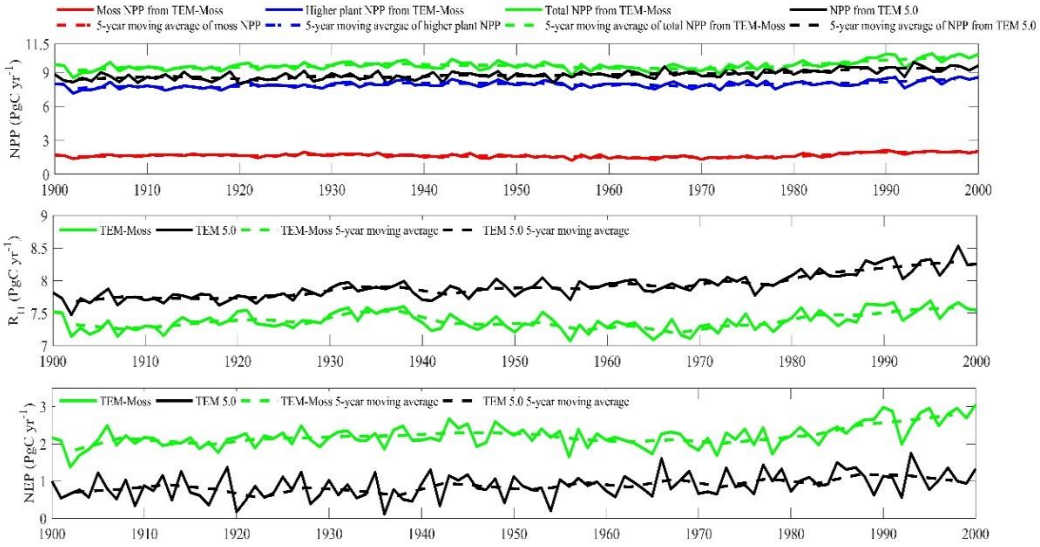

Figure 4.8. Simulated annual net primary production (NPP, a), heterotrophic respiration (R_H, b), and net ecosystem production (NEP, c) during the 20th century by TEM_Moss and TEM 5.0.

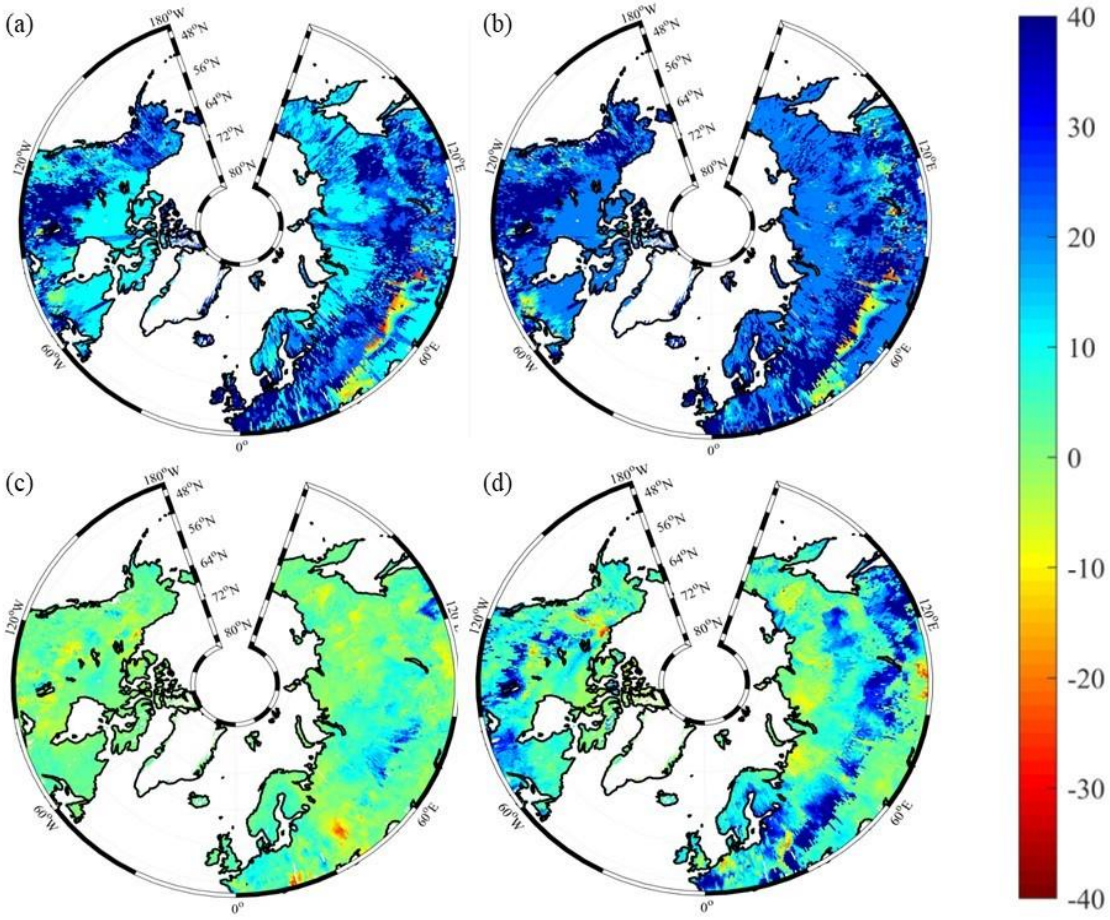

Figure 4.9. Spatial distribution of NEP simulated by TEM_Moss for the periods (a) 1900–1950, (b) 1951–2000, and by TEM 5.0 for the periods (c) 1900–1950, (d) 1951–2000. Positive values of NEP represent sinks of CO_2 into terrestrial ecosystems, while negative values represent sources of CO_2 to the atmosphere.

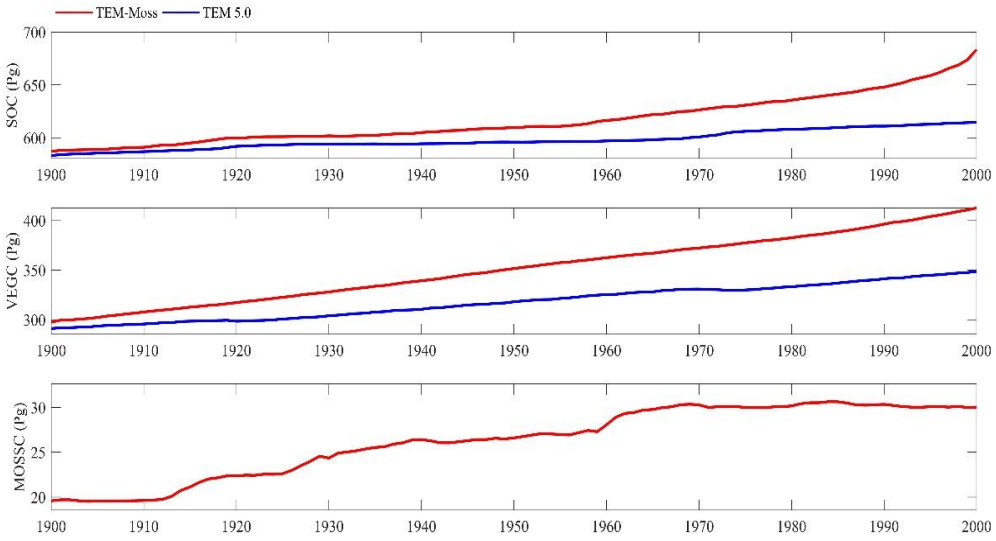

Figure 4.10. Simulated annual soil organic carbon (SOC, a), vegetation carbon (VEGC, b), and moss carbon (MOSSC, c) during the 20th century by TEM_Moss and TEM 5.0

Table 4.9. Average annual NPP, R_H and NEP (as Pg C per year) during the 20th century estimated by two models.

Average annual carbon fluxes (PgC yr^{-1})		TEM_Moss	TEM 5.0	Difference	Moss NPP/ Higher plant NPP
NPP	Moss NPP	1.69	-	-	21.3%
	Higher plant NPP	7.93	8.8	-	
	Total NPP	9.6	8.8	0.8	
R_H		7.38	7.91	-0.53	
NEP		2.22	0.89	1.33	

Table 4.10. Increasing of SOC, vegetation carbon (VGC), and moss carbon (MOSSC) from 1900 to 2000, and total carbon storage during the 20th century predicted by two models.

Models	Carbon pools	Carbon pool amounts in 1900/2000 (units: Pg)	Changes in carbon pools during the 20th century (units: Pg)
TEM-Moss	SOC	587.1/683.4	96.3
	VEGC	297.5/412.7	115.2
	MOSSC	19.6/30	10.4
	Total	904.2/1126.1	221.9
TEM 5.0	SOC	583.2/614.9	31.7
	VEGC	291.1/348.6	57.5
	Total	874.3/963.5	89.2

4.4.3 Regional carbon dynamics during the 21st century

Under the RCP 2.6 scenario, TEM-Moss simulated NEP of 2.07 PgC yr^{-1} with the range from 0.41 PgC yr^{-1} to 3.2 PgC yr^{-1}, and the inter-annual standard deviation of 0.59 PgC yr^{-1} during the 21st century (Figure 4.11 (a)). The regional sink shows a decreasing pattern in the 2000s and then generally increases over the remaining years of the 21st century (Figure 4.11 (a)). For comparison, TEM 5.0 predicted that the average NEP of 0.28 PgC yr^{-1} with the range from -1.48 PgC yr^{-1} to 1.69 PgC yr^{-1} during the 21st century (Figure 4.11 (a), Table 4.11 (b)). Thus, TEM 5.0 projected 179.1 PgC stored in northern ecosystems is less than the estimation from TEM-Moss in the 21st century (Table 4.11 (b)). Besides, TEM 5.0 simulated that the regional NEP showed a decreasing trend and the region fluctuates between sinks and sources during the century (Figure 4.11 (a)). The spatial patterns from two models also showed differences. TEM-Moss indicated that the region accumulates carbon over this century, while TEM 5.0 simulated that some regions changed from a carbon sink to a source in the second half of the century (Figure 4.12 (a)). Simulated regional NPP by TEM-Moss ranges from 11.2 to 13.7 PgC yr^{-1} with a mean of 12.98 PgC yr^{-1} in this century, while average NPP predicted by TEM 5.0 is 1.46 PgC yr^{-1} lower than that value (11.52 PgC yr^{-1} (Figure 4.11(a), Table 4.11(b)). TEM-Moss simulated NPP has 3.74 PgC yr^{-1} from moss and 9.24 PgC yr^{-1} from higher plants, which account for 28.8% and 71.2% of total NPP, respectively (Figure 4.11(a), Table 4.11(b)). Meanwhile, TEM-Moss estimated that R_H is 10.91 PgC yr^{-1}, while TEM 5.0 predicted it as 0.33 PgC yr^{-1}, which is higher (Figure 4.11(a), Table 4.11(b)). Both models projected that soil organic carbon and vegetation carbon accumulate in this century but with different magnitudes (Figure 4.13 (a)). TEM-Moss predicted that regional SOC and VEGC accumulated 84.7 PgC and 112.6 PgC, respectively, during the 21st century, while TEM 5.0 predicted that a smaller increase with 12.1 and 15.5 PgC in SOC and VEGC, respectively

(Figure 4.13 (a), Table 4.12 (a)). Besides, TEM-Moss also predicted an increasing of 9.4 PgC in MOSSC, accounting for 4.5% of the total carbon uptake in this region (Table 4.12(a)).

Under the RCP 8.5 scenario, TEM-Moss simulated annual NPP of 13.84 PgC yr^{-1} with a range from 11.09 to 16.94 PgC yr^{-1}, which is 1.31 PgC yr^{-1} higher than the projection from TEM 5.0 (Figure 4.11 (b)). Total NPP estimated by TEM-Moss has 3.84 PgC yr^{-1} from moss and 10 PgC yr^{-1} from higher plants (Figure 4.11(b), Table 4.11(a)). Annual R_H was 11.28 PgC yr^{-1} estimated by TEM-Moss and 11.54 PgC yr^{-1} by TEM 5.0, respectively (Figure 4.11(b), Table 4.11(a)). Consequently, TEM-Moss projected NEP was 2.56 PgC yr^{-1} with the inter-annual standard deviation of 0.93 PgC yr^{-1} in this century (Figure 4.11 (b)). NEP ranges from 0.67 PgC yr^{-1} to 4.78 PgC yr^{-1} estimated with TEM-Moss, while from -1.69 PgC yr^{-1} to 2.65 PgC yr^{-1} with a mean of 0.99 PgC yr-1 was estimated by TEM 5.0 (Figure 4.11 (b)). TEM-Moss predicted more carbon uptake of 157.5 Pg than TEM 5.0 during the 21st century. Both models predicted that NEP showed an increasing trend during the 21st century (Figure 4.11 (b)). Moreover, similar spatial patterns of carbon sinks and sources appeared in the projections from two models (Figure 4.12 (b)). Soil organic carbon and vegetation carbon shows an increasing trend from both models (Figure 4.13 (b)). Regional SOC and VEGC increased by 92.5 PgC and 153.6 PgC, respectively by the end of the 21st century predicted by TEM-Moss. In contrast, the increase of 44.2 PgC and 54.5 PgC of SOC and VEGC, respectively, was predicted by TEM 5.0 (Figure 4.13 (b), Table 4.12 (b)). TEM-Moss predicted an increase of 10.1 PgC in MOSSC (Table 4.12(b)).

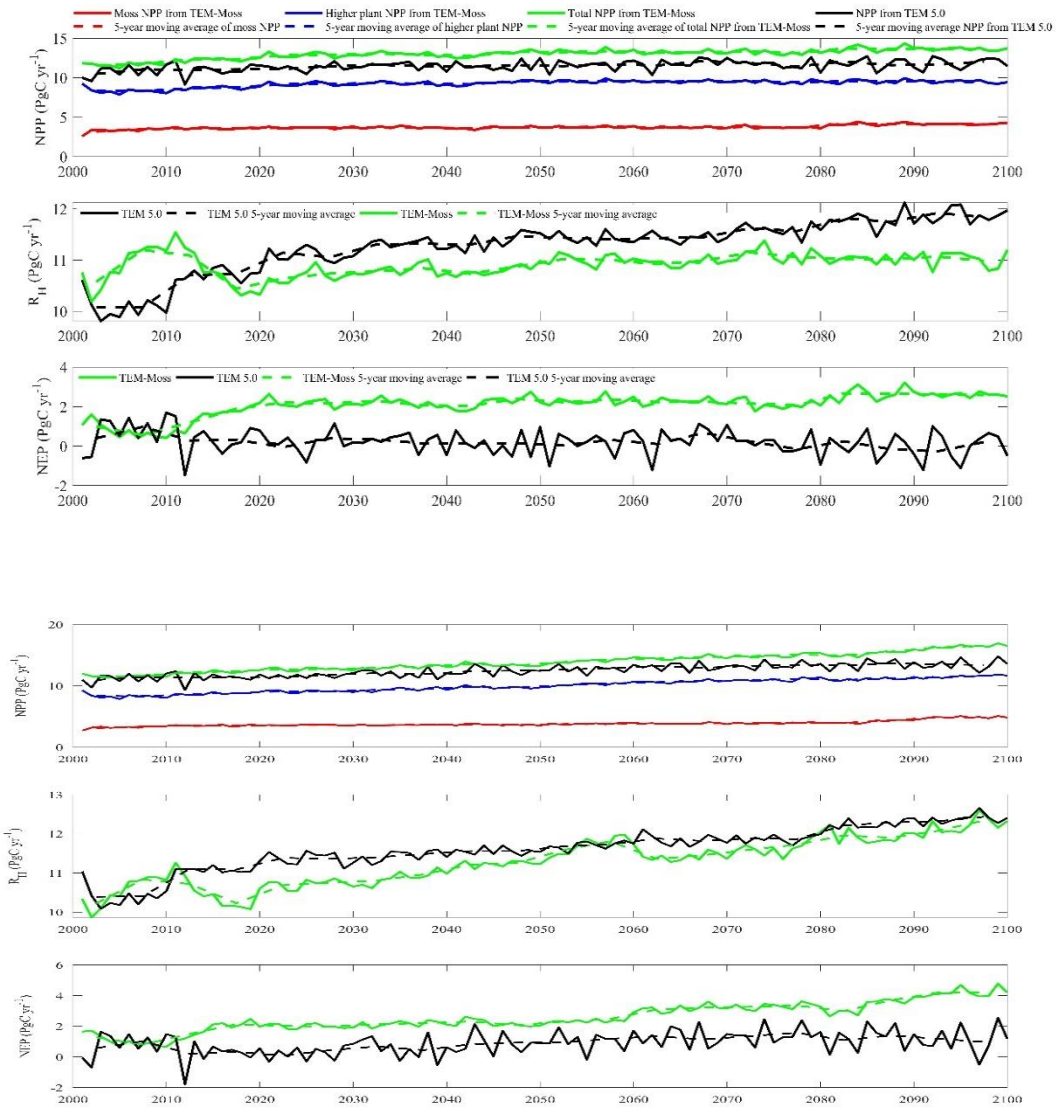

Figure 4.11. Predicted changes in carbon fluxes: annual net primary production (NPP, (a, d)), heterotrophic respiration (R_H, (b, e)), and net ecosystem production (NEP, (c, f)) during the 21st century under RCP 2.6 scenario (a, b, c, upper panel) and RCP 8.5 scenario (d, e, f, bottom panel) by TEM_Moss and TEM 5.0.

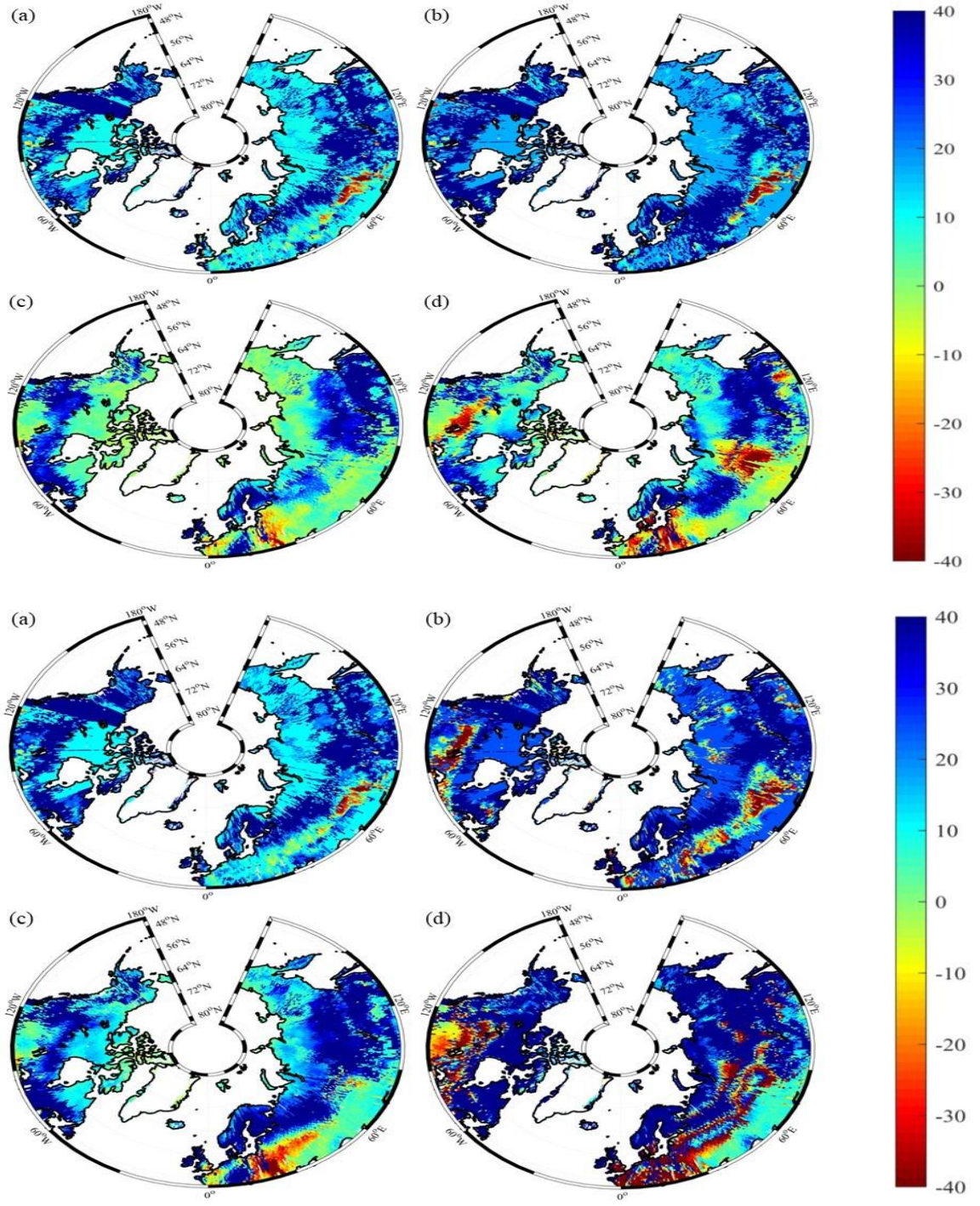

Figure 4.12. Spatial distribution of NEP simulated for the periods (a) 2000–2050, (b) 2051–2099 by TEM_Moss, and by TEM 5.0 (c, d) during the 21st century under RCP 2.6 scenario (upper panel) and RCP 8.5 scenario (bottom panel). Positive values of NEP represent sinks of CO_2 into terrestrial ecosystems, while negative values represent sources of CO_2 to the atmosphere.

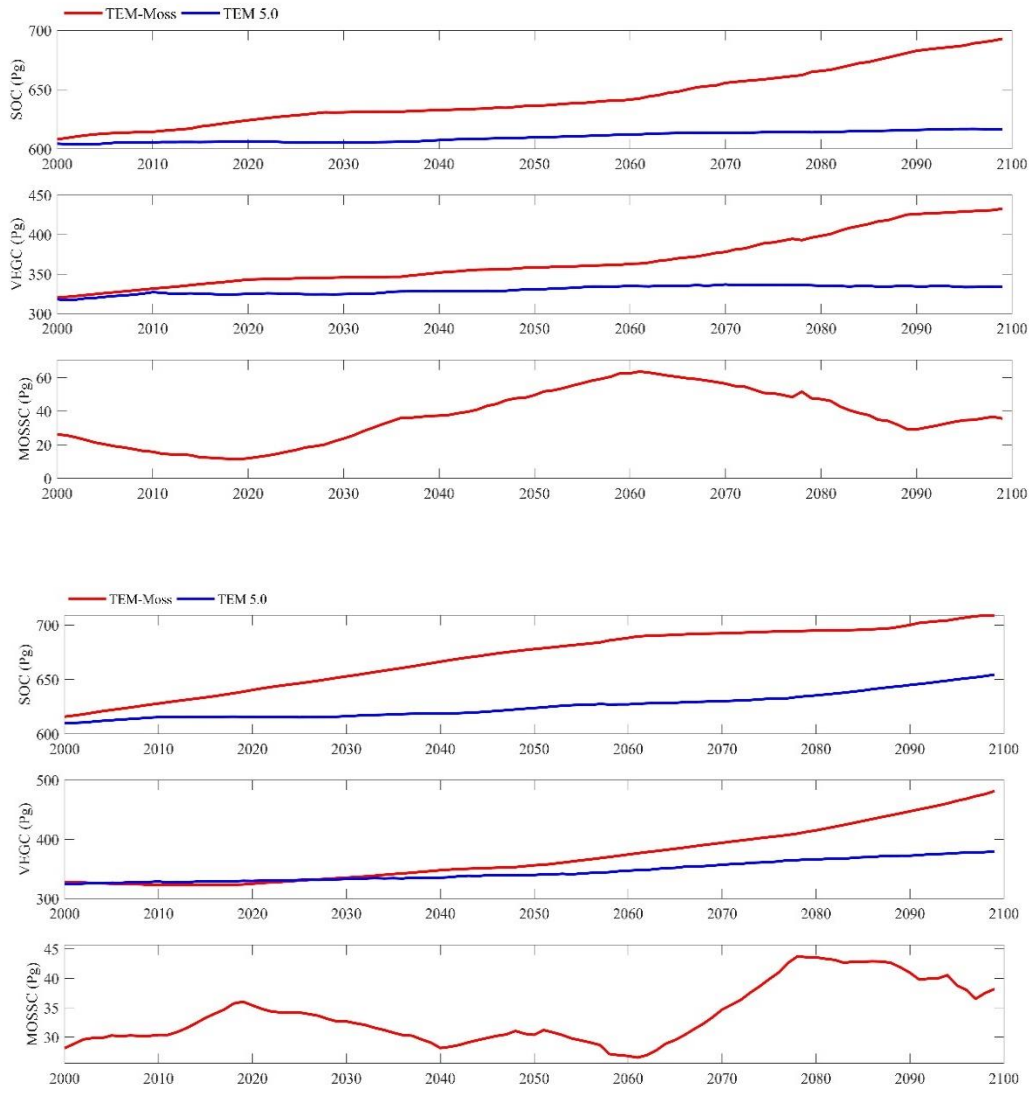

Figure 4.13. Simulated annual soil organic carbon (SOC, a), vegetation carbon (VEGC, b), and moss carbon (MOSSC, c) during the 21st century by TEM_Moss and TEM 5.0 under RCP 2.6 scenario (upper panel) and RCP 8.5 scenario (bottom panel).

Table 4.11. Average annual NPP, R_H and NEP (as Pg C per year) during the 21st century estimated by two models under (a) RCP 8.5 scenario and (b) RCP 2.6 scenario.

(a)

Average annual carbon fluxes (PgC yr^{-1})		TEM_Moss	TEM 5.0	Difference	Moss Higher NPP	NPP/ plant
NPP	Moss NPP	3.84	-	-	38.4%	
	Higher plant NPP	10	12.53	-		
	Total NPP	13.84	12.53	1.31		
R_H		11.28	11.54	-0.21		
NEP		2.56	0.99	1.57		

(b)

Average annual carbon fluxes (PgC yr^{-1})		TEM_Moss	TEM 5.0	Difference	Moss Higher NPP	NPP/ plant
NPP	Moss NPP	3.74	-	-	40.5%	
	Higher plant NPP	9.24	11.52	-		
	Total NPP	12.98	11.52	1.46		
R_H		10.91	11.24	-0.33		
NEP		2.07	0.28	1.79		

Table 4.12. Increasing of SOC, vegetation carbon (VGC), and moss carbon (MOSSC) from 1900 to 2000, and total carbon storage during the 21st century predicted by two models under (a) RCP 2.6 scenario and (b) RCP 8.5 scenario.

(a)

Models	Carbon pools	Carbon pool amounts in 2000/2099 (units: Pg)	Changes in carbon pools during the 21st century (units: Pg)
TEM-Moss	SOC	608.1/692.8	84.7
	VEGC	320.2/432.8	112.6
	MOSSC	26.2/35.6	9.4
	Total	954.5/1161.2	206.7
TEM 5.0	SOC	604.4/616.5	12.1
	VEGC	318.2/333.7	15.5
	Total	922.6/950.2	27.6

(b)

Models	Carbon pools	Carbon pool amounts in 2000/2099 (units: Pg)	Changes in carbon pools during the 21st century (units: Pg)
TEM-Moss	SOC	615.9/708.4	92.5
	VEGC	327.8/481.4	153.6
	MOSSC	28.1/38.2	10.1
	Total	971.8/1228.0	256.2
TEM 5.0	SOC	610.2/654.4	44.2
	VEGC	324.9/379.4	54.5
	Total	935.1/1033.8	98.7

4.5 Discussion

4.5.1 The role of moss in the regional carbon dynamics

Global warming has been pronounced in recent decades, particularly at high latitudes (IPCC, 2014; Tape et al., 2006; Stow et al., 2004). An enormous amount of soil organic carbon stored in northern high-latitude regions (Tarnocai et al., 2009; Schuur et al., 2008) is expected to affect a broad spectrum of ecological and human systems, and cause rapid changes in the Earth system when undergoing substantial climate change (Serreze and Francis 2006; Davidson and Janssens, 2006; McGuire et al., 2009). Improving projections for carbon budget of high latitude terrestrial ecosystems is essential for understanding global carbon–climate feedbacks (Melillo et al., 2011; Todd-Brown et al., 2013).

Our simulations suggest that mosses play an important role in the regional carbon dynamics, which is consistent with previous studies (McGuire et al., 2009; Turetsky et al., 2012). First of all, mosses are productive with carbon assimilation even during low temperature, water content and irradiance (Kallio and Heinonen, 1975; Harley et al., 1989). For example, mosses can tolerate drought through physiological responses, such as by suspending metabolism and by withstanding cell dessication (Turetsky et al., 2012; Oechel and Van Cleve, 1986). The key functional traits related to water, nutrient, and thermal tolerances of mosses enable them to fit in harsh northern conditions (Shetler et al., 2008; Turetsky et al., 2012). Thus, with incorporation of moss into our models, NPP estimation in our model is improved. Mosses also act as a powerful competitor with vascular plants for nutrient uptake. Their rapid nutrient acquisition and slow nutrient loss through slow decomposition may constrain concentrations of plant-available nitrogen (Hobbie et al., 2000; Turetsky et al., 2010; Oechel and Van Cleve, 1986; Gornall et al., 2007), which will further decrease NPP of higher plant. Our model results suggested that the NPP of higher plants

considering moss is indeed lower than previous NPP estimates without considering moss, but the total NPP is larger than before. We estimated that mosses contribute 17.6% of NPP in the 20th century, and 28.8% and 27.6% in the 21st century under the RCP 2.6 and RCP 8.5 scenarios, respectively. This is comparable with the results reported by Turetsky et al. (2010), which suggested an average contribution of 20% of aboveground NPP from moss in boreal forests. Frolking et al. (1996) even reported a contribution of 38.4% to total NPP by moss at a boreal forest site. Moreover, mosses can also influence heterotrophic respiration (R_H) through their effects on soil thermal and hydrologic dynamics (Zhuang et al., 2001). With the layer of moss, soil temperature tends to decrease but soil moisture tends to increase (Oechel and Van Cleve, 1986), which will further decrease soil respiration in summer. This supports our results that TEM_Moss simulated R_H is lower than that by TEM 5.0. With a combination of higher NPP and lower R_H, NEP predicted by TEM_Moss is larger than that by TEM 5.0. The two contrasting regional simulations by TEM-Moss and TEM 5.0 indicated the region is currently a carbon sink, which is consistent with previous studies (White et al., 2000; McGuire et al., 2009; Schimel et al., 2001). Our study estimated that regional NEP during the 20th century is 2.2 Pg C yr^{-1} by TEM_Moss and 0.89 Pg C yr^{-1} by TEM 5.0, respectively. In the 1990s, the regional sink is projected to be 2.7 and 1.1 Pg C yr^{-1} by TEM_Moss and TEM 5.0 respectively. Compared with other existing studies, our regional estimates of NEP are within the reasonable range from other existing studies. McGuire et al. (2009) estimated a land sink of 0.3–0.6 Pg C yr^{-1} for the pan-arctic region for the 1990s, which is closer to our estimation by TEM 5.0 but less than the projection by TEM_Moss. The top-down atmospheric analyses indicate that the sink of pan-arctic region is between 0 and 0.8 Pg C yr^{-1} in the 1990s (Menon et al. 2007). Besides, Schimel et al. (2001) reported an estimation of the northern extratropical NEP is from 0.6 to 2.3 PgC yr^{-1} in the late 20th century, which is comparable to our

estimates. Our simulations also confirmed that mosses and higher plants respond to climate change similarly in terms of their productivity (Turetsky et al. 2010).

4.5.2 Model Uncertainty and limitations

There are a number of uncertainty sources in our model simulations. First, the errors in the observed data will influence our parameterization results, which will bias our regional estimates of carbon dynamics. Second, climatic driving data are also a source of uncertainty for historical and future simulations. Third, model assumptions will also induce additional uncertainties. For instance, we assumed that vegetation distribution will remain unchanged during the transient simulation. However, vegetation will change in response to warming climate and disturbances such as fire and insect outbreaks in the region (Hansen et al., 2006), which will affect carbon budget. Missing potential responses to disturbances in our model shall introduce additional uncertainties (Soja et al. 2007; Kasischke and Turetsky, 2006).

We conducted ensemble regional simulations with 50 sets of parameters to quantify model uncertainty due to uncertain parameters. The 50 sets of parameters were obtained using the method in Tang and Zhuang (2008). The ensemble means and the inter-simulation standard deviations are used to measure the model uncertainty (Figure 4.14). TEM_Moss predicted that the regional cumulative carbon ranges from a carbon loss of 266 Pg C to a carbon sink of 567.3 Pg C by different ensemble members, with a mean of 161.1±142.1 Pg during the 21st century under the RCP 2.6 scenario. Under the RCP 8.5 scenario, TEM_Moss predicted that the region acts from a carbon source of 79.1 Pg C to a carbon sink of 625.9 Pg C, with a mean of 186.7±166.1 Pg during the 21st century (Figure 4.14).

This study took an important step to incorporate moss into an extant ecosystem model that has not explicitly consider the role of moss and its interactions with higher plants. Our model

simulations showed that mosses have strong influences on regional ecosystem carbon cycling, by affecting the soil thermal, nitrogen availability, and water conditions of terrestrial ecosystems. However, there are still limitations in our model. First, we did not differentiate various kinds of mosses because they have their own functional traits. The structural and physiological traits of mosses will differ largely in different moss groups, such as feather moss versus Sphagnum (Turetsky et al., 2010). In addition, we lack spatially explicit information of moss distribution in the region, which will lead to a large regional uncertainty of carbon quantification. Another limitation is that some important physiological traits of moss have not been modeled. For example, moss abundance may change following shifts in vascular species composition due to shading or burial by vascular litter (Turetsky et al., 2010; Cornelissen et al., 2007). Furthermore, disturbance such as wildfires can also influence moss activities.

(a)

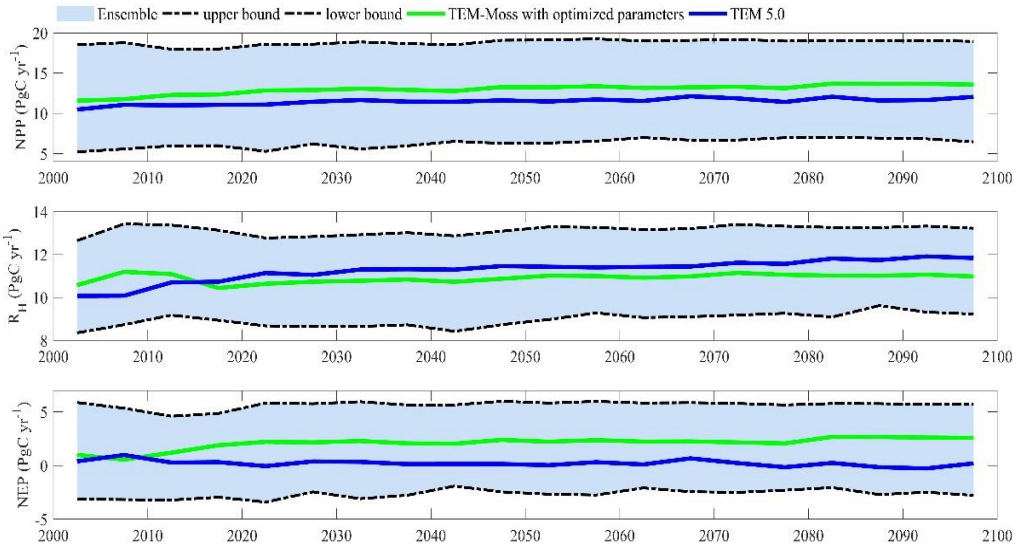

(b)

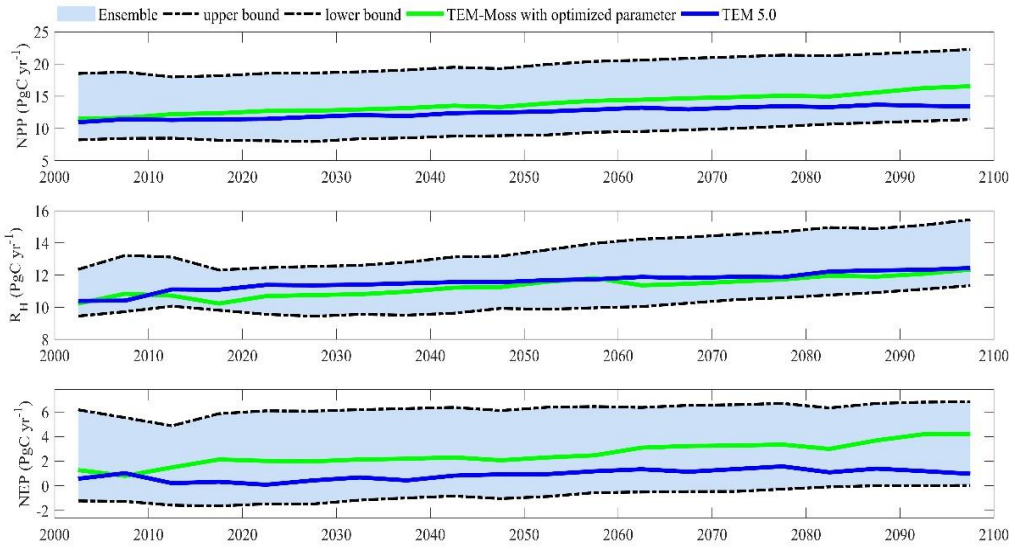

Figure 4.14. 5-year moving average plots for carbon fluxes under the (a) RCP 2.6 scenario and (b) RCP 8.5 scenario. The blue area represents the upper and lower bounds of simulations.

4.6 Conclusions

This study explicitly incorporated moss into an extant process-based terrestrial ecosystem model to investigate the carbon dynamics in the Arctic for the past and this century. Historical regional simulations with TEM_Moss indicated that the region is a carbon sink of 221.9 PgC over the 20th century, and this sink may decrease to 206.7 PgC under the RCP 2.6 scenario or increase to 256.2 PgC under the RCP 8.5 scenario during the 21st century. Compared with an earlier version of TEM that has not explicitly modeled moss, TEM_Moss projected that the region stored 132.7 Pg more C over the last century, 179.1 Pg and 157.5 Pg more C under the RCP 2.6 and RCP 8.5 scenarios, respectively. This study demonstrated that moss activities have large effects on ecosystem soil thermal, water, and carbon dynamics through their interactions with higher plants. This study highlights the importance of considering the moss dynamics in Earth System Models to adequately quantify the carbon–climate feedbacks in the Arctic.

4.7 Acknowledgments

This research was supported by an NSF project (IIS-1027955), a DOE project (DE-SC0008092), and a NASA LCLUC project (NNX09AI26G). We acknowledge the Rosen High Performance Computing Center at Purdue for computing support. We also acknowledge the World Climate Research Programme's Working Group on Coupled Modeling Intercomparison Project CMIP5, and we thank the climate modeling groups for producing and making available their model output.

CHAPTER 5. CONCLUSION AND FUTURE WORK

Climate over northern high latitudes regions (> 45 °N) has been warming with elevated atmospheric CO_2 in recent decades. The large amount of carbon stored in this region is particularly vulnerable to climate change. To better understand the carbon–climate feedbacks, more accurate models that are incorporated with the new knowledge of microbe and plant sciences are needed. This dissertation research seeks to improve the Arctic carbon budget quantification by refining model representation and investigates the interactions between northern high-latitude ecosystems and climate change. Through inter-comparisons among models, the importance of representation of detailed microbial physiology and the moss dynamics in Earth System Models were highlighted. A series of model developments, model calibration and verification with in-situ observations and remote sensing data, and model simulations and uncertainty analysis have been conducted to fulfill the research tasks. In this chapter, I first summarized main findings of this dissertation research corresponding to research questions raised in Chapter 1. Second, I will discuss limitations in current models and provided suggestions and directions for future earth system modeling to enhance our understanding to interactions of climate change and ecosystems.

5.1 Summary and Conclusions

1) Chapter 2 evaluates the necessity of replacing the traditional Q_{10}-based soil decomposition processes with detailed microbial-based soil decay process, and investigates the carbon dynamics in northern high-latitude regions for the past and this century by applying these two contrasting models. Although both models can reproduce the observed net ecosystem production (NEP) from field studies reasonably well, the model with more detailed microbial mechanisms tends to perform better than traditional model at site level. Meanwhile, microbial

models also show better results on net primary production (NPP) estimation than traditional model at regional level. Contrasting regional simulations with two models differ in last and this century. Specifically, microbial model indicated the region is a carbon sink in the 20th century, and this sink will increase in the 21st century under the RCP 8.5 scenario but shift to a carbon source under the RCP 2.6 scenario. Whereas traditional model estimated the region always acts as a carbon sink with larger magnitude during the 20th century and the 21st century under both scenarios.

2) Chapter 3 quantified impacts of microbial dormancy on Arctic terrestrial ecosystem carbon budget by comparing microbial-based model with and without dormancy trait consideration, and examined the fate of large Arctic soil carbon under changing climate conditions during the 20th and 21st century. The dormancy model produced a better match with field observed net ecosystem production (NEP) and heterotrophic respiration (R_H) in comparison with the no-dormancy model. The long-term trajectories of Arctic carbon dynamics also differ in two models. The regional modeling results by the dormancy model indicated the region is a carbon sink in the 20th century, and this sink could decrease under both RCP 8.5 and RCP 2.6 scenarios during the 21st century. While the carbon sink estimated by no-dormancy model during the 20th and 21st century is much less compared to the dormancy model. Whether considering microbial dormancy or not can cause large differences in carbon budget estimation between two models, which highlights the critical role of microbial dormancy in high latitudes.

3) In Chapter 2 and Chapter 3 studies, the microbial-based model (MIC-TEM) predicted less carbon accumulation than traditional terrestrial ecosystem model (TEM 5.0) in last and this century, while the dormancy version (MIC-TEM-dormancy) projected much more carbon accumulation than MIC-TEM. Considering the collective effects of microbial physiology and

microbial dormancy, the MIC-TEM-dormancy also predicted large magnitude of carbon sink than TEM 5.0 in last and this century.

4) Chapter 4 assessed the role of moss dynamics in Arctic carbon–climate feedbacks by explicitly incorporating moss into an extant process-based terrestrial ecosystem model to investigate the carbon dynamics in the Arctic for the past and this century. In the new model, moss was treated as a plant functional type to adequately model the interactions between higher plants and mosses and their competition for energy, water, and nutrient. With considering the activities of moss, the new model simulations better match observed net ecosystem production (NEP), soil moisture and soil temperature data than previous model without moss. We applied two models to project historical and future carbon budgets in the Arctic. Both models estimated that this region acted as a carbon sink in the 20th century, and this sink will increase in the 21st century under the RCP 8.5 scenario but decrease under the RCP 2.6 scenario. However, compared to the traditional model without moss, the new model estimated a much higher carbon accumulation in the region during last and this century. Thus, this study highlights the necessity of coupling moss into Earth System Models to adequately quantify carbon dynamics in the Arctic.

5.2 Limitations and Future Research Directions

In this dissertation research, although results presented here are promising and encouraging, it is inevitable that some generic limitations still exist in current models. Main limitations may include insufficient model representations, simplified model structures, inadequate understanding on parameters, and limited data availability. Thus, more efforts are needed to make up these deficiencies in the future. In this section, I will discuss some existing limitations and point out several future research directions.

In Chapter 2 and Chapter 3, microbial activities including microbial-based soil decomposition and microbial dormancy were explicitly considered in my models. However, some other important microbial traits are still missing. For example, shift in microbial community structure, which is a vital common evolutionary trait of microbe, was not considered. Many documents have demonstrated that microbial community could shift with changing environment, including warming, precipitation and N fertilization (Treseder et al., 2011; Frey et al., 2013; Allison et al., 2009; Evans & Wallenstein, 2011). This shift will affect microbial physiology, growth rates, and its temperature sensitivity of heterotrophic respiration (Classen et al., 2015; Stone et al., 2012), which will further influence the soil decomposition and carbon dynamics (Treseder et al., 2011; Schimel & Schaeffer, 2012; Todd-Brown et al., 2011). Besides, mechanisms such as microbial acclimation have not yet been included in my models. Their adaption to temperature regime could decrease the warming-induced elevated respiration over time (Melillo et al. 1993; Todd-Brown et al., 2011), thus ignoring this mechanism could bias future soil decomposition analysis. Moreover, functional discrimination in microbial community compositions is another "missing part" (Strickland et al., 2009; Moorhead et al., 2006). Different functional microbial groups could vary in responses to environmental conditions (Balser et al. 2002; Fierer et al. 2007). Inexplicit representation of microbial functional groups may also induce uncertainty in carbon dynamics predictions (McGuire & Treseder, 2010; Schimel, 1995). Therefore, future modeling work should incorporate these new details into model structure to better represent microbial life-history traits and microbial community dynamics. At the same time, more experiments should be conducted to examine the functions of these key microbial physiology metrics to support the modeling work.

In addition to the limitation in model representation and model structure, our knowledge on related parameters also need to be updated. For example, temperature sensitivity of microbial carbon decomposition is currently modeled as involving a critical but controversial parameter, carbon-use-efficiency (CUE). Some empirical studies suggested that CUE decreases as temperature increases (Steinweg et al., 2008; Manzoni et al., 2012), while some found that CUE is invariant with temperature (López-Urrutia and Morán, 2007). Besides, theoretical and empirical studies also indicated that CUE decreases as nutrient substrate quality and availability decreases (Frey et al., 2013; Manzoni et al., 2012). In our models, CUE is assumed as a simple linear relationship with temperature, but no connection with nutrient availability. Thus, more experiments are needed in the future to adequately measure the important parameters that drive microbial and enzyme turnover since those parameters are commonly used across microbial-based models. Modelers are also required to advance their understanding on these functions and parameters with times.

In Chapter 4, I incorporated moss into an extant ecosystem model to explore the role of moss and its interactions with higher plants. I found that mosses affect regional ecosystem carbon cycling through influencing soil thermal, nitrogen availability, and water conditions of terrestrial ecosystems. Nevertheless, our model parameterization and validations were constrained on data availability. More data related moss physiology such as moss moisture, moss carbon and moss temperature, and regional spatial information of moss distribution are necessary to make the model calibration and validations more accurate. Thus, future field work needs to collect more data corresponding to the requirements of modeling work. In addition, similar to microbes in previous models, dissimilarity in structural and physiological traits of moss groups were also ignored in our moss model, which may bias regional carbon budgets prediction (Turetsky et al., 2010). Besides,

important physiological traits of moss such as changing of moss abundance following shifts in vascular species composition are still missing in current models (Turetsky et al., 2010; Cornelissen et al., 2007). Future work may include these essential moss physiological traits and moss community dynamics into modeling. Last but not least, symbiotic relationships between higher plants and fungi could be important to ecosystem carbon dynamics. Recent studies have shown that these symbiotic relationships are common in regions where soil nitrogen is in short supply (Schimel and Hättenschwiler, 2007), and in these cases the hyphae can provide nitrogen to plants, and in return, plants provide sugar to fungi (Hobbie and Hobbie, 2008, 2006). Although our study modeled the interactions between higher plants and moss, other interactions among higher plants and understory should be also explored in future modeling.

In addition, vegetation distributions are assumed to remain unchanged during the transient simulation in my analysis. However, vegetation can shift from one type to another to compete for light, nutrient, and water along with the climate change (White et al., 2000; Hansen et al., 2006; Lloyd, 2005). Besides, potential responses to disturbances such as fire and insect outbreaks are also neglected in my models. For instance, fire may alter the nitrogen cycle and water and energy exchanges between the atmosphere and ecosystems by destroying aboveground biomass and consuming organic soils (Harden et al., 2000; Kasischke and Turetsky, 2006; Soja et al., 2007). These disturbances and vegetation dynamics shall be factored into future regional carbon quantifications.

REFERENCES

Allison, E. H., Perry, A. L., Badjeck, M.-C., Neil Adger, W., Brown, K., Conway, D., Halls, A. S., Pilling, G. M., Reynolds, J. D., Andrew, N. L., and Dulvy, N. K.: Vulnerability of national economies to the impacts of climate change on fisheries, Fish and Fisheries, 10, 173-196, 10.1111/j.1467-2979.2008.00310.x, 2009.

Allison, S. D. and Martiny, J. B.: Colloquium paper: resistance, resilience, and redundancy in microbial communities, P. Natl. Acad. Sci. USA, 105, 11512–11519, https://doi.org/10.1073/pnas.0801925105, 2008.

Allison, S. D., and Treseder, K. K.: Warming and drying suppress microbial activity and carbon cycling in boreal forest soils, Global change biology, 14, 2898-2909, 10.1111/j.1365-2486.2008.01716.x, 2008.

Allison, S. D., Wallenstein, M. D., and Bradford, M. A.: Soil-carbon response to warming dependent on microbial physiology, Nature Geoscience, 3, 336-340, 10.1038/ngeo846, 2010.

Amiro, B. D., Orchansky, A. L., Barr, A. G., Black, T. A., Chambers, S. D., Chapin Iii, F. S., Goulden, M. L., Litvak, M., Liu, H. P., McCaughey, J. H., McMillan, A., and Randerson, J. T.: The effect of post-fire stand age on the boreal forest energy balance, Agr. Forest Meteorol., 140, 41–50, https://doi.org/10.1016/j.agrformet.2006.02.014, 2006.

Balser, T. C., Kinzig, A. P., and Firestone, M. K.: Linking soil microbial communities and ecosystem functioning, The functional consequences of biodiversity: Empirical progress and theoretical extensions, 265-293, 2002.

Barichivich, J., Briffa, K. R., Myneni, R. B., Osborn, T. J., Melvin, T. M., Ciais, P., Piao, S., and Tucker, C.: Large-scale variations in the vegetation growing season and annual cycle of atmospheric CO2 at high northern latitudes from 1950 to 2011, Glob. Change Biol., 19, 3167–3183, https://doi.org/10.1111/gcb.12283, 2013.

Basilier, K.: Moss-associated nitrogen fixation in some mire and coniferous forest environments around Uppsala, Sweden, Lindbergia, 5, 84-88, 1979.

Ben Bond-Lamberty, S. T. G., Douglas E. Ahl and Peter E. Thornton: Reimplementation of the Biome-BGC model to simulate successional change, Tree Physiology, 25, 413–424, 2005.

Beringer, J., Chapin, F. S., Thompson, C. C., and McGuire, A. D.: Surface energy exchanges along a tundra-forest transition and feedbacks to climate, Agricultural and Forest Meteorology, 131, 143-161, 10.1016/j.agrformet.2005.05.006, 2005.

Blagodatskaya, E. and Kuzyakov, Y.: Active microorganisms in soil: Critical review of estimation criteria and approaches, Soil Biol. Biochem., 67, 192–211, https://doi.org/10.1016/j.soilbio.2013.08.024, 2013.

Blagodatskaya, E., Khomyakov, N., Myachina, O., Bogomolova, I., Blagodatsky, S., and Kuzyakov, Y.: Microbial interactions affect sources of priming induced by cellulose, Soil Biology and Biochemistry, 74, 39-49, 10.1016/j.soilbio.2014.02.017, 2014.

Blagodatsky, S. A., Heinemeyer, O., and Richter, J.: Estimating the active and total soil microbial biomass by kinetic respiration analysis, Biol Fertil Soils, 32, 73-81, 2000.

Blagodatsky, S., Grote, R., Kiese, R., Werner, C., and Butterbach-Bahl, K.: Modelling of microbial carbon and nitrogen turnover in soil with special emphasis on N-trace gases emission, Plant and soil, 346, 297-330, 10.1007/s11104-011-0821-z, 2011.

Bond-Lamberty, B. and Thomson, A.: Temperature-associated increases in the global soil respiration record, Nature, 464, 579– 582, https://doi.org/10.1038/nature08930, 2010.

Bond-Lamberty, B., Bailey, V. L., Chen, M., Gough, C. M., and Vargas, R.: Globally rising soil heterotrophic respiration over recent decades, Nature, 560, 80-83, 10.1038/s41586-018-0358-x, 2018.

Bond-Lamberty, B., Peckham, S. D., Ahl, D. E., and Gower, S. T.: Fire as the dominant driver of central Canadian boreal forest carbon balance, Nature, 450, 89–92, https://doi.org/10.1038/nature06272, 2007.

Bouskill, N. J., Tang, J., Riley, W. J., and Brodie, E. L.: Trait-based representation of biological nitrification: model development, testing, and predicted community composition, Frontiers in microbiology, 3, 364, 10.3389/fmicb.2012.00364, 2012.

Cahoon, S. M., Sullivan, P. F., Shaver, G. R., Welker, J. M., Post, E., and Holyoak, M.: Interactions among shrub cover and the soil microclimate may determine future Arctic carbon budgets, Ecology letters, 15, 1415-1422, 10.1111/j.1461-0248.2012.01865.x, 2012.

Callaghan, T., Björn, L. O., Chernov, Y., Chapin, T., Christensen, T. R., Huntley, B., Ims, R., Jolly, D., Jonasson, S., Matveyeva, N., Panikov, N., Oechel,W., and Shaver, G.: Chapter 7: Arctic tundra and polar desert ecosystems, Arctic climate impact assessment, 243–352, ACIA Overview report. Cambridge University Press, 1020 pp., 2005.

Carney, K. M., and Matson, P. A.: The influence of tropical plant diversity and composition on soil microbial communities, Microbial ecology, 52, 226-238, 10.1007/s00248-006-9115-z, 2006.

Chadburn, S. E., Burke, E. J., Cox, P. M., Friedlingstein, P., Hugelius, G., and Westermann, S.: An observation-based constraint on permafrost loss as a function of global warming, Nature Climate Change, 7, 340-344, 10.1038/nclimate3262, 2017.

Chapin, F. S. and Starfield, A. M.: Time lags and novel ecosystems in response to transient climatic change in arctic Alaska, Climatic Change, 35, 449–461, 1997. Christensen, J. H. and Christensen, O. B.: A summary of the PRUDENCE model projections of changes in European climate by the end of this century, Climatic Change, 81, 7–30, https://doi.org/10.1007/s10584-006-9210-7, 2007.

Charles J. Vörösmarty, B. M. I., Annette L. Grace, and M. Patricia Gildea: Continental scale models of water balance and fluvial transport: an application to South America, Global biogeochemical cycles, 3, 241-265, 1989.

Chmlelewrki, R. A. N., and Frank, J. F.: Formation of viable but nonculturable Salmonella during starvation in chemically defined solutions, Letters in Applied Microbiology, 20, 380-384, 1995.

Ciais, P., Sabine, C., Bala, G., Bopp, L., Brovkin, V., Canadell, J., Chhabra, A., DeFries, R., Galloway, J., Heimann, M., Jones, C., Quéré, C. L., Myneni, R. B., Piao, S., and Thornton, P.: Carbon and other biogeochemical cycles, Climate change 2013: the physical science basis. Contribution of Working Group I to the Fifth Assessment Report of the Intergovernmental Panel on Climate Change, 465–570, 2013.

Clarke, G. C. S.: Productivity of Bryophytes in Polar Regions, Annals of botany, 35, 99–108, 1971.

Classen, A. T., Sundqvist, M. K., Henning, J. A., Newman, G. S., Moore, J. A. M., Cregger, M. A., Moorhead, L. C., and Patterson, C. M.: Direct and indirect effects of climate change on soil microbial and soil microbial-plant interactions: What lies ahead?, Ecosphere, 6, art130, 10.1890/es15-00217.1, 2015.

Cole, C. V., Duxbury, J., Freney, J., Heinemeyer, O., Minami, K., Mosier, A., Paustian, K., Rosenberg, N., Sampson, N., Sauerbeck, D., and Zhao, Q.: Global estimates of potential mitigation of greenhouse gas emissions by agriculture, Nutr. Cycl. Agroecosys., 49, 221–228, 1997.

Collins, W. C. O. a. N. J.: Comparative COz exchange patterns in mosses from two tundra habitats at Barrow, Alaska, Canadian Journal of Botany, 54, 1355-1369, 1976.

Conant, R. T., Ryan, M. G., Ågren, G. I., Birge, H. E., Davidson, E. A., Eliasson, P. E., Evans, S. E., Frey, S. D., Giardina, C. P., Hopkins, F. M., Hyvönen, R., Kirschbaum, M. U. F., Lavallee, J. M., Leifeld, J., Parton, W. J., Megan Steinweg, J., Wallenstein, M. D., Martin Wetterstedt, J. Å., and Bradford, M. A.: Temperature and soil organic matter decomposition rates - synthesis of current knowledge and a way forward, Global change biology, 17, 3392-3404, 10.1111/j.1365-2486.2011.02496.x, 2011.

Cook, F. J. and Orchard, V. A.: Relationships between soil respiration and soil moisture, Soil Biol. Biochem., 40, 1013–1018, https://doi.org/10.1016/j.soilbio.2007.12.012, 2008.

Cornelissen, J. H., Lang, S. I., Soudzilovskaia, N. A., and During, H. J.: Comparative cryptogam ecology: a review of bryophyte and lichen traits that drive biogeochemistry, Annals of botany, 99, 987-1001, 10.1093/aob/mcm030, 2007.

Coursolle, C., Margolis, H. A., Barr, A. G., Black, T. A., Amiro, B. D., McCaughey, J. H., Flanagan, L. B., Lafleur, P. M., Roulet, N. T., Bourque, C. P. A., Arain, M. A., Wofsy, S. C., Dunn, A., Morgenstern, K., Orchansky, A. L., Bernier, P. Y., Chen, J. M., Kidston, J., Saigusa, N., and Hedstrom, N.: Late-summer carbon fluxes from Canadian forests and peatlands along an east–west continental transect, Canadian Journal of Forest Research, 36, 783-800, 10.1139/x05-270, 2006.

Davidson, E. A. and Janssens, I. A.: Temperature sensitivity of soil carbon decomposition and feedbacks to climate change, Nature, 440, 165–173, https://doi.org/10.1038/nature04514, 2006.

Davidson, E. A., Janssens, I. A., and Luo, Y.: On the variability of respiration in terrestrial ecosystems: moving beyond Q10, Global change biology, 12, 154-164, 10.1111/j.1365-2486.2005.01065.x, 2006.

Davidson, E. A., Samanta, S., Caramori, S. S., and Savage, K.: The Dual Arrhenius and Michaelis-Menten kinetics model for decomposition of soil organic matter at hourly to seasonal time scales, Global change biology, 18, 371-384, 10.1111/j.1365-2486.2011.02546.x, 2012.

Davidson, E. A., Trumbore, S. E., and Amundson, R.: Biogeochemistry: soil warming and organic carbon content, Nature, 408, 789–790, https://doi.org/10.1038/35048672, 2000.

DeLuca, T. H., Zackrisson, O., Gentili, F., Sellstedt, A., and Nilsson, M. C.: Ecosystem controls on nitrogen fixation in boreal feather moss communities, Oecologia, 152, 121-130, 10.1007/s00442-006-0626-6, 2007.

Dong, Y. and Somero, G. N.: Temperature adaptation of cytosolic malate dehydrogenases of limpets (genus Lottia): differences in stability and function due to minor changes in sequence correlate with biogeographic and vertical distributions, J. Exp. Biol., 212, 169–177, https://doi.org/10.1242/jeb.024505, 2009.

Duan, Q., Sorooshian, S., and Gupta, V. K.: Optimal use of the SCE-UA global optimization method for calibrating watershed models, Journal of Hydrology, 158, 265-284, 1994.

E. S. Euskirchen, A. D. M., F. S. Chapin, III, S. Yi, and C. C. Thompson: Changes in vegetation in northern Alaska under scenarios of climate change, 2003–2100: implications for climate feedbacks, Ecological Applications, 19, 1022–1043, 2009.

Edward A. G. Schuur, J. B., Josep G. Canadell, Eugenie Euskirchen, Christopher B., Field, S. V. G., Stefan Hagemann, Peter Kuhry, Peter M. Lafleur, Hanna Lee, Galina, Mazhitova, F. E. N., Annette Rinke, Vladimir E. Romanovsky, Nikolay Shiklomanov,, and Charles Tarnocai, S. V., Jason G. Vogel, And Sergei A. Zimov: Vulnerability of Permafrost Carbon to Climate Change: Implications for the Global Carbon Cycle, BioScience, 58, 701-714, 2008.

Esteban G. Jobbágy, and Jackson, R. B.: The vertical distribution of soil organic carbon and its relation to climate and vegetation, Ecological applications, 10, 423-436, 2000.

Evans, S. E., and Wallenstein, M. D.: Soil microbial community response to drying and rewetting stress: does historical precipitation regime matter?, Biogeochemistry, 109, 101-116, 10.1007/s10533-011-9638-3, 2011.

F. S. Chapin III, M. S., M. C. Serreze, J. P. McFadden, J. R. Key, A. H. Lloyd, A. D. McGuire, T. S. Rupp, A. H. Lynch, J. P. Schimel, J. Beringer, W. L. Chapman, H. E. Epstein, E. S. Euskirchen, L. D. Hinzman, G. Jia, C.-L. Ping, K. D. Tape, C. D. C. Thompson, D. A. Walker, J. M. Welker: Role of Land-Surface Changes in Arctic Summer Warming, Science, 310, 657-660, 2005.

Fierer, N., Morse, J. L., Berthrong, S. T., Bernhardt, E. S., and Jackson, R. B.: Environmental controls on the landscape - scale biogeography of stream bacterial communities, Ecology, 88, 2162-2173, 2007.

Frey, S. D., Lee, J., Melillo, J. M., and Six, J.: The temperature response of soil microbial efficiency and its feedback to climate, Nature Climate Change, 3, 395-398, 10.1038/nclimate1796, 2013.

Frolking, S., Roulet, N. T., Tuittila, E., Bubier, J. L., Quillet, A., Talbot, J., and Richard, P. J. H.: A new model of Holocene peatland net primary production, decomposition, water balance, and peat accumulation, Earth System Dynamics, 1, 1-21, 10.5194/esd-1-1-2010, 2010.

Gangsheng Wang, M. A. M., Lianhong Gu, Christopher W. Schadt: Representation of Dormant and Active Microbial Dynamics for Ecosystem Modeling, Public Library of Science, 9, 10.1371/journal.pone.0089252.g001, 2014.

Gear, A. J. and Huntley, B.: Rapid changes in the range limits of Scots pine 4000 years ago, Science, 251, 544–547, 1991.

German, D. P., Marcelo, K. R. B., Stone, M. M., and Allison, S. D.: The Michaelis Menten kinetics of soil extracellular enzymes in response to temperature: a cross latitudinal study, Glob. Change Biol., 18, 1468–1479, https://doi.org/10.1111/j.1365-2486.2011.02615.x, 2012.

Gilmanov, T. G., Tieszen, L. L., Wylie, B. K., Flanagan, L. B., Frank, A. B., Haferkamp, M. R., Meyers, T. P., and Morgan, J. A.: Integration of CO2flux and remotely-sensed data for primary production and ecosystem respiration analyses in the Northern Great Plains: potential for quantitative spatial extrapolation, Global Ecology and Biogeography, 14, 271-292, 10.1111/j.1466-822X.2005.00151.x, 2005.

Goetz, S. J., Mack, M. C., Gurney, K. R., Randerson, J. T., and Houghton, R. A.: Ecosystem responses to recent climate change and fire disturbance at northern high latitudes: observations and model results contrasting northern Eurasia and North America, Environ. Res. Lett., 2, 045031, https://doi.org/10.1088/1748-9326/2/4/045031, 2007.

Gornall, J. L., Jonsdottir, I. S., Woodin, S. J., and Van der Wal, R.: Arctic mosses govern below-ground environment and ecosystem processes, Oecologia, 153, 931-941, 10.1007/s00442-007-0785-0, 2007.

Gornall, J. L., Woodin, S. J., Jonsdottir, I. S., and van der Wal, R.: Balancing positive and negative plant interactions: how mosses structure vascular plant communities, Oecologia, 166, 769-782, 10.1007/s00442-011-1911-6, 2011.

Gough, C. M., Hardiman, B. S., Nave, L. E., Bohrer, G., Maurer, K. D., Vogel, C. S., Nadelhoffer, K. J., and Curtis, P. S.: Sustained carbon uptake and storage following moderate disturbancein a Great Lakes forest, Ecological Applications, 23, 1202-1215, 2013.

Goulden, M. L., Winston, G. C., McMillan, A. M. S., Litvak, M. E., Read, E. L., Rocha, A. V., and Rob Elliot, J.: An eddy covariance mesonet to measure the effect of forest age on land?atmosphere exchange, Global change biology, 12, 2146-2162, 10.1111/j.1365-2486.2006.01251.x, 2006.

Graham, E. B., Knelman, J. E., Schindlbacher, A., Siciliano, S., Breulmann, M., Yannarell, A., Beman, J. M., Abell, G., Philippot, L., Prosser, J., Foulquier, A., Yuste, J. C., Glanville, H. C., Jones, D. L., Angel, R., Salminen, J., Newton, R. J., Burgmann, H., Ingram, L. J., Hamer, U., Siljanen, H. M., Peltoniemi, K., Potthast, K., Baneras, L., Hartmann, M., Banerjee, S., Yu, R. Q., Nogaro, G., Richter, A., Koranda, M., Castle, S. C., Goberna, M., Song, B., Chatterjee, A., Nunes, O. C., Lopes, A. R., Cao, Y., Kaisermann, A., Hallin, S., Strickland, M. S., Garcia-Pausas, J., Barba, J., Kang, H., Isobe, K., Papaspyrou, S., Pastorelli, R., Lagomarsino, A., Lindstrom, E. S., Basiliko, N., and Nemergut, D. R.: Microbes as Engines of Ecosystem Function: When Does Community Structure Enhance Predictions of Ecosystem Processes?, Frontiers in microbiology, 7, 214, 10.3389/fmicb.2016.00214, 2016.

Graham, E. B., Wieder, W. R., Leff, J. W., Weintraub, S. R., Townsend, A. R., Cleveland, C. C., Philippot, L., and Nemergut, D. R.: Do we need to understand microbial communities to predict ecosystem function? A comparison of statistical models of nitrogen cycling processes, Soil Biology and Biochemistry, 68, 279-282, 10.1016/j.soilbio.2013.08.023, 2014.

Griffis, T. J., Lee, X., Baker, J. M., Billmark, K., Schultz, N., Erickson, M., Zhang, X., Fassbinder, J., Xiao, W., and Hu, N.: Oxygen isotope composition of evapotranspiration and its relation to C4photosynthetic discrimination, Journal of Geophysical Research, 116, 10.1029/2010jg001514, 2011.

Hagerty, S. B., van Groenigen, K. J., Allison, S. D., Hungate, B. A., Schwartz, E., Koch, G. W., Kolka, R. K., and Dijkstra, P.: Accelerated microbial turnover but constant growth efficiency with warming in soil, Nat. Clim. Change, 4, 903–906, https://doi.org/10.1038/nclimate2361, 2014.

Hansen, J., Sato, M., Ruedy, R., Lo, K., Lea, D. W., and Medina- Elizade, M.: Global temperature change, P. Natl. Acad. Sci. USA, 103, 14288–14293, https://doi.org/10.1073/pnas.0606291103, 2006.

Hanson, P. J., Edwards, N. T., Garten, C. T., and Andrews, J. A.: Separating root and soil microbial contributions to soil respiration: A review of methods and observations, Biogeochemistry, 48, 115–146, 2000.

Hao, G., Zhuang, Q., Zhu, Q., He, Y., Jin, Z., and Shen, W.: Quantifying microbial ecophysiological effects on the carbon fluxes of forest ecosystems over the conterminous United States, Climatic Change, 133, 695–708, https://doi.org/10.1007/s10584- 015-1490-3, 2015.

Harden, J. W., Trumbore, S. E., Stocks, B. J., Hirsch, A., Gower, S. T., O'neill, K. P., and Kasischke, E. S.: The role of fire in the boreal carbon budget, Glob. Change Biol., 6, 174–184, 2000.

Harder, w., and Dijkhuizen, L.: Physiological responses to nutrient limitation, Annual Review of Microbiology, 37, 1983.

Harris, I., Jones, P. D., Osborn, T. J., and Lister, D. H.: Updated high-resolution grids of monthly climatic observations - the CRU TS3.10 Dataset, International Journal of Climatology, 34, 623-642, 10.1002/joc.3711, 2014.

Hayes, D. J., Kicklighter, D. W., McGuire, A. D., Chen, M., Zhuang, Q., Yuan, F., Melillo, J. M., and Wullschleger, S. D.: The impacts of recent permafrost thaw on land atmosphere greenhouse gas exchange, Environ. Res. Lett., 9, 045005, https://doi.org/10.1088/1748-9326/9/4/045005, 2014.

Hayes, D. J., McGuire, A. D., Kicklighter, D. W., Gurney, K. R., Burnside, T. J., and Melillo, J. M.: Is the northern high-latitude land-based CO2sink weakening?, Global Biogeochemical Cycles, 25, n/a-n/a, 10.1029/2010gb003813, 2011.

He, Y., Yang, J., Zhuang, Q., Harden, J. W., McGuire, A. D., Liu, Y., Wang, G., and Gu, L.: Incorporating microbial dormancy dynamics into soil decomposition models to improve quantification of soil carbon dynamics of northern temperate forests, J. Geophys. Res.-Biogeo., 120, 2596–2611, https://doi.org/10.1002/2015jg003130, 2015.

Henning Pedersen, K. A. D. M. F.: The relative importance of autotrophic and heterotrophic nitrification in a conifer forest soil as measured by 15N tracer and pool dilution techniques, Biogeochemistry, 44, 135–150, 1999.

Hiller, R. V., McFadden, J. P., and Kljun, N.: Interpreting CO2 Fluxes Over a Suburban Lawn: The Influence of Traffic Emissions, Boundary-Layer Meteorology, 138, 215-230, 10.1007/s10546-010-9558-0, 2010.

Hobbie, E. A. and Hobbie, J. E.: Natural Abundance of 15N in Nitrogen-Limited Forests and Tundra Can Estimate Nitrogen Cycling Through Mycorrhizal Fungi: A Review, Ecosystems, 11, 815–830, https://doi.org/10.1007/s10021-008-9159-7, 2008.

Hobbie, J. E. and Hobbie, E. A.: 15N in symbiotic fungi and plants estimates nitrogen and carbon flux rates in Arctic tundra, Ecology, 87, 816–822, 2006.

Holland, M. M. and Bitz, C. M.: Polar amplification of climate change in coupled models, Clim. Dynam., 21, 221–232, https://doi.org/10.1007/s00382-003-0332-6, 2003.

Houghton, R. A.: Balancing the Global Carbon Budget, Annu. Rev. Earth Pl. Sc., 35, 313–347, https://doi.org/10.1146/annurev.earth.35.031306.140057, 2007.

https://www.nature.com/articles/nature02887#supplementary-information, 2004.

Hugelius, G., Strauss, J., Zubrzycki, S., Harden, J. W., Schuur, E. A. G., Ping, C. L., Schirrmeister, L., Grosse, G., Michaelson, G. J., Koven, C. D., amp, apos, Donnell, J. A., Elberling, B., Mishra, U., Camill, P., Yu, Z., Palmtag, J., and Kuhry, P.: Estimated stocks of circumpolar permafrost carbon with quantified uncertainty ranges and identified data gaps, Biogeosciences, 11, 6573-6593, 10.5194/bg-11-6573-2014, 2014.

Jägerbrand, A. K., Alatalo, J. M., Chrimes, D., and Molau, U.: Plant community responses to 5 years of simulated climate change in meadow and heath ecosystems at a subarctic-alpine site, Oecologia, 161, 601-610, 10.1007/s00442-009-1392-z, 2009.

Jägerbrand, A. K., Lindblad, K. E. M., Björk, R. G., Alatalo, J. M., and Molau, U.: Bryophyte and Lichen Diversity Under Simulated Environmental Change Compared with Observed Variation in Unmanipulated Alpine Tundra, Biodiversity and Conservation, 15, 4453-4475, 10.1007/s10531-005-5098-1, 2006.

James E. Overland, M. C. S., Donald B. Percival, Muyin Wang, and Harold O. Mofjeld: Seasonal and Regional Variation of Pan-Arctic Surface Air Temperature over the Instrumental Record, American Meteorological Society: Journal of Climate, 17, 3263-3282, 2004.

Jason Beringer, A. H. L., F. Stuart Chapin III, Michelle Mack, Gordon B. Bonan: The Representation of Arctic Soils in the Land Surface Model: The Importance of Mosses, American Meteorological Society: Journal of Climate, 14, 3324-3335, 2001.

Jenkins, J. P., Richardson, A. D., Braswell, B. H., Ollinger, S. V., Hollinger, D. Y., and Smith, M. L.: Refining light-use efficiency calculations for a deciduous forest canopy using simultaneous tower-based carbon flux and radiometric measurements, Agricultural and Forest Meteorology, 143, 64-79, 10.1016/j.agrformet.2006.11.008, 2007.

Johnstone, J. F. and Kasischke, E. S.: Stand-level effects of soil burn severity on postfire regeneration in a recently burned black spruce forest, Can. J. Forest Res., 35, 2151 2163, https://doi.org/10.1139/x05-087, 2005.

Kaiser, C., Franklin, O., Dieckmann, U., and Richter, A.: Microbial community dynamics alleviate stoichiometric constraints during litter decay, Ecology letters, 17, 680-690, 10.1111/ele.12269, 2014.

Kallio, P. and Heinonen, S. : CO_2 exchange and growth of Rhacomitrium lanuginosum and Dicranum elongatum. In *Fennoscandian tundra ecosystems*, Springer, Berlin, Heidelberg, 138-148, 1975.

Kasischke, E. S. and Turetsky, M. R.: Recent changes in the fire regime across the North American boreal region – Spatial and temporal patterns of burning across Canada and Alaska, Geophys. Res. Lett., 33, L09703, https://doi.org/10.1029/2006gl025677, 2006.

Kasischke, E. S.: Boreal ecosystems in the global carbon cycle. In Fire, climate change, and carbon cycling in the boreal forest, Ecological Studies (Analysis and Synthesis), 138, 19-30, https://doi.org/10.1007/978-0-387-21629-4_2, 2000.

Kip, N., Ouyang, W., van Winden, J., Raghoebarsing, A., van Niftrik, L., Pol, A., Pan, Y., Bodrossy, L., van Donselaar, E. G., Reichart, G. J., Jetten, M. S., Damste, J. S., and Op den Camp, H. J.: Detection, isolation, and characterization of acidophilic methanotrophs from Sphagnum mosses, Applied and environmental microbiology, 77, 5643-5654, 10.1128/AEM.05017-11, 2011.

Knorr, W., Prentice, I. C., House, J. I., and Holland, E. A.: Long-term sensitivity of soil carbon turnover to warming, Nature, 433, 2005.

Knorr, W.: Annual and interannual CO2 exchanges of the terrestrial biosphere: process-based simulations and uncertainties, Global Ecology and Biogeography, 9, 225-252, 2000.

L. Kulmala, J. P., P. Hari and T. Vesala: Photosynthesis of ground vegetation in different aged pine forests: Effect of environmental factors predicted with a process-based model, Journal of Vegetation Science, 22, 96–110, 2011.

Launiainen, S., Katul, G. G., Lauren, A., and Kolari, P.: Coupling boreal forest CO2, H2O and energy flows by a vertically structured forest canopy – Soil model with separate bryophyte layer, Ecological Modelling, 312, 385-405, 10.1016/j.ecolmodel.2015.06.007, 2015.

Lawrence, C. R., Neff, J. C., and Schimel, J. P.: Does adding microbial mechanisms of decomposition improve soil organic matter models? A comparison of four models using data from a pulsed rewetting experiment, Soil Biology and Biochemistry, 41, 1923-1934, 10.1016/j.soilbio.2009.06.016, 2009.

Lawrence, D. M., Oleson, K. W., Flanner, M. G., Thornton, P. E., Swenson, S. C., Lawrence, P. J., Zeng, X., Yang, Z.-L., Levis, S., Sakaguchi, K., Bonan, G. B., and Slater, A. G.: Parameterization improvements and functional and structural advances in Version 4 of the Community Land Model, J. Adv. Model. Earth Sy., 3, M03001, https://doi.org/10.1029/2011ms000045, 2011.

Lennon, J. T. and Jones, S. E.: Microbial seed banks: the ecological and evolutionary implications of dormancy, Nature reviews, Microbiology, 9, 119–130, https://doi.org/10.1038/nrmicro2504, 2011.

Lindo, Z., and Gonzalez, A.: The Bryosphere: An Integral and Influential Component of the Earth's Biosphere, Ecosystems, 13, 612-627, 10.1007/s10021-010-9336-3, 2010.

Lloyd, A. H., Rupp, T. S., Fastie, C. L., and Starfield, A. M.: Patterns and dynamics of treeline advance on the Seward Peninsula, Alaska, Journal of Geophysical Research, 108, 10.1029/2001jd000852, 2002.

Lloyd, A. H.: Ecological histories from Alaskan tree lines provide insight into future change, Ecology, 86, 1687–1695, 2005.

Longton, R. E.: Adaptations and strategies of polar bryophytes, Botanical Journal of the Linnean Society, 98, 253-268, 1988.

López-Urrutia, A., and Morán, X. A. G.: Resource limitation of bacterial production distorts the temperature dependence of oceanic carbon cycling, Ecology, 88, 817–822, 2007.

M. C. Serreze, J. E. W., F. S.Chapin III, T. Osterkamp, M. Dyurgerov, V. Romanovsky, W. C. Oechel, J. Morison, T. Zhang and R. G. Barry: Observational Evidence of Recent Change in the Northern High-Latitude Environment, Climatic Change, 46, 159–207, 2000.

M. Torre Jorgenson, C. H. R., James C. Walters and Thomas E. Osterkamp: Permafrost Degradation and Ecological Changes Associated with a warming Climate in Central Alaska, Climatic Change, 48, 551–579, 2001.

Mack, M. C., Schuur, E. A. G., Bret-Harte, M. S., Shaver, G. R., and Chapin III, F. S. C.: Ecosystem carbon storage in arctic tundra reduced by long-term nutrient fertilization, Nature, 431, 440–443, 2004.

Mack, M. C., Schuur, E. A. G., Bret-Harte, M. S., Shaver, G. R., and Chapin Iii, F. S.: Ecosystem carbon storage in arctic tundra reduced by long-term nutrient fertilization, Nature, 431, 440, 10.1038/nature02887

Manzoni, S., Taylor, P., Richter, A., Porporato, A., and Agren, G. I.: Environmental and stoichiometric controls on microbial carbon-use efficiency in soils, The New phytologist, 196, 79-91, 10.1111/j.1469-8137.2012.04225.x, 2012.

Markham, J. H.: Variation in moss-associated nitrogen fixation in boreal forest stands, Oecologia, 161, 353-359, 10.1007/s00442-009-1391-0, 2009.

McEwing, K. R., Fisher, J. P., and Zona, D.: Environmental and vegetation controls on the spatial variability of CH4 emission from wet-sedge and tussock tundra ecosystems in the Arctic, Plant and soil, 388, 37-52, 10.1007/s11104-014-2377-1, 2015.

McGuire, A. D. and Hobbie, J. E.: Global climate change and the equilibrium responses of carbon storage in arctic and subarctic regions, in: Modeling the Arctic system: A workshop report on the state of modeling in the Arctic System Science program, 53– 54, 1997.

McGuire, A. D., Anderson, L. G., Christensen, T. R., Dallimore, S., Guo, L., Hayes, D. J., Heimann, M., Lorenson, T. D., Macdonald, R. W., and Roulet, N.: Sensitivity of the carbon cycle in the Arctic to climate change, Ecological Monographs, 79, 523-555, 2009.

McGuire, A. D., Christensen, T. R., Hayes, D., Heroult, A., Euskirchen, E., Kimball, J. S., Koven, C., Lafleur, P., Miller, P. A., Oechel, W., Peylin, P., Williams, M., and Yi, Y.: An assessment of the carbon balance of Arctic tundra: comparisons among observations, process models, and atmospheric inversions, Biogeosciences, 9, 3185–3204, https://doi.org/10.5194/bg-9-3185- 2012, 2012.

McGuire, A. D., Melillo, J. M., Joyce, L. A., Kicklighter, D. W., Grace, A. L., III, B. M., and Vorosmarty, C. J.: Interactions between carbon and nitrogen dynamics in estimating net primary productivity for potential vegetation in North America, Global Biogeochemical Cycles, 6, 101-124, 1992.

McGuire, A. D., Melillo, J. M., Kicklighter, D. W., and Joyce, L. A.: Equilibrium responses of soil carbon to climate change: Empirical and process-based estimates, Journal of Biogeography, 785-796, 1995.

McGuire, K. L., and Treseder, K. K.: Microbial communities and their relevance for ecosystem models: Decomposition as a case study, Soil Biology and Biochemistry, 42, 529-535, 10.1016/j.soilbio.2009.11.016, 2010.

Me´tris, A., Gerrard, A. M., Cumming, R. H., Weigner, P., and Paca, J.: Modelling shock loadings and starvation in the biofiltration of toluene and xylene, Journal of Chemical Technology and Biotechnology, 76, 565-572, 2001.

Melillo, J. M., Butler, S., Johnson, J., Mohan, J., Steudler, P., Lux, H., Burrows, E., Bowles, F., Smith, R., Scott, L., Vario, C., Hill, T., Burton, A., Zhou, Y.-M., and Tang, J.: Soil warming, carbon - nitrogen interactions, and forest carbon budgets, PNAS, 108, 9508-9512, 2011.

Melillo, J. M., McGuire, A. D., Kicklighter, D. W., Moore III, B., Vorosmarty, C. J., and Schloss, A. L.: Global climate change and terrestrial net primary production, Nature, 363, 234–240, https://doi.org/10.1038/363234a0, 1993.

Merbold, L., Kutsch, W. L., Corradi, C., Kolle, O., Rebmann, C., Stoy, P. C., Zimov, S. A., and Schulze, E. D.: Artificial drainage and associated carbon fluxes (CO2/CH4) in a tundra ecosystem, Global change biology, 15, 2599-2614, 10.1111/j.1365-2486.2009.01962.x, 2009.

Moorhead, D. L., and Sinsabaugh, R. L.: A theoretical model of litter decay and microbial interaction, Ecological Monographs, 76, 151-174, 2006.

Naomi Oreskes, K. S.-F., Kenneth Belitz: Verification, validation, and confirmation of numerical models in the earth sciences, Science, 263, 641-646, 1994.

O. Skre, W. C. O.: Moss production in a black spruce Picea mariana forest with permafrost near Fairbanks, Alaska, as compared with two permafrost-free stands, Ecography, 2, 249-254, 1979.

Oechei, O. S. a. W. C.: Moss production in a black spruce Picea mariana forest with permafrost near Fairbanks, Alaska, as compared with two permafrost-free stands, Ecography, 2, 249-254, 1979.

Oechel, W. C., Laskowski, C. A., Burba, G., Gioli, B., and Kalhori, A. A. M.: Annual patterns and budget of CO2flux in an Arctic tussock tundra ecosystem, Journal of Geophysical Research: Biogeosciences, 119, 323-339, 10.1002/2013jg002431, 2014.

Oechel, W.C. and Van Cleve, K. : The role of bryophytes in nutrient cycling in the taiga. In *Forest ecosystems in the Alaskan taiga*, Springer, New York, NY, 121-137, 1986

Oechel,W. C., Vourlitis, G. L., Hastings, S. J., Zulueta, R. C., Hinzman, L., and Kane, D.: Acclimation of ecosystem CO2 exchange in the Alaskan Arctic in response to decadal climate warming, Nature, 406, 978–981, https://doi.org/10.1038/35023137, 2000.

Okland, R. H.: Population Biology of the Clonal Moss Hylocomium Splendens in Norwegian Boreal SpruceForests. I. Demography, Journal of Ecology, 83, 697-712, 1995.

P. D. Jones, A. M.: Hemispheric and Large-Scale Surface Air Temperature Variations: An Extensive Revision and an Update to 2001, American Meteorological Society: Journal of Climate, 16, 206-223, 2003.

P. Friedlingstein, P. C., R. Betts, L. Bopp, W. Von Bloh, V. Brovkin, P. Cadule, S. Doney, M. Eby, I. Fung, G. Bala, J. John, C. Jones, F. Joos, T. Kato, M. Kawamiya, W. Knorr, K. Lindsay, H. D. Matthews, T. Raddatz, P. Rayner, C. Reick, E. Roeckner, K.-G. Schnitzler, R. Schnur, K. Strassmann, A. J. Weaver, C. Yoshikawa, And N. Zeng: Climate–Carbon Cycle Feedback Analysis: Results from the C4MIP Model Intercomparison, American Meteorological Society: Journal of Climate, 19, 3337-3353, 2006.

P.C. Harley, J. D. T., K.J. Murray, and J. Beyers: Irradiance and temperature effects on photosynthesis of tussock tundra Sphagnum mosses from the foothills of the Philip Smith Mountains, Alaska, Oecologia, 79, 251-259, 1989.

P.J. Hanson, N. T. E., C.T. Garten, J.A. Andrews: Separating root and soil microbial contributions to soil respiration: A review of methods and observations, Biogeochemistry, 48, 115-146, 2000.

Pakarinen, P., and D. H. Vitt: Primary production of plant communities of the Truelove Lowland, Devon Island, Canada–Moss communities, Primary production and production processes, tundra biome. International Biological Programme, Tundra Biome Steering Committee, Edmonton Oslo, 37-46, 1973.

Pan, Y., McGuire, A. D., Melillo, J. M., Kicklighter, D. W., Sitch, S., and Prentice, I. C.: A biogeochemistry-based dynamic vegetation model and its application along a moisture gradient in the continental United States, J. Vegetation Sci., 13, 369–382, 2002.

Parton, W. J., Ojima, D. S., Cole, C. V., and Schimel, D. S.: A general model for soil organic matter dynamics: sensitivity to litter chemistry, texture and management, SSSA Spec. Publ., 39, 147– 167, 1994.

Parton, W. J., Scurlock, J. M. O., Ojima, D. S., Gilmanov, T. G., Scholes, R. J., Schimel, D. S., Kirchner, T., Menaut, J. C., Seastedt, T., Moya, E. G., Kamnalrut, A., and Kinyamario, J. I.: Observations and modeling of biomass and soil organic matter dynamics for the grassland biome worldwide, Global Biogeochemical Cycles, 7, 785-809, 1993.

Pharo, E. J., and Zartman, C. E.: Bryophytes in a changing landscape: The hierarchical effects of habitat fragmentation on ecological and evolutionary processes, Biological Conservation, 135, 315-325, 10.1016/j.biocon.2006.10.016, 2007.

Potter, C. S., Randerson, J. T., Field, C. B., Matson, P. A., Vitousek, P. M., Mooney, H. A., and Klooster, S. A.: Terrestrial ecosystem production: a process model based on global satellite and surface data, Global Biogeochem. Cy., 7, 811–841, 1993.

Qian, H., Joseph, R., and Zeng, N.: Enhanced terrestrial carbon uptake in the Northern High Latitudes in the 21st century from the Coupled Carbon Cycle Climate Model Intercomparison Project model projections, Glob. Change Biol., 16, 641–656, https://doi.org/10.1111/j.1365-2486.2009.01989.x, 2010.

Raich, J. W., Rastetter, E. B., Melillo, J. M., Kicklighter, D. W., Steudler, P. A., Peterson, B. J., Grace, A. L., III, B. M., and Vorosmarty, C. J.: Potential net primary productivity in South America: application of a global model, Ecological Applications, 1, 399-429, 1991.

Raich, J.W. and Schlesinger,W. H.: The global carbon dioxide flux in soil respiration and its relationship to vegetation and climate, Tellus B, 44, 81–99, 1992.

Randerson, J. T., Liu, H., Flanner, M. G., Chambers, S. D., Jin, Y., Hess, P. G., Pfister, G., Mack, M. C., Treseder, K. K., Welp, L. R., Chapin, F. S., Harden, J.W., Goulden, M. L., Lyons, E., Neff, J. C., Schuur, E. A. G., and Zender, C. S.: The impact of boreal forest fire on climate warming, Science, 314, 1130–1132, 2006.

Richardson, A. D., Jenkins, J. P., Braswell, B. H., Hollinger, D. Y., Ollinger, S. V., and Smith, M. L.: Use of digital webcam images to track spring green-up in a deciduous broadleaf forest, Oecologia, 152, 323-334, 10.1007/s00442-006-0657-z, 2007.

Running, S. W., and Coughlan, J. C.: A general model of forest ecosystem processes for regional applications I. Hydrologic balance, canopy gas exchange and primary production processes., Ecological Modelling, 42, 125-154, 1988.

S. Frolking, M. L. G., S.C. Wofsy, S-M. Fan, D.J. Sutton, J.W. Munger, A.M. Bazzaz, B.C. Daube, P.M. Crill, J.D, Aber, L.E. Band, X. Wang, K. Savage, T. Moore And R.C. Harriss: Modelling temporal variability in the carbon balance of a spruce/moss boreal forest, Global change biology, 2, 343-366, 1996.

Sarah E. Hobbie, J. P. S., Susan E. Trumbore And James R. Randerson: Controls over carbon storage and turnover in high-latitude soils, Global change biology, 6, 196-210, 2000.

Schaphoff, S., Heyder, U., Ostberg, S., Gerten, D., Heinke, J., and Lucht, W.: Contribution of permafrost soils to the global carbon budget, Environ. Res. Lett., 8, 014026, https://doi.org/10.1088/1748-9326/8/1/014026, 2013.

Schimel, D. S., House, J. I., Hibbard, K. A., Bousquet, P., Ciais, P., Peylin, P., Braswell, B. H., Apps, M. J., Baker, D., Bondeau, A., Canadell, J., Churkina, G., Cramer, W., Denning, A. S., Field, C. B., Friedlingstein, P., Goodale, C., Heimann, M., Houghton, R. A., Melillo, J. M., III, B. M., Murdiyarso, D., Noble, I., Pacala, S. W., Prentice, I. C., Raupach, M. R., Rayner, P. J., Scholes, R. J., Steffen, W. L., and Wirth, C.: Recent patterns and mechanisms of carbon exchange by terrestrial ecosystems, Nature, 414, 2001.

Schimel, D. S.: Terrestrial ecosystems and the carbon cycle, Global change biology, 1, 77-91, 1995.

Schimel, J. P. and Hättenschwiler, S.: Nitrogen transfer between decomposing leaves of different N status, Soil Biol. Biochem., 39, 1428–1436, https://doi.org/10.1016/j.soilbio.2006.12.037, 2007.

Schimel, J. P. and Schaeffer, S. M.: Microbial control over carbon cycling in soil, Front. Microbiol., 3, 348, https://doi.org/10.3389/fmicb.2012.00348, 2012.

Schimel, J. P. and Weintraub, M. N.: The implications of exoenzyme activity on microbial carbon and nitrogen limitation in soil: a theoretical model, Soil Biol. Biochem., 35, 549–563, https://doi.org/10.1016/s0038-0717(03)00015-4, 2003.

Schimel, J.: Microbes and global carbon, Nature Climate Change, 3, 867-868, 10.1038/nclimate2015, 2013.

Schlesinger, W. H., and Andrews, J. A.: Soil respiration and the global carbon cycle, Biogeochemistry, 48, 7-20, 2000.

Schmidt, M. W., Torn, M. S., Abiven, S., Dittmar, T., Guggenberger, G., Janssens, I. A., Kleber, M., Kogel-Knabner, I., Lehmann, J., Manning, D. A., Nannipieri, P., Rasse, D. P., Weiner, S., and Trumbore, S. E.: Persistence of soil organic matter as an ecosystem property, Nature, 478, 49–56, https://doi.org/10.1038/nature10386, 2011.

Schuur, E. A. G., Bockheim, J., Canadell, J. G., Euskirchen, E., Field, C. B., Goryachkin, S. V., Hagemann, S., Kuhry, P., Lafleur, P. M., Lee, H., and Mazhitova, G.: Vulnerability of permafrost carbon to climate change: Implications for the global carbon cycle, BioScience, 58, 701–714, 2008.

Serreze, M. C. and Francis, J. A.: The Arctic on the fast track of change, Weather, 61, 65–69, 2006.

Shetler, G., Turetsky, M. R., Kane, E., and Kasischke, E.: Sphagnum mosses limit total carbon consumption during fire in Alaskan black spruce forests, Canadian Journal of Forest Research, 38, 2328-2336, 10.1139/x08-057, 2008.

Sinsabaugh, R. L.: Enzymic analysis of microbial pattern and process, Biol Fertil Soils, 17, 69-74, 1994.

Soja, A. J., Tchebakova, N. M., French, N. H. F., Flannigan, M. D., Shugart, H. H., Stocks, B. J., Sukhinin, A. I., Parfenova, E. I., Chapin, F. S., and Stackhouse, P. W.: Climate-induced boreal forest change: Predictions versus current observations, Global and Planetary Change, 56, 274-296, 10.1016/j.gloplacha.2006.07.028, 2007.

Somero, G. N.: Adaptation of enzymes to temperature: searching for basic “strategies”, Comp. Biochem. Phys. B, 139, 321–333, https://doi.org/10.1016/j.cbpc.2004.05.003, 2004.

Steinweg, J. M., Dukes, J. S., Paul, E. A., and Wallenstein, M. D.: Microbial responses to multi-factor climate change: effects on soil enzymes, Front. Microbiol., 4, 146, https://doi.org/10.3389/fmicb.2013.00146, 2013.

Steinweg, J. M., Plante, A. F., Conant, R. T., Paul, E. A., and Tanaka, D. L.: Patterns of substrate utilization during long-term incubations at different temperatures, Soil Biol. Biochem., 40, 2722–2728, https://doi.org/10.1016/j.soilbio.2008.07.002, 2008.

Stolpovsky, K., Martinez-Lavanchy, P., Heipieper, H. J., Van Cappellen, P., and Thullner, M.: Incorporating dormancy in dynamic microbial community models, Ecological Modelling, 222, 3092-3102, 10.1016/j.ecolmodel.2011.07.006, 2011.

Stone, M. M., Weiss, M. S., Goodale, C. L., Adams, M. B., Fernandez, I. J., German, D. P., and Allison, S. D.: Temperature sensitivity of soil enzyme kinetics under N fertilization in two temperate forests, Glob. Change Biol., 18, 1173–1184, https://doi.org/10.1111/j.1365-2486.2011.02545.x, 2012.

Stone, R. S., Dutton, E. G., Harris, J. M., and Longenecker, D.: Earlier spring snowmelt in northern Alaska as an indicator of climate change, Journal of Geophysical Research: Atmospheres, 107, ACL 10-11-ACL 10-13, 10.1029/2000jd000286, 2002.

Stow, D. A., Hope, A., McGuire, D., Verbyla, D., Gamon, J., Huemmrich, F., Houston, S., Racine, C., Sturm, M., Tape, K., Hinzman, L., Yoshikawa, K., Tweedie, C., Noyle, B., Silapaswan, C., Douglas, D., Griffith, B., Jia, G., Epstein, H., Walker, D., Daeschner, S., Petersen, A., Zhou, L., and Myneni, R.: Remote sensing of vegetation and land-cover change in Arctic Tundra Ecosystems, Remote Sensing of Environment, 89, 281-308, 10.1016/j.rse.2003.10.018, 2004.

Strickland, M. S., Lauber, C., Fierer, N., and Bradford, M. A.: Testing the functional significanceof microbial community composition, Ecology, 90, 441-451, 2009.

Sturm, M., Racine, C., and Tape, K.: Climate change: increasing shrub abundance in the Arctic, Nature, 411, 546–547, https://doi.org/10.1038/35079180, 2001.

T. G. Williams, L. B. F.: Measuring and modelling environmental influences on photosynthetic gas exchange in Sphagnum and Pleurozium, Plant, Cell and Environment, 21, 555–564, 1998.

Tang, J. and Zhuang, Q.: Equifinality in parameterization of process-based biogeochemistry models: A significant uncertainty source to the estimation of regional carbon dynamics, J. Geophys. Res.-Biogeo., 113, G04010, https://doi.org/10.1029/2008jg000757, 2008.

Tang, J., and Riley, W. J.: Weaker soil carbon–climate feedbacks resulting from microbial and abiotic interactions, Nature Climate Change, 5, 56-60, 10.1038/nclimate2438, 2014.

Tape, K. E. N., Sturm, M., and Racine, C.: The evidence for shrub expansion in Northern Alaska and the Pan-Arctic, Glob. Change Biol., 12, 686–702, https://doi.org/10.1111/j.1365-2486.2006.01128.x, 2006.

Tarnocai, C., Canadell, J. G., Schuur, E. A. G., Kuhry, P., Mazhitova, G., and Zimov, S.: Soil organic carbon pools in the northern circumpolar permafrost region, Global Biogeochemical Cycles, 23, n/a-n/a, 10.1029/2008gb003327, 2009.

Thullner, M., Van Cappellen, P., and Regnier, P.: Modeling the impact of microbial activity on redox dynamics in porous media, Geochimica et Cosmochimica Acta, 69, 5005-5019, 10.1016/j.gca.2005.04.026, 2005.

Todd-Brown, K. E. O., Hopkins, F. M., Kivlin, S. N., Talbot, J. M., and Allison, S. D.: A framework for representing microbial decomposition in coupled climate models, Biogeochemistry, 109, 19–33, https://doi.org/10.1007/s10533-011-9635-6, 2011.

Todd-Brown, K. E. O., Randerson, J. T., Post, W. M., Hoffman, F. M., Tarnocai, C., Schuur, E. A. G., and Allison, S. D.: Causes of variation in soil carbon simulations from CMIP5 Earth system models and comparison with observations, Biogeosciences, 10, 1717–1736, https://doi.org/10.5194/bg-10-1717-2013, 2013.

Treseder, K. K., Balser, T. C., Bradford, M. A., Brodie, E. L., Dubinsky, E. A., Eviner, V. T., Hofmockel, K. S., Lennon, J. T., Levine, U. Y., MacGregor, B. J., Pett-Ridge, J., and Waldrop, M. P.: Integrating microbial ecology into ecosystem models: challenges and priorities, Biogeochemistry, 109, 7-18, 10.1007/s10533-011-9636-5, 2011.

Treseder, K. K., Marusenko, Y., Romero-Olivares, A. L., and Maltz, M. R.: Experimental warming alters potential function of the fungal community in boreal forest, Global change biology, 22, 3395-3404, 10.1111/gcb.13238, 2016.

Turetsky, M. R., Bond-Lamberty, B., Euskirchen, E., Talbot, J., Frolking, S., McGuire, A. D., and Tuittila, E. S.: The resilience and functional role of moss in boreal and arctic ecosystems, The New phytologist, 196, 49-67, 10.1111/j.1469-8137.2012.04254.x, 2012.

Turetsky, M. R., Mack, M. C., Hollingsworth, T. N., and Harden, J. W.: The role of mosses in ecosystem succession and function in Alaska's boreal forestThis article is one of a selection of papers from The Dynamics of Change in Alaska's Boreal Forests: Resilience and Vulnerability in Response to Climate Warming, Canadian Journal of Forest Research, 40, 1237-1264, 10.1139/x10-072, 2010.

Van't Hoff, J.H. and Lehfeldt, R.A. : *Lectures on theoretical and physical chemistry*, London: E. Arnold, 1, 1899.

W. D. Billings, K. M. P., G. R. Shaver, A. W. Trent: Root Growth, Respiration, and Carbon Dioxide Evolution in an Arctic Tundra Soil, Arctic and Alpine Research, 9, 129-137, 10.1080/00040851.1977.12003908, 1977.

Wang G., M. A. M., Lianhong Gu, Christopher W. Schadt: Representation of Dormant and Active Microbial Dynamics for Ecosystem Modeling, Public Library of Science, 9, 10.1371/journal.pone.0089252.g001, 2014.

Wang Wei, F. J., T. Oikawa: Contribution of Root and Microbial Respiration to Soil CO2 Efflux and Their Environmental Controls in a Humid Temperate Grassland of Japan, Pedosphere, 19, 31-39, 2009.

Wang, G., Jagadamma, S., Mayes, M. A., Schadt, C. W., Steinweg, J. M., Gu, L., and Post, W. M.: Microbial dormancy improves development and experimental validation of ecosystem model, The ISME journal, 9, 226-237, 10.1038/ismej.2014.120, 2015.

Wardle, M.-C. N. a. D. A.: Understory vegetation as a forest ecosystem driver: evidence from the northern Swedish boreal forest, The Ecological Society of America, 3, 421–428, 2005.

Wardle, M.-C. N. a. D. A.: Understory vegetation as a forest ecosystem driver: evidence from the northern Swedish boreal forest, The Ecological Society of America, 3, 421–428, 2005.

Werf, H. V. d., and Verstraete, W.: Estimation of active soil microbial biomass by mathematical analysis of respiration curves: relation to conventional estimation of total biomass, Soil Biology and Biochemistry, 19, 267-271, 1987.

White, A., Cannell, M. G. R., and Friend, A. D.: The high-latitude terrestrial carbon sink: a model analysis Global change biology, 6, 227-245, 2000.

Wieder, W. R., Bonan, G. B., and Allison, S. D.: Global soil carbon projections are improved by modelling microbial processes, Nat. Clim. Change, 3, 909–912, https://doi.org/10.1038/nclimate1951, 2013.

Xu, X., Schimel, J. P., Thornton, P. E., Song, X., Yuan, F., and Goswami, S.: Substrate and environmental controls on microbial assimilation of soil organic carbon: a framework for Earth system models, Ecology letters, 17, 547-555, 10.1111/ele.12254, 2014.

Zha, J., and Zhuang, Q.: Microbial decomposition processes and vulnerable arctic soil organic carbon in the 21st century, Biogeosciences, 15, 5621-5634, 10.5194/bg-15-5621-2018, 2018a.

Zhou, L., Tucker, C. J., Kaufmann, R. K., Slayback, D., Shabanov, N. V., and Myneni, R. B.: Variations in northern vegetation activity inferred from satellite data of vegetation index during 1981 to 1999, Journal of Geophysical Research: Atmospheres, 106, 20069-20083, 10.1029/2000jd000115, 2001.

Zhuang, Q., Chen, M., Xu, K., Tang, J., Saikawa, E., Lu, Y., Melillo, J. M., Prinn, R. G., and McGuire, A. D.: Response of global soil consumption of atmospheric methane to changes in atmospheric climate and nitrogen deposition, Global Biogeochem. Cy., 27, 650–663, https://doi.org/10.1002/gbc.20057, 2013.

Zhuang, Q., He, J., Lu, Y., Ji, L., Xiao, J., and Luo, T.: Carbon dynamics of terrestrial ecosystems on the Tibetan Plateau during the 20th century: an analysis with a process based biogeochemical model, Global Ecol. Biogeogr., 19, 649–662, https://doi.org/10.1111/j.1466-8238.2010.00559.x, 2010.

Zhuang, Q., McGuire, A. D., Melillo, J. M., Clein, J. S., Dargaville, R. J., Kicklighter, D. W., Myneni, R. B., Dong, J., Romanovsky, V. E., Harden, J., and Hobbie, J. E.: Carbon cycling in extratropical terrestrial ecosystems of the Northern Hemisphere during the 20th century: a modeling analysis of the influences of soil thermal dynamics, Tellus B, 55, 751–776, https://doi.org/10.3402/tellusb.v55i3.16368, 2003.

Zhuang, Q., McGuire, A. D., O'Neill, K. P., Harden, J. W., Romanovsky, V. E., and Yarie, J.: Modeling soil thermal and carbon dynamics of a fire chronosequence in interior Alaska, Journal of Geophysical Research, 108, 10.1029/2001jd001244, 2002.

Zhuang, Q., Melillo, J. M., Sarofim, M. C., Kicklighter, D. W., McGuire, A. D., Felzer, B. S., Sokolov, A., Prinn, R. G., Steudler, P. A., and Hu, S.: CO2and CH4exchanges between land ecosystems and the atmosphere in northern high latitudes over the 21st century, Geophysical Research Letters, 33, 10.1029/2006gl026972, 2006.

Zhuang, Q., Romanovsky, V. E., and McGuire, A. D.: Incorporation of a permafrost model into a large-scale ecosystem model: Evaluation of temporal and spatial scaling issues in simulating soil thermal dynamics, Journal of Geophysical Research: Atmospheres, 106, 33649-33670, 10.1029/2001jd900151, 2001.

Zhuang, Q., Zhu, X., He, Y., Prigent, C., Melillo, J. M., David McGuire, A., Prinn, R. G., and Kicklighter, D. W.: Influence of changes in wetland inundation extent on net fluxes of carbon dioxide and methane in northern high latitudes from 1993 to 2004, Environmental Research Letters, 10, 095009, 10.1088/1748-9326/10/9/095009, 2015.

VITA
Junrong Zha

550 Stadium Mall Drive, Department of EAPS, West Lafayette, IN 47907 USA

EDUCATION

Purdue University 2015.8 - 2019. 6

Ph.D. in Earth Science. Advised by **Dr. Qianlai Zhuang**.

Dissertation: Modeling the Impacts of Changes in Soil Microbes and Mosses on Arctic Terrestrial Ecosystem Carbon Dynamics

University of Science & Technology of China (USTC) 2011.8 - 2015.6

B.S. in Atmospheric Physics

PUBLICATIONS

- **Zha, J.** and Zhuang, Q.: Microbial decomposition processes and vulnerable arctic soil organic carbon in the 21st century, ***Biogeosciences***, 15, 5621-5634, https://doi.org/10.5194/bg-15-5621-2018, 2018.
- **Zha, J.** and Zhuang, Q.: Microbial dormancy and its impacts on Arctic terrestrial ecosystem carbon budget, ***Biogeosciences Discuss.***, https://doi.org/10.5194/bg-2019-72, in review, 2019.
- **Zha, J.** and Zhuang, Q (2019), Modeling the role of moss in terrestrial ecosystem carbon dynamics in northern high-latitudes (Submitted to ***Journal of Advances in Modeling Earth Systems***).

PROFESSIONAL EXPERIENCE

Graduate Research Assistant, Purdue University 2015.8-2019.7

Graduate Teaching Assistant, Purdue University

- Teaching Assistant for EAPS 577 Remote Sensing of the Planets, Spring, 2018
- Teaching Assistant for EAPS 327 Great Issues: Climate, Science and Society, Spring, 2018

PRESENTATION

Terrestrial Ecosystem Model (TEM) Workshop at Purdue University. Oral presentation. 2017

HONORS & AWARDS (SELECTED)

- Outstanding Student Scholarship of USTC 2012-2014
- Innovation Scholarship by Aegon-Industrial Fund 2014
- Chinese National Endeavor Fellowship 2012
- Second prize in National Undergraduate Mathematical Contest 2012